Modelling the extracellular environment of pancreatic ductal adenocarcinoma to study different aspects of disease progression

Nausica Betriu Rosselló

http://hdl.handle.net/10803/687371

Data defensa: 15-12-2022

UNIVERSITAT RAMON LLULL

DOCTORAL THESIS

Title	Modelling the extracellular environment of pancreatic ductal adenocarcinoma to study different aspects of disease progression
Presented by	Nausica Betriu Rosselló
Centre	IQS School of Engineering
Department	Bioengineering
Directed by	Carlos E. Semino Margrett

ACKNOWLEDGEMENTS

This thesis also belongs

To my parents and my sisters, who have supported me my entire life. I have no words for you other than thank you.

To my Biochemist friends, who have been with me since the beginning of this long journey in 2012. I think none of us thought at that time we would end up doing a PhD, but here we are.

To my appreciated students Claire Jarrosson, Anna Andreeva and Anna Alonso, who have accompanied me in each chapter of this thesis. I am so happy I could be a mentor for you and I am very proud of each one of you.

Finally, this thesis specially belongs to my supervisor, Dr. Carlos Semino, for his endless support, guidance and trust.

SUMMARY

Pancreatic ductal adenocarcinoma (PDAC) is the most relevant pancreatic disease, accounting for more than 90% of all pancreatic malignancies. PDAC is the fourth most common cause of cancer-related deaths in Europe and US, with an extremely low five-year survival rate of around 10%. One of the main hallmarks of PDAC is the presence of a dense and remarkably stiff extracellular matrix produced by stromal cells, which generates a unique microenvironment that fosters sustained cancer cell proliferation and resistance to drug-induced toxicity and apoptosis. During approximately the last five decades, two-dimensional (2D) cell cultures have been classically used to study cancer cell biology. However, it has been widely demonstrated that in 2D cultures cells are exposed to a non-physiological environment as compared to 3D cultures, which provide the normal cellular conformation, matrix dimensionality and stiffness, as well as molecular gradients. The microenvironment of solid tumors is better recreated in 3D cultures, and therefore they are becoming a more physiological alternative to study different aspects of cancer progression such as angiogenesis, sustained proliferation, resistance to apoptosis and drug resistance capacities. In the present thesis, 3D in vitro models to study different aspects of PDAC have been developed. Specifically, the extracellular milieu has been deconstructed in three main parameters, being dimensionality, stiffness and biological signaling, and the contribution of each one in triggering different cell responses such as cell proliferation, drug resistance and signal mechanotransduction has been explored.

Part of this thesis focused on the study of the Epithelial Growth Factor Receptor (EGFR), a well-known tyrosine kinase receptor that is overexpressed in PDAC. Results show that treatment with the tyrosine kinase inhibitor erlotinib promoted EGFR degradation in 3D cultures of PDAC cell lines but not in 2D cultures. Moreover, receptor degradation did not occur in normal fibroblast cells, regardless of culture dimensionality. Therefore, not only erlotinib had a distinct effect on tumor and normal cells but also pancreatic ductal adenocarcinoma cells responded differently to drug treatment when cultured in a 3D microenvironment.

Moreover, researchers are increasingly developing cell culture models to mimic the increased stiffness associated with these kinds of tumors. In this thesis, the relationship between tumor cells and their biomechanical environment in terms of matrix stiffness has been studied. Both synthetic and natural 3D matrices were used to analyze the effect of matrix stiffness in terms of focal adhesion kinase (FAK) activation, as this protein has been widely reported to sense the stiffness of the environment and participate in signal mechanotransduction pathways. In addition, FAK is hyperactivated in many epithelial cancers and its expression correlates with tumor malignancy and invasion potential. Results show that increased matrix stiffness in synthetic but not in natural scaffolds promoted FAK downregulation at a protein level. Altogether, these findings highlight the importance of culture systems that can more accurately mimic the in vivo tumor physiology, since cell response strongly depends on the microenvironment in which they exist.

RESUM

L'adenocarcinoma ductal pancreàtic (ADP) és la malaltia pancreàtica més rellevant, que representa més del 90% de totes les patologies pancreàtiques. L'ADP és la quarta causa més comuna de mort per càncer a Europa i els Estats Units, amb una taxa de supervivència de 5 anys de només el 10%. Una de les característiques més importants de l'ADP és la presència d'una matriu extracel·lular molt densa i dura, produïda per cèl·lules estromals, que genera un microambient únic que promou la proliferació cel·lular i la resistència a l'apoptosi induïda per fàrmacs. Durant aproximadament les últimes cinc dècades, els cultius bi-dimensionals (2D) s'han emprat clàssicament per estudiar la biologia cel·lular del càncer. No obstant, s'ha demostrat que en cultius 2D, les cèl·lules queden exposades a un ambient no fisiològic comparat amb els cultius en 3D, que proveeixen una conformació cel·lular, una dimensió i una duresa normals, així com la formació de gradients moleculars. El microambient dels tumors sòlids es recrea millor en cultius 3D, i per tant, aquest tipus de cultiu es considera una alternativa més fisiològica per a estudiar diferents aspectes de la progressió del càncer, com per exemple la capacitat d'angiogènesis, proliferació cel·lular, resistència a apoptosis i resistència a fàrmacs. En aquesta tesis s'han desenvolupat models in vitro 3D per tal d'estudiar diferents aspectes de l'ADP. En concret, l'ambient extracel·lular s'ha deconstruït en tres paràmetres principals: dimensió, duresa i senyals biològiques, i s'ha estudiat el paper de cadascun d'ells en el desencadenament de diferents respostes cel·lulars com per exemple la proliferació, la resistència a fàrmacs i la mecanotransducció de senyals.

Part d'aquesta tesis s'ha centrat en l'estudi del receptor del factor de creixement epitelial (*Epithelial Growth Factor Receptor*, EGFR), un receptor de tirosina quinasa que es troba sobre-expressat en l'ADP. Els resultats mostren com el tractament amb erlotinib, un inhibidor de receptors tirosina quinasa, promou la degradació del EGFR en cultius 3D de diferents línies cel·lulars de càncer de pàncrees, però no en cultius 2D. A més, la degradació d'aquest receptor no succeeix en fibroblasts, cèl·lules no tumorals, en cap dels dos tipus de cultius (2D o 3D). Per tant, no només l'erlotinib té un efecte diferent en cèl·lules tumorals i no tumorals, sinó que, a més a més, les cèl·lules responen de manera diferent al fàrmac quan es cultiven en un ambient 3D.

A més, els científics estan progressivament desenvolupant models de cultiu cel·lular per imitar l'augment de duresa associada a aquest tipus de tumors. En aquesta tesi s'ha estudiat la relació entre les cèl·lules tumorals i el seu ambient biomecànic en termes de duresa de la matriu. S'han utilitzat matrius 3D sintètiques i naturals per a analitzar l'efecte de la duresa de la matriu en termes d'activació de la quinasa d'adhesions focals (*focal adhesion kinase*, FAK), ja que aquesta proteïna és capaç de sentir la duresa de l'ambient i de participar en vies de mecanotransducció de senyals. A més, FAK es troba hiperactivada en molts càncers epitelials, i la seva expressió es correlaciona amb la malignitat i el potencial invasiu dels tumors. Els resultats obtinguts mostren que les matrius sintètiques d'elevada duresa, però no pas les matrius naturals, promouen la regulació negativa de FAK a nivell de proteïna. En conjunt, els resultats ressalten la importància de sistemes de cultiu que siguin capaços de recrear la fisiologia tumoral de manera més acurada, ja que la resposta cel·lular depèn del microambient en el qual es troben les cèl·lules.

RESUMEN

El adenocarcinoma ductal pancreático (ADP) es la enfermedad pancreática más relevante, representando más del 90% de todas las patologías pancreáticas. El ADP es la cuarta causa más común de muerte por cáncer en Europa y Estados Unidos, con una tasa de supervivencia de 5 años de solo el 10%. Una de las características más importantes del ADP es la presencia de una matriz extracelular muy densa i dura, producida por células estromales, que genera un microambient único que promueve la proliferación celular i la resistencia a la apoptosis inducida por fármacos. Durante aproximadamente las últimas 5 décadas, los cultivos bidimensionales (2D) se han usado clásicamente para estudiar la biología celular del cáncer. No obstante, se ha demostrado que en cultivos 2D, las células quedan expuestas a un ambiente no fisiológico en comparación con los cultivos en 3D, que aportan una conformación celular, dimensionalidad y dureza normales, así como la generación de gradientes moleculares. El microambiente de los tumores sólidos se recrea mejor en cultivos 3D, y por lo tanto, este tipo de cultivo se considera una alternativa más fisiológica para estudiar diferentes aspectos de la progresión del cáncer, como por ejemplo la capacidad de angiogénesis, proliferación celular, resistencia a apoptosis y resistencia a fármacos. En esta tesis se han desarrollado modelos in vitro 3D para estudiar diferentes aspectos del ADP. En concreto, el ambiente extracelular se ha deconstruido en tres parámetros principales: dimensionalidad, dureza y señales biológicas, y se ha estudiado la contribución de cada uno en desencadenar diferentes respuestas celulares como por ejemplo la proliferación, la resistencia a fármacos y la mecanotransducción de señales.

Parte de esta tesis se ha centrado en el estudio del receptor del factor de crecimiento epitelial (*Epithelial Growth Factor Receptor*, EGFR), un receptor de tirosina quinasa que se encuentra sobre-expresado en el ADP. Los resultados muestran como el tratamiento con erlotinib, un inhibidor de receptores tirosina quinasa, promueve la degradación del EGFR en cultivos 3D de diferentes líneas celulares de cáncer de páncreas, pero no en cultivos 2D. Además, la degradación de este receptor no sucede en fibroblastos, células no tumorales, en ninguno de los dos tipos de cultivos (2D o 3D). Por lo tanto, no sólo el erlotinib tiene un efecto diferente en células tumorales y no tumorales y sino que además, las células responden de modo diferente al fármaco cuando se cultivan en un ambiente 3D.

Además, los científicos están progresivamente desarrollando modelos de cultivo celular para imitar el augmento de dureza asociada a este tipo de tumores. En esta tesis, se ha estudiado la relación entre les células tumorales y su ambiente biomecánico en términos de dureza de la matriz. Se han utilizado matrices 3D sintéticas y naturales para analizar el efecto de la dureza de la matriz en términos de activación de la quinasa de adhesiones focales (*focal adhesion kinase*, FAK), ya que esta proteína es capaz de sentir la dureza del ambiente y participar en vías de mecanotransducción de señales. Además, FAK se encuentra hiperactivada en muchos cánceres epiteliales, y su expresión se correlaciona con la malignidad y el potencial invasivo de los tumores. Los resultados obtenidos muestran que las matrices sintéticas de elevada dureza, pero no las matrices naturales, promueven la regulación negativa de FAK a nivel de proteína. En conjunto, estos resultados destacan la importancia de sistemas de cultivo que puedan recrear la fisiología tumoral de manera más acurada, ya que la respuesta celular depende del microambiente en el cual se encuentran las células.

LIST OF CONTENTS

LIST OF FIGURES

LIST OF TABLES

LIST OF ABBREVIATIONS

2D	Two-dimensional	**MLC**	Myosin Light Chain
3D	Three-dimensional	**MLCP**	Myosin Light Chain Phosphatase
BME	Basal Membrane Extract	**MRE**	Magnetic Resonance Elastography
CAF	Cancer-associated fibroblast	**MSC**	Mesenchymal Stem Cell
Cdk2	Cyclin-dependent kinase 2	**NMuMG**	Normally murine mammary gland cells
E	Elastic Young's modulus		
ECM	Extracellular Matrix	**PDAC**	Pancreatic Ductal Adenocarcinoma
EMT	Epithelial-to-Mesenchymal transition	**PDGF**	Platelet-derived Growth Factor
		PA	Polyacrylamide
FA	Focal Adhesion	**PEG**	Poly(ethylene glycol)
FAK	Focal Adhesion Kinase	**PLA**	Polylactic acid
FBS	Fetal Bovine Serum	**PLG**	Poly(lactide-co-glycolide)
FC	Focal Complex	**PLGA**	Poly(lactic-co-glycolic acid)
G	Shear modulus	**PI3K**	Phosphatidylinositol 3-kinase
GAG	Glycosaminoglycan	**PIP$_2$**	Phosphatidylinositol 4,5-bisphosphate
GelMA	Gelatin-methacrylate		
GFR	Growth Factor Receptor	**PIP$_3$**	Phosphatidylinositol (3,4,5)-trisphosphate
HA	Hyaluronic Acid		
HAS	Hyaluronic Acid Synthase	**PSC**	Pancreatic Stellate Cell
HCC	Hepatocellular carcinoma	**rBM**	reconstituted Basal Membrane
IAC	Integrin-Associated Complex	**ROCK**	Rho-Associated coiled-coil containing protein kinase
IDC	Invasive Ductal Carcinoma		
IPN	Interpenetrating Polymer Network	**ROS**	Reactive Oxygen Specie
LIMK	LIM-Kinase	**SAP**	Self-assembling Peptide
LOX	Lysyl Oxidase	**SSM**	Steady-State-Modulus
MAPK	Mitogen-Activated protein kinase	**SWUE**	Shear Wave Ultrasound Elastography
MDCK	Madin-Darby canine kidney epithelial cells		
		TE	Tissue Engineering
MEC	Mammary Epithelial Cell	**TKR**	Tyrosine Kinase Receptor
MET	Mesenchymal-to-Epithelial transition	**TKI**	Tyrosine Kinase Receptor Inhibitor
		TME	Tumor Microenvironment
MMP	Matrix Metalloproteinase	**TG2**	Transglutaminase 2

Chapter 1. Introduction

1.1 Pancreatic ductal adenocarcinoma

The pancreas is an organ that functions as part of the gastrointestinal system (**Figure 1a**) and undergoes both exocrine and endocrine functions. The endocrine pancreas is constituted of many pancreatic islets, called islets of Langerhans, which contain specific cells that produce and secrete hormones such as glucagon (alpha cells) and insulin (beta cells) that regulate blood glucose levels and glucose intake by the cells (**Figure 1b**). Moreover, the islets of Langerhans also secrete two other hormones: the pancreatic polypeptide (PP cells), that regulates pancreatic secretion processes as well as glycogen storage in the liver, and somatostatin (delta cells), that inhibits the release of pancreatic hormones such as insulin, glucagon and pancreatic exocrine enzymes. The exocrine pancreas instead is constituted by duct cells and acinar cells, the latter ones in charge of producing enzymes such as proteases, lipases and amylases, that travel through the pancreatic duct to be finally released into the duodenum to support nutrient digestion. Therefore, pancreatic dysfunction can lead to digestion problems as well as dysregulation of blood glucose homeostasis due to different diseases such as diabetes, chronic and acute pancreatitis, cystic fibrosis and hereditary pancreatitis.
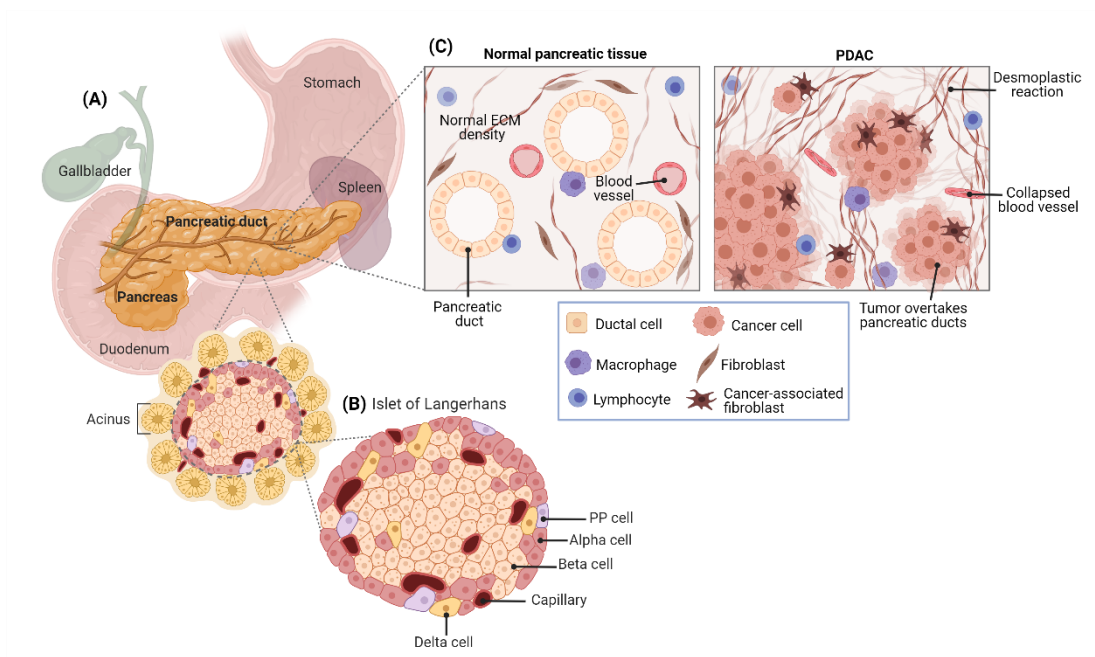
Figure 1. Pancreas physiology in homeostasis and disease. (a) The pancreas functions as part of the gastrointestinal system; **(b)** The pancreas undergoes both an exocrine (acinar and duct cells) and an endocrine function (islets of Langerhans); **(c)** Pancreatic ductal adenocarcinoma (PDAC) arises in ductal cells and its progression is characterized by both the proliferation of tumor cells that overtake the pancreatic duct and the secretion of vast amounts of ECM (desmoplastic reaction) by cancer-associated fibroblasts. The figure was created using Biorender.

However, the most relevant pancreatic disease in terms of patient survival, with an extremely low five-year survival rate of around 10%[1] is, without doubt, pancreatic ductal adenocarcinoma (PDAC) (**Figure 1c**). PDAC accounts for more than 90% of all pancreatic malignances and is usually diagnosed at very advanced stages due to the lack of efficient screening tests for early disease detection as well as due to its asymptomatic nature at early stages. Moreover, some of its symptoms, like abdominal pain, jaundice and dark urine are not specific to this disease, which makes it even more difficult to diagnose[2]. The cause of pancreatic cancer remains unknown, but some of the risks of developing PDAC are cigarette smoking, a diet based on a high intake of fat and meat, diabetes, alcohol abuse and family history[2,3]. There are three precursors from which PDAC can originate[4], namely intraductal papillary mucinous neoplasm (IPMN), mucinous cystic neoplasm (MCN) and pancreatic intraepithelial neoplasm (PanIN), the last one being the most common precursor lesion of pancreatic cancer. PanINs are non-invasive epithelial neoplasms usually located at the head of the pancreas, which can be divided into PanIN-1, PanIN-2 and PanIN-3, depending on its stage. These neoplasms are considered to be the first steps before PDAC development and each one is associated with specific mutations. For example, PanIN-1 is characterized by alterations in EGFR signaling and KRAS mutations, while PanIN-2 and PanIN-3 are characterized by the inactivation of tumor suppressor genes like CDKN2A, SMAD4 and TP53[5].

As mentioned above, KRAS mutation is one of the first events in PanIN progression into PDAC. Constitutive activation of mutant KRas promotes plasticity of neoplastic cells and tumor development. Moreover, Ras activates signaling events such as MAPK and PI3K/Akt pathways, which regulate genes involved in cell proliferation, migration, survival/apoptosis and metastasis[5]. These signaling pathways are normally activated through different cellular receptors such as tyrosine kinase receptors (TKRs), a receptor family which participates in a wide range of cellular processes, like cell proliferation, growth and invasion[6]. Most of these biochemical pathways, such as cell proliferation, survival and metastasis, can be modulated by the dynamical property of the extracellular matrix (ECM), suggesting that any change in its integrity, stiffness and composition may directly affect organ physiology as well as the development of some pancreatic diseases including cancer progression.

Specifically, the ECM is a three-dimensional network of fibrous proteins, glycoproteins, proteoglycans and polysaccharides with different biochemical and physical properties synthesized and secreted by stromal cells, mainly fibroblasts. Furthermore, the ECM provides structural and biochemical support for organs and tissues, for epithelial cell layers as basal membrane (BM) and for individual cells as a substrate for migration[7,8]. The ECM, as well as cell-cell contact and diverse signaling molecules, serves as an information exchanger between cells forming a tissue. These interactions provide the necessary information to preserve cellular differentiation and thus, create complex tissue structures. During the early stages of tumorigenesis, epithelial cells undergo a complex process called epithelial-to-mesenchymal transition (EMT). During this process, pre-cancer epithelial cells experience a series of changes such as the downregulation of cell-cell interaction proteins (cadherins), upregulation of cell-matrix receptors (integrins), and remodeling of the entire cytoskeleton to acquire cell motility, proper of a mesenchymal migrating cell type. Also important, cells undergoing EMT overexpress matrix metalloproteinases (MMP), that actively remodel the surrounding ECM. MMPs are overexpressed in

most early stages of human cancers[9]. Interestingly, pancreatic cancer is characterized by a desmoplastic reaction, in which the deposition of abundant amounts of ECM exert biochemical and mechanical effects on PDAC cells[10] (**Figure 1c**). During pancreatic cancer progression, degradation of the normal ECM is followed by synthesis and deposition of a new ECM, with a particular property of being a high desmoplastic matrix stroma, which promotes tumor development. This new tumor-associated matrix stroma has attracted the attention of many researchers in terms of targeting the ECM for the development of new PDAC treatments. However, special care should be taken to avoid the depletion of the entire ECM, as this could have dramatic consequences[11]. The degradation of the ECM components and the basal membrane implies the destruction of a physical barrier, which would allow stromal invasion by cancer cells as well as the migration of endothelial cells into the matrix, resulting in neovascularization. Moreover, during the ECM degradation, different growth factors and cytokines may be released, a fact that would support the proliferation of cancer cells and tumor growth.

1.1.1 The hallmarks of PDAC

Pancreatic ductal adenocarcinoma (PDAC) is considered one of the most aggressive carcinomas that often presents with locally invasive or metastatic disease. PDAC is the fourth most common cause of cancer-related death worldwide, despite it only represents about 3% of all cancer occurrences. The most common driver gene mutations found in PDAC are *KRAS* (88-100% of cases), *CDKN2A* (90% of cases), *TP53* (85% of cases) and *SMAD4* (55% of cases) (**Figure 2a**), which all fulfill key roles in pancreatic tumorigenesis[12] (**Table 1**).

Table 1. Driver gene mutations in PDAC and its role in tumorigenesis

Gene	Tumor suppressor/Oncogene	Protein	Pathway	Mutation effect	Role in tumorigenesis
KRAS	Oncogene	K-Ras	RAS-ERK signaling	Activating	Ligand-dependent receptor tyrosine kinase growth independence
CDKN2A	Tumor suppressor	p16^{INK4A} p19^{ARF}	G1/S transition	Inactivating	Loss of the G1/S checkpoint
TP53	Tumor suppressor	p53	DNA damage response	Inactivating	Loss of the G1/S checkpoint Loss of the G2/M checkpoint Resistance to apoptotic signals
SMAD4	Tumor suppressor	SMAD4	TGFβ signaling	Inactivating	Loss of homeostatic mechanisms

The origin of PDAC is complex, but it has been described that it can arise either from a precursor cell of intralobular ducts or from acinar cells. PDAC is initiated by KRAS mutations and requires the repression of the epithelial differentiation program and the activation of other factors that are normally expressed during the embryonic development. Precursors of pancreatic cancer such as PanINs participate in this process[13] (**Figure 2b**).

Apart from this genetic landscape, PDAC has also a unique tumor microenvironment (TME), which also favors malignant progression (**Figure 2c**). One of the hallmarks of PDAC, and probably the most important, is the presence of high quantities of extracellular matrix (ECM) proteins, specially type I collagen, but also other proteins such as fibronectin and laminin, which are produced by stromal cells. Interestingly, ECM production is such large, that stromal components can account for up to 80% of the tumor[16]. During malignant progression, pancreatic cancer cells release profibrotic factors that activate stromal cells resident in the pancreas, called pancreatic stellate cells (PSCs), which migrate from different sites of the pancreas towards the tumor core, where produce large amounts of ECM components around the tumor tissue, which process is called desmoplastic reaction (DR).
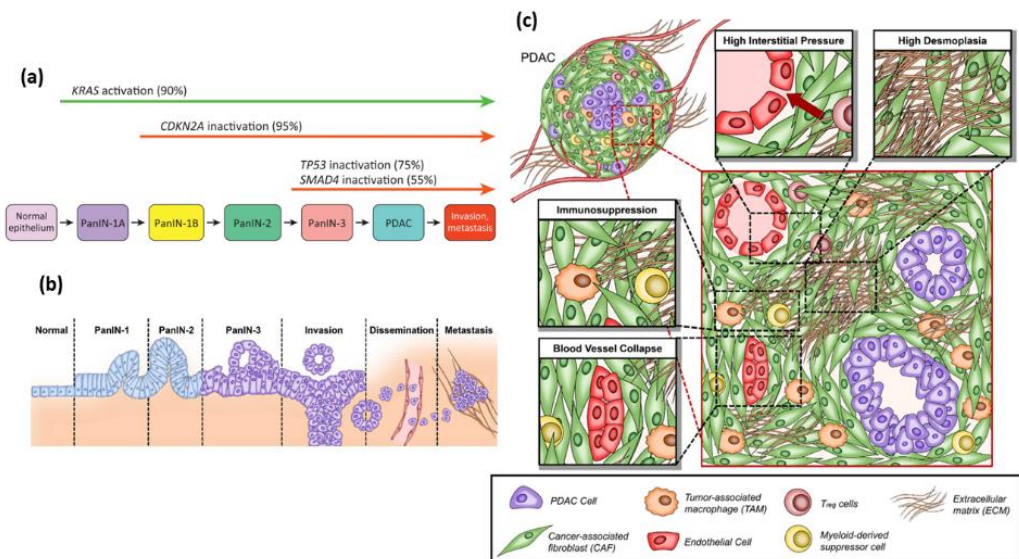
Figure 2. Hallmarks of pancreatic ductal adenocarcinoma. **(a)** Genetic progression of PDAC; **(b)** Development of PDAC describing different PanIN lesions towards invasive PDAC and metastasis; **(c)** The PDAC microenvironment. Adapted from[14,15].

This leads to a positive feedback loop of cancer cell proliferation and subsequent growth factors and cytokines release, perpetuating PSC activity, and therefore promoting the accumulation of more and more ECM components. Is therefore widely accepted that the crosstalk between activated PSCs and cancer cells promotes PDAC carcinogenesis and chemoresistance. Moreover, this stromal reaction also causes tissue stiffening, which accelerates PDAC progression via changes in integrin-mediated signal mechano-transduction and also produces a feedback loop that sustains PSC fibrotic activity. Therefore, one of the principal features of PDAC and probably one of the main properties of the

malignant phenotype, is the presence of a dense and remarkably stiff ECM surrounding the tumor, which generates a unique microenvironment that fosters cancer cell proliferation and resistance to drug-induced apoptosis[17–24].

1.1.2 Treatment of PDAC

Most PDAC patients are not eligible for surgery because of the advanced stage of disease. In such cases, chemotherapies are the treatment of choice. The asymptomatic nature at early stages, the extreme metastatic behavior, the lack of efficient diagnostic tools and the limited response to chemotherapy and radiotherapy characterize this disease -since detected- to have a median survival time of about 3 to 4 months. With good treatment, the survival time could increase between 6 to 12 months. Despite all efforts, little improvements have been accomplished in PDAC therapy, being chemotherapy the standard treatment for PDAC in all stages of disease.

Currently, Gemcitabine (Gemzar®) is considered the gold-standard chemotherapy for treating PDAC. However, chemoresistance associated with this drug limits its effectivity. Different combinatorial therapies have been proposed to overcome drug resistance to Gemcitabine. For example, adjuvant therapy with modified FOLFIRINOX (combination of 5-Fluorouracil (5-FU), leucovorin, irinotecan and oxaliplatin) showed longer overall survival than gemcitabine therapy in patients with resected PDAC (ClinicalTrials.gov Identifier: NCT01526135)[25]. In another study, patients were treated with gemcitabine alone or combined with *nab*-paclitaxel (ClinicalTrials.gov Identifier: NCT01964430). However, combinatorial treatment did not improve patient's survival when compared with gemcitabine alone[26]. Notably, such drug cocktails are very toxic not only to the tumor but also at a systemic level.

In addition to chemoresistance, the poor therapeutic outcome of PDAC has been ascribed to the intrinsic complexity of the tumor, which is protected by a dense and hypoxic stroma. Therefore, it has been suggested that PDAC therapies should combine a chemotherapeutic and a co-adjuvant drug for reducing the stroma to give access to the drug. To this end, several combined treatments have been proposed. Among them, administration of nab-paclitaxel/gemcitabine along with pegvorhyaluronidase alfa (PEGPH20)[27], which degrades hyaluronic acid present in the tumor stroma (ClinicalTrials.gov Identifier: NCT01839487), Gemcitabine and LY364947[28], a TGFβ inhibitor that decreases pericyte coverage of the vasculature, and more recently Gemcitabine with Metformin[29]. Although these therapeutic regimes could accomplish an improvement compared with standard treatment, PDAC patients' survival is still extremely low.

1.1.3 The extracellular matrix in PDAC

PDAC is without doubt one of the tumors in which more ECM amounts are produced and deposited, which causes the stiffening of the tissue. The responsible for this desmoplastic reaction are the stromal cells resident in the stromal compartment of the pancreas, named pancreatic stellate cells (PSCs). Under homeostasis, PSCs are found in a quiescent state, in which they synthesize both ECM proteins and ECM-degrading enzymes[30,31], regulating therefore ECM turnover and maintaining a balance between ECM synthesis and degradation[30]. However, during cancer initiation and progression, pancreatic cancer cells release molecules such as TGFβ1, FGF2 and PDGF, that activate PSCs[32–35] and attract them to the tumor core. Once there, they produce large amounts of ECM components around the tumor tissue, thus unbalancing ECM synthesis and degradation and promoting the accumulation of ECM components.

Collagens are the most abundant components of the ECM in PDAC. In particular, collagen type I (COLI) is the main responsible for the desmoplastic reaction[36–39]. Among other functions, it serves as ligand for integrin receptors in cancer cells, specifically for β1-integrins. This interaction can trigger other intracellular signaling pathways and activate molecules such as FAK[40] and WNT[41,42], with both ending up promoting EMT, migration, invasion and metastasis[43–45]. Collagen I also promotes inhibition of apoptosis, proliferation and MMP expression[11]. Moreover, tissue stiffening is not only caused by the over-deposition of ECM components, but also by the cross-linking of collagen fibers by the presence of enzymes such as lysyl oxidase (LOX)[46,47] and transglutaminase 2 (TG2)[48].

Fibronectin is another ECM component that plays a key role in tumorigenesis. It is a glycoprotein that, similar to collagen, binds to integrin receptors (α5β1) and activates the FAK pathway[49]. Fibronectin has been associated to radiotherapy resistance[50], proliferation[51], production of ROS[52] and the promotion of PSCs fibrotic activity[53].

Proteoglycans such as hyaluronic acid (HA) are also expressed in abundant amounts in the PDAC ECM[54]. HA contributes to the increased intratumoral tissue pressure reducing the delivery of chemotherapeutic drugs[55,56]. Moreover, it promotes cell survival, proliferation and invasion via CD44 binding[57,58].

1.2 ECM and signal mechanotransduction in tissue homeostasis and disease

Tissue engineering (TE) is a scientific field focused on creating functional 3D tissues for tissue repair and regeneration, the study of stem cell behavior as well as the development of tissue and organ models to study diseases. The TE "triad" includes the combination of cells, soluble factors and engineered extracellular matrices (ECM) that facilitate cell growth, organization, and differentiation. Moreover, for the successful of TE approaches it is important to recreate not only the 3D environment and the chemical signaling itself but also the mechanical environment, that is the mechanical properties of the synthetic extracellular matrix. In the *in vivo* tissues, cells are found surrounded by a complex extracellular matrix. There are mainly two types of ECM: the interstitial connective tissue matrix, that embeds cells an provide structural scaffolding for tissues, and the basement membranes, which is a specialized ECM that separates epithelial tissues from its stroma. Therefore, the ECM provides structural and biochemical support for organs and tissues, for epithelial cells layers as basal membranes and for individuals cells as a substrate for migration[7,8]. Moreover, body tissues are under mechanical influence, which is composed of both endogenous and exogenous force sources such as pressure generated by loaded forces on tissues, shear stress generated by fluid flow, etc. Endogenous forces are those generated by the cytoskeletal contractility within cells while exogenous forces include gravity, shear stress, tension and compression. In particular, local ECM stiffness importantly affects cellular behavior. Cells experience and sense deformation by these endogenous or exogenous forces, affecting mainly two types of interactions: Cell-ECM and cell-cell interactions, which are internally transduced by specific mechanosignaling pathways that regulate cell lineage commitment and maintenance, survival, proliferation and specific tissue-cell function.

1.2.1 ECM and tissue mechanical homeostasis

The ECM is essential for connective tissues to perform normal function. Cells within a tissue synthesize and secrete the ECM constituents during development, while maintain it in health, remodel it during adaptation and repair it in response of injury or disease[59]. Each tissue, depending on its function, has a different ECM composition that define its biomechanical properties in terms of stiffness (elastic modulus). For example, tissues with structural functions that are under a high mechanical loading, such as bone, cartilage and skeletal muscle are much stiffer than mechanically static tissues such as brain or tissues constituting the gastrointestinal system (**Figure 3**).

In soft connective tissues, the ECM is built and maintained mainly by tissue-specific fibroblasts, such as cardiac fibroblasts in heart[60], pulmonary fibroblasts in lungs[61] and muscle fibroblasts in muscle[62]. Fibroblasts in each tissue not only synthesize the constituents of each tissue-specific ECM, but also can secrete matrix metalloproteinases (MMPs) that degrade the structural components of the ECM[63]. Importantly, interaction between cells and its ECM is governed not only by the chemical composition

but also by the mechanical properties of the ECM. To promote tissue mechanical homeostasis- the maintaining of structural integrity and functionality- cells must sense and regulate ECM mechanics. The key players in maintaining mechanical homeostasis are the components of the mechanostransduction machinery: extracellular matrix molecules, transmembrane receptors (integrins) and their linker proteins to the actomyosin cytoskeleton. The mechanical properties of the ECM depend mainly on three components: elastic fibers, collagens and glycosaminoglycans (GAGs). Elastic fibers consist of a core of elastin associated with microfibrils such as fibrillin and fibulin and its role is to provide tissues with elastic recoil and resilience. Elastic fibers are deposited and organized only during childhood, and therefore, any damage or degradation associated with ageing results in permanent changes in tissue function[64]. In contrast, collagens endow connective tissues with stiffness and strength and are constantly remodeled, degraded and re-synthesized to maintain tissue homeostasis under stress. Finally, GAGs are highly hydrated molecules that not only contribute to the compressive stiffness of tissues but also play an important function binding and presenting growth factors[65].
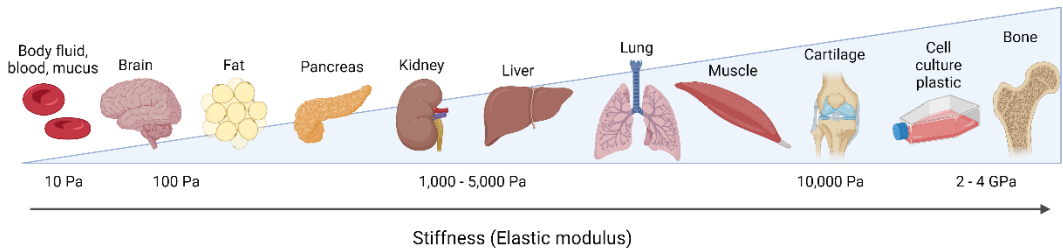
Figure 3. Variations in tissue stiffness. The biomechanical properties of a tissue in terms of stiffness (elastic modulus, Pa) differ between organs and tissues, and are inherently related to tissue function. Mechanically static tissues such as brain or compliant tissues such as lung exhibit low stiffness, whereas tissues exposed to high mechanical loading, such as bone or skeletal muscle, exhibit elastic moduli with a stiffness that is several orders of magnitude greater. The figure was created using Biorender. Adapted from[66,67].

Mechanical homeostasis in soft connective tissues depends mainly on the rate of ECM production and removal, the mechanical properties of the ECM constituents and the degree of pre-stress that is built into these constituents when deposited[68]. To preserve mechanical properties (such as stress, strain, stiffness and elasticity) and therefore, promote mechanical homeostasis, cells must sense changes in the ECM and restore its normal values through negative feedback mechanisms. Under normal conditions an increase or decrease in matrix stiffness triggers mechanisms that make the ECM more compliant or stiffer, respectively. This negative feedback is characterized by and ECM reorganization as well as the regulation in the balance between degradation and deposition of ECM constituents. However, in pathologic conditions the negative feedback to compensate mechanical changes is lost[69–72] or switched to positive feedback mechanisms. For instance, stress and strain increase can result in ECM stiffening due to the abnormal and excessive production and deposition of ECM, often called fibrosis.

Cells not only sense and transduce forces into biochemical signals but also adjust their own mechanical state in response to them[73]. This concept is known as tensional homeostasis, first

described as a basal equilibrium stress state -or steady state-[74] which was later used to describe the tendency of fibroblasts cultured in 3D collagens hydrogels to counteract the application of external loading and move toward a previous force setpoint that had been stablished before external force application (pre-stress)[75]. This process develops a tensile stress that within hours is stablished as part of the steady state[76]. Since stress increases proportionally ECM stiffness, tensional homeostasis represents one way to regulate ECM stiffness.

1.2.2 Signal mechanotransduction and molecular regulation of focal adhesions

At a cellular level, matrix stiffness is sensed through specific transmembrane receptors called integrins, which convert mechanical stimuli into a chemical response, which process is called signal mechanotransduction. Integrins are activated by engagement with the ECM and recruit a set of proteins that links them to the actin cytoskeleton[77], forming the so-called integrin-associated complexes (IACs). The formation, maturation and disassembly of these protein complexes are highly regulated in time and space. Small integrin-associated complexes that form at the leading edge of a cell are named focal complexes (FCs). Focal complex assembly is independent of actomyosin-mediated forces and disassemble fast in the absence of force. However, FCs can maturate into focal adhesions (FAs) (**Figure 4a**). This process requires integrin clustering and the recruitment and activation of specific proteins. The association of FA proteins between integrins and the actin cytoskeleton is complex, and it has been reported to involve 180 different proteins[78,79], including adaptor proteins such as vinculin[80], paxillin[81], talin[82] and focal adhesion kinases (FAKs) (**Figure 4a**). Upon integrin activation, the actin cytoskeleton is reorganized into stress fibers to mediate cell contractility, which is translated into the activation of different signaling pathways that can promote cell proliferation[83], migration[84], and differentiation[85].

IACs dynamics, that is, formation of FCs, maturation into FAs and disassembly, are regulated in a force-dependent manner. In this context, the Rho/ROCK signaling pathway plays a crucial role in FAs maturation through the activation of myosin II and the formation of actin stress fibers, that drive cell contractility[86]. Moreover, the tension generated from the actomyosin contractility to linked FA is needed to maintain the molecular composition of FA[87,88]. The maturation of FA is also accompanied by an increment of focal adhesion proteins such as vinculin, FAK, α-actinin, and filamin[89], which produce a reinforcement in the actin-integrin-ECM linkage. The strengthening of this linkage is also force-dependent. For example, it has been reported that vinculin, through binding to talin, localizes in FA when external forces are applied to adhesion sites[90], while a decrease in the actomyosin-generated force results in delocalization of vinculin from focal adhesions[91]. Moreover, the residence time of vinculin at FAs is also proportional to the magnitude of actomyosin-based forces exerted to FAs.

Once integrin-associated complexes are stablished within a cell, several signaling pathways that regulate cell activities are activated. Importantly, it has been reported that stiff matrices increase the

number of FAs compared to soft ones, enhancing thus the recruitment of adaptor and signaling proteins. Therefore, some of these signaling pathways are intensified under stiff matrix conditions. Additionally, in most situations signal mechanotransduction is complemented by chemical stimulation through soluble ligands that bind and activate growth factor receptors.

FAK protein plays a critical role in the downstream activation of diverse signaling pathways. FAK is an adaptor protein found in focal adhesions that also acts as a signaling protein kinase[92] that mediates the regulation of Rho-family GTPases (Rho, Rac, and Cdc42). Rho-family GTPases control the formation and disassembly of actin structures (stress fibers, lamellipodia and filopodia) and therefore control cell motility[93,94]. In particular, the RhoA/ROCK signaling pathway plays a critical role in signal mechanotransduction to regulate actin cytoskeleton dynamics. RhoA is positively regulated by matrix stiffness, with rigid matrices leading to an increase in RhoA activation. RhoA acts activating its principal downstream effector, Rho-Associated coiled-coil containing protein kinase (ROCK), a serine/threonine kinase that in turn phosphorylates a variety of substrates. For example, ROCK phosphorylates and inhibits the myosin light chain phosphatase (MLCP), allowing myosin light chain (MLC) phosphorylation to promote actin crosslinking by myosin and thus enhancing actomyosin contractility[95]. ROCK also phosphorylates and activates LIM-kinase (LIMK), which in turns inactivates Cofilin, an actin depolymerizing factor, promoting therefore the stabilization of existing actin filaments[96]. Thus, the combination of ROCK actions induces the formation of actin stress fibers, which are actomyosin bundles formed by anti-parallel actin filaments crosslinked with myosin (**Figure 4b**).

Integrins are essential not only for controlling cell contractility and motility but also for cell cycle progression and proliferation. Indeed, the role of integrins is so important for cell division that in the absence of integrin-mediated adhesions, normal cells cannot progress into cell cycle and proliferation, even in the presence of growth factors[97–100]. However, integrins cannot trigger proliferation by their own, but they need to cooperate with growth factor receptors (GFRs). There are two major different mechanisms of cooperation between integrins and GFRs: 1) via indirect signal crosstalk, in which both integrins and GFRs activate the same pathway (for example PI3K/Akt, MAPK/Erk and small GTPase pathways) and 2) via physical association between integrins and GFRs, in which is included both the activation of integrins by GFRs to enhance mitogenic signals and the activation of GFRs by integrins in the absence of growth factors.

An example of cooperation between integrins and GFs is the MAPK pathway. In most cell types, this pathway is vital to trigger cell division through cyclin D1 expression, which promotes formation of Cdk2/cyclin E complex, allowing the cell to enter to S phase and thus proliferate. Even though Erk is induced by growth factors via GFRs, the sustained activation required to induce cyclin D expression is accomplished via integrins (**Figure 4c**). In particular, integrin activation mediates Erk translocation into the nucleus, where it exerts its mitogenic effect[97,99]. Moreover, because Erk does not have a conventional nuclear localization signal it requires anchoring proteins to regulate its distribution. It is not clear how integrin-mediated adhesion regulates Erk nuclear shuttling but the fact that paxillin and actin interact with Erk supports the idea that cytoskeleton rearrangements upon integrin activation allow Erk translocation[101,102].

12

Another example of signal transduction pathway triggered by integrin-associated complexes in response to ECM signals is the PI3K/Akt pathway. Importantly, this pathway can also be activated by tyrosine kinase receptors (TKRs) and G protein-coupled receptors (GPCRs). In the case of mechanotransduction through integrins, the regulatory p85 subunit of PI3K binds to FAK at phosphorylated Tyr397, which leads to PI3K activation[103]. Activated PI3K phosphorylates plasma membrane lipids, which then recruit and activate Akt. Akt is a serine/threonine kinase that, once activated, translocates to the cytosol and nucleus where phosphorylates downstream effectors and thus mediates cellular responses such as cell survival and apoptosi[104], proliferation[105] and migration[106] (**Figure 4d**).
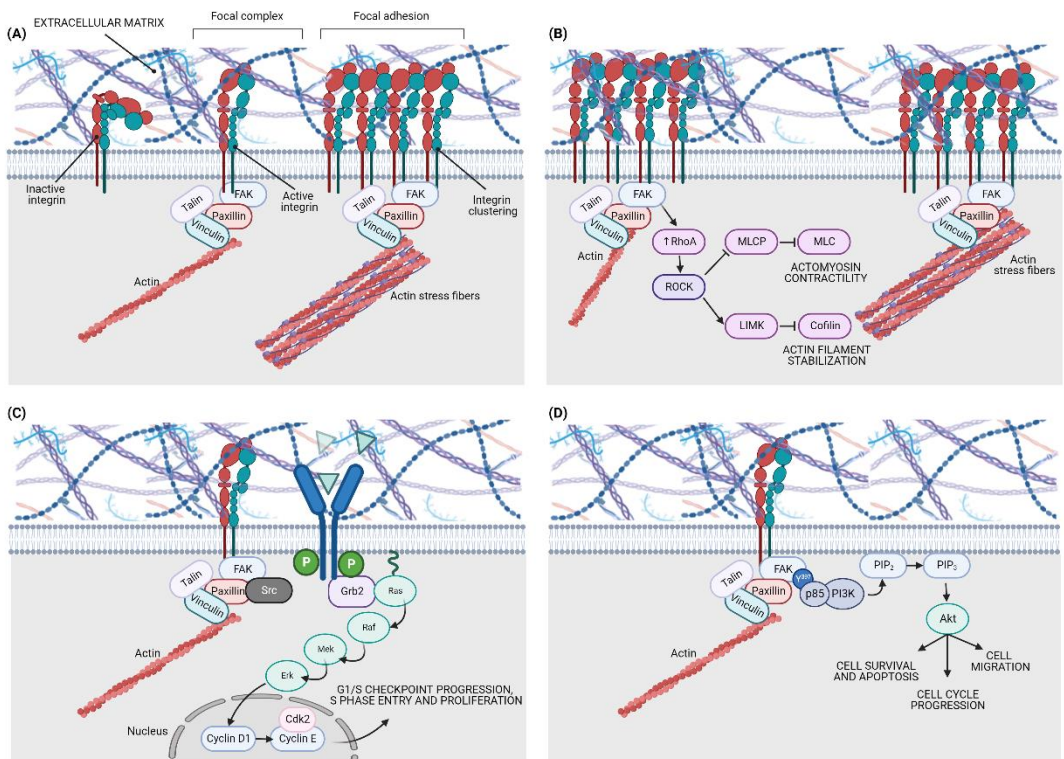
Figure 4. Integrin-mediated signaling. (a) Integrin-associated complex maturation. Integrins are activated by engagement with the ECM, forming focal complexes that can mature into focal adhesions in the presence of force; **(b)** Role of Rho/ROCK signaling pathway in signal mechanotransduction. Stiff matrices stimulate RhoA activity increase and ROCK activation, which promotes actomyosin contractility and actin filament stabilization through the phosphorylation of MLCP and LIMKP intermediate substrates; **(c)** MAPK/Erk signaling pathway via integrin cooperation; **(d)** PI3K/Akt signaling pathway via pFAK[Y397] in signal mechanotransduction. The figure was created using Biorender.

1.2.3 Influence of ECM stiffness, composition and structural organization on cell behavior

IACs dynamics are regulated in a force-dependent manner by both endogenous forces such as those generated by actomyosin contractility, and exogenous forces such as the local ECM stiffness. Changes in ECM stiffness alters the cytoskeleton and triggers signaling pathways that affect cell fate. For example, it has been described that mesenchymal stem cells (MSCs) can be differentiated into neuron-like cells when cultured on soft substrates mimicking brain tissue (0.1-1 kPa) while culturing the same cells on stiffer substrates mimicking muscle (8-17 kPa) or bone (25-40 kPa) promote myogenic and osteogenic differentiation[85].

The dynamics of integrin-associated complexes are not only influenced by the local stiffness of the ECM but also by its chemical composition[107]. On its extracellular domain, integrins recognize and bind to ECM molecules. The function of each integrin in controlling contractile forces and cell migration will depend on the specific ligand that is recognized[108]. For example, the binding of α5β1 integrins to fibronectin forms stronger cytoskeletal interactions, resulting in acceleration of cell spreading, membrane protrusions and cell migration, when compared to the binding of α4β1 integrins to VCAM-1[109]. Therefore, the chemical composition of the ECM controls the combination of integrins with specific ligands, which in turn results in a specific IAC-mediated signaling that allows the attribution of specific cellular responses.

Moreover the structural organization of the ECM in terms of ligand spacing[84,110,111] and geometry[112,113] also plays an important role on cell behavior. For example, studies using RGD-functionalized surfaces such as PEG[114] or hydrogels[115] together with microcontact printing have shown that ligand spacing, size and arrangement influence cell adhesion and motility[84,116]. Also, the application of adhesive micropattern confines cells in a specific geometry that controls cell shape and the organization of traction forces[117]. The spatial distribution of ECM ligands, and therefore the distribution of FAs also plays an important role in cell differentiation, mediating the switch in MSCs commitment toward adipogenic or osteogenic fate[118].

Finally, apart from mechanics, the ECM also confers dimensionality. Dimensional constraints on 2D substrates have been shown to influence stem cell fate, implying that the three-dimensionality of the ECM is also an important parameter in signal mechanotransduction[112].

1.2.4 ECM stiffness and remodeling in cancer progression

In healthy tissue, homeostatic mechanisms are able to preserve normal tissue mechanics and therefore, proper tissue function. However, persistent changes in ECM mechanics may lead to the development and progression of fibrotic diseases, which are characterized by an excessive matrix deposition. Fibrotic diseases include for example pulmonary fibrosis, systemic sclerosis and liver

cirrhosis, in which there is an hyperproliferation of fibroblasts and their differentiation into myofibroblasts, which synthesize and secrete excessive amounts of ECM constituents. Interestingly, some fibrotic diseases have been identified to increase the risk for malignant transformation. For example, hepatocellular carcinoma (HCC) is the most common cause of death in patients with liver cirrhosis[119] and the incidence of lung cancer is 4-fold higher in patients with idiopathic pulmonary fibrosis compared to patients with pulmonary emphysema[120]. Moreover, some types of cancer such as pancreatic ductal adenocarcinoma (PDAC)[20] are characterized by a dense and fibrotic stroma, synthesized by cancer-associated fibroblasts (CAFs). Constitutive production of collagen by activated fibroblasts promote an increase in collagen concentration, which alters not only ECM amount but also its normal composition, leading to an increase in matrix stiffness. Pulmonary fibrosis represents a clear example of how alteration in matrix composition can result in tissue stiffening. In the lung, elastin, with an elastic Young's modulus of approximately 1 MPa[121,122], represents the major ECM protein, forming a continuous network that allows a passive recoil during expiration. During pulmonary fibrosis, great amounts of collagen fibrils, which present an elastic Young's modulus in the range of 100-360 MPa[123], are deposited, leading to tissue stiffening that consequently results in dyspnea[124–126]. Thus, increased matrix deposition as well as alteration in its composition, promotes tissue stiffening that in turn modify cellular behavior and impair tissue function.

Alterations in ECM remodeling and matrix stiffening also play a crucial role in tumor development and progression. Increased matrix stiffness is a characteristic of many cancers and therefore is not surprising that clinicians often diagnose tumors by palpation based on differences in tissue rigidity. The best examples are the physical breast exam by palpation to detect breast cancer and the digital rectal examination test for the diagnosis of prostate cancer. Tumor tissues such as breast cancer[69], colorectal cancer[127], pancreatic ductal adenocarcinoma (PDAC)[128] and hepatocellular carcinoma (HCC)[129] can be several folds stiffer than their healthy counterparts (**Table 2**).

During cancer progression the ECM of tumoral cells experiments changes in composition, density, stiffness and topography. A common feature in some cancers, such as breast cancer[69], PDAC[20] and gastric cancer[130] is an increased deposition of ECM components, mainly collagen I, which is in part responsible for the increased stiffness in these tumors. Matrix stiffness promotes a malignant phenotype and enhances cell migration and invasion in a process called durotaxis, in which cells migrate from soft to stiffer regions[131–133]. Moreover, the rearrangement of randomly oriented collagen fibers, found in normal tissues, into aligned fibers has been described in tumor tissues such as breast cancer[134,135], colon carcinoma[136] and PDAC[128]. This alignment of collagen fibers has been reported to direct and enhance breast cancer cells migration *in vitro*[137], implying that ECM topography plays a significant role in cell migration and local invasion.

Table 2. Mechanical moduli of tissues under homeostatic and pathological conditions

Tissue	Pathology	Stiffness (kPa)	Modulus	Technique
Breast	Normal stroma	0.4	E	AFM[135]
	IDC	5		
	Normal fibroglandular tissue	3.24	E	Indentation[138]
	Low-grade IDC	10.4		
	Medium-grade IDC	19.9		
	High-grade IDC	42.5		
	Normal stroma	0.87	G	MRE[139]
	Breast cancer	2.9		
Thyroid	Normal Thyroid	9-11.4	E	Compressive deformation[140]
	Papillary adenocarcinoma	44-110		
Colon	Normal colon	0.93	E	Tactile sensor[127]
	Colorectal cancer	7.51		
Liver	Normal liver	2.3	G	MRE[141]
	Fibrosis	5.9		
	HCC	10.3		
	Normal liver	3.9	E	SWUE[142]
	Fibrosis	8.3		
	Cirrhosis	17		
	HCC	42		
Pancreas	Normal pancreas	2.47	G	MRE[143]
	Pancreatic cancer	6.06		
	Normal pancreas	1.06	SSM	Indentation[144]
	Pancreatitis	2.15		
	PDAC	5.46		
	Normal pancreas	1	E	AFM (Mouse model)[128]
	Pancreatitis	2		
	PDAC	4		
Prostate	Normal prostate	24.1	E	SWUE[145]
	Prostate cancer	63.6		

IDC, invasive ductal carcinoma; HCC, hepatocellular carcinoma; PDAC, pancreatic ductal adenocarcinoma; E, Elastic Young's modulus; G, Shear modulus; SSM, steady-state modulus; MRE; magnetic resonance elastography; SWUE, Shear wave ultrasound elastography. Data represent human tumors if not stated the contrary.

1.3 Taking the study of cancer to the third dimension

Organs are made up of tissues, which in turn are formed by cells that interact both with each other and with the extracellular matrix (ECM). Multicellular tissues are constituted by two types of cells: epithelial and mesenchymal cells. Epithelial cell monolayers are tightly adhered to each other by their lateral domain while laying on a specialized ECM called basal membrane. Thus, epithelial cells in monolayers are polarized cells, with an apical domain often facing a lumen (in the case of ducts, such as breast and pancreatic ducts, vessel endothelial cells or epithelial intestinal cells) (**Figure 5a**). Instead, epithelial cells might form stratified tissues, such as the skin epidermis, where cells form layers from the basal membrane to the skin surface (**Figure 5b**). At the basal domain, basal cells resting on a 2D basal membrane are covered at the apical side with differentiated epithelial cells tightly attached to each other (**Figure 5b**). In contrast, mesenchymal cells are usually arranged as individual cells embedded within a 3D ECM, also called stroma. Therefore, it could be considered that, while epithelial cell monolayers are resting on a thin basal membrane in a two-dimensional configuration, the natural configuration of mesenchymal cells is three-dimensional. Moreover, tissues and organs are also three-dimensional, but our ability to study their function and pathology *in vitro* has classically relied on two-dimensional cell cultures, usually performed on plastic surfaces.
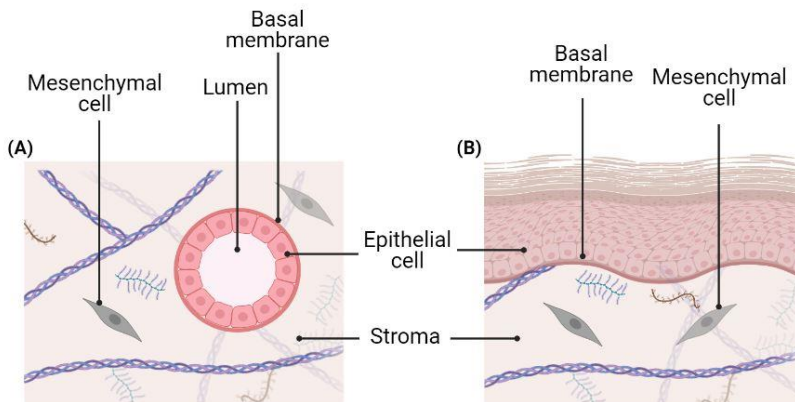
Figure 5. Organization of multicellular tissues. (a) Epithelial cells are polarized cells facing a lumen in the case of ducts or; **(b)** the outside of the body in the case of the skin epidermis that lay on a thin specialized ECM called basal membrane. Mesenchymal cells instead are embedded within an interstitial matrix called stroma. The figure was created using Biorender.

It is evident that given these complex interactions within a tissue, important biological features may be missed if they are only studied in unnatural and constraining 2D cell cultures. It has been extensively reported that cell proliferation, morphology, behavior and signaling are dramatically modified when culturing cells in 2D *versus* 3D conditions. When cancer cells are cultured in 2D monolayer, all the cells are exposed to the same oxygen and nutrients level, fact that leads to a relatively uniform proliferation rate. Nevertheless, growing the same cells in 3D spheroids induces zones of differential proliferation, with cell division occurring more rapidly in the outer part of the

spheroid[146]. This is due to the generation of molecular gradients (oxygen, nutrient and growth factors) across the 3D spheroid, which are not reproduced in 2D culture. Growing cells on 2D surfaces also results in morphology changes. Cells are forced to adhere to a stiff and flat substrate, which leads to a false apical-basal polarity and changes in cell shape, that ultimately modify cellular function[147]. For example, fibroblasts cultured in 2D present an altered cytoskeletal organization and an artificial polarity, adopting a spread-out morphology, which is not present in 3D cultures, where they adopt a bipolar or stellate morphology, similar to the seen *in vivo*[148]. Importantly, the ECM composition and configuration are strongly modified in 2D cultures, and consequently cells do not receive the proper signals that provides a normal ECM configuration[149]. Studies of gene expression and mRNA patterns also reveal differences between cells cultured in 2D *versus* 3D[150]. The culmination of these genetic changes has impact on different cell behaviors such as migration and differentiation, which are linked to the extent of tumor progression. Moreover, growing cells in a 3D environment reveals a more realistic drug response. It has been reported that 3D cultured cells are more resistant to chemotherapy, when compared to the same cells grown in 2D monolayer. Different mechanisms have been attributed to this enhanced drug resistance, but the most straightforward explanation is that the microenvironment provided by the 3D system protect the cells from drug penetration[151]. Besides, since most drugs have rapidly dividing cells as a target, those quiescent cells that exist in the inner of the 3D culture remain protected[152]. In addition, some pancreatic cancer cell lines have shown increased expression of diverse drug resistance genes in 3D culture compared to 2D culture[153]. This reveals that 3D cultured cells can recapitulate mechanisms of drug resistance found in tumors, offering therefore the opportunity to analyze these mechanisms and test multidrug therapies *in vitro* before animal experimentation. 3D cell culture can also capture the phenotypic heterogeneity found in a tumor. Finally, *in vitro* 3D cancer models allow to mimic the tumor microenvironment and manipulate each component in order to study its implications in tumor progression.

First attempts to took cancer cell biology to the third dimension were the development of multicellular spheroids. Spheroids, which are tumor cell aggregates, have been used since the 1970s to study the mechanisms of action of radiotherapy and chemotherapy as well as drug resistance[154]. 3D spheroids recreate the heterogeneity found in the *in vivo* tumor, in terms of cell growth and drug resistance. Cells within the tumor are exposed to environmental differences due to nutrient and oxygen gradients. Thus, the cells on the outside receive the most nutrients and oxygen, and therefore are under an active proliferating state. On the other hand, cells that exist in the inner part of the tumor, that is in hypoxic and nutrient depletion conditions, are found to be in a quiescent state, and often necrotic. Multicellular spheroids can recreate these molecular gradient-associated features, being a good option to test drug efficacy. Nevertheless, they have important limitations, since they grow as independent aggregates and show poor interactions with the extracellular environment[155,156].

To overcome this limitation and considering that the microenvironment has a critical role in tumorigenesis, ECM analogs, also called *scaffolds*, were introduced in 3D cell culture systems. In these systems, cells are embedded in a natural or synthetic scaffold that mimics the ECM, providing thus, the chemical, mechanical and physical cues that cells need to form physiological tissue structures *in vitro*. The scaffold properties, such as molecular composition and stiffness, will have an important

effect on cellular morphology and behavior (migration, proliferation rate and gene expression). For this reason, the selection of the scaffold is a key point when planning experiments and should depend on different factors, such as the application of the 3D model, the tumor etiology, and the concrete step of tumor progression to be recreated. Moreover, the results obtained should be interpreted in the context of each experimental design[157].

Natural scaffolds are mainly hydrogels made of natural materials or proteins, such as Matrigel[TM], collagen type I, laminin and gelatin, which provide chemical cues, principally ECM binding motifs. The advantages of natural scaffolds are their easy processing and low cost. Moreover, the structural properties of the gel, such as pore size and stiffness, can be modulated by increasing concentration or introducing chemical cross-linking compounds. However, natural scaffolds present biodegradability *in vitro*, fact that risks the maintaining of biophysical, biomechanical and structural properties along culture time. Besides, due to its natural origin, they frequently contain residual growth factors, undefined constituents or non-quantified impurities. Thus, animal-derived biomaterials present variations from batch to batch, compromising assay reproducibility[149].

The development of synthetic biomaterials could overcome the disadvantages of natural scaffolds. Synthetic scaffolds have minimal variation from batch-to-batch production, providing thus, a reproducible cellular microenvironment. Moreover, they present low biodegradability *in vitro*, fact that permits to maintain structural and mechanical properties over time. Alike natural scaffolds, structural properties, such as matrix stiffness, can be modulated by increasing concentration. The lack of chemical cues provides a non-instructive environment, making these biomaterials more challenging, since factors that drive tumor progression need to be identified and precisely incorporated. In fact, these kind of scaffolds only serve to hold the cells in the 3D space until they produce their own physiological matrix environment[158]. This limitation can be overcome functionalizing the scaffold with specific motifs and/or soluble signaling molecules.

In the last decades, polymeric scaffolds, such as poly(lactide-co-glycolide) (PLG), poly(lactic-co-glycolic acid) (PLGA)[159] and polylactic acid (PLA)[160,161] have been developed in an attempt to culture cells in 3D. These polymeric scaffolds can be functionalized with specific motifs, such as integrin binding sites and proteolytic degrading sites[162]. However, synthetic polymer's structure consists of 50-500 μm fibers and 50-100 μm pore size, which are similar in size to most mammalian cells. Thus, cells attached on microfibers are in fact in a 3D-like environment with a curvature depending on the diameter of the microfibers. Moreover, the micropores between the fibers are 1,000-10,000-fold greater than the size of biomolecules, and consequently, diffuse away very quickly. Therefore, to culture cells in a truly 3D environment, the fibers and pores must be of around 1,000 fold smaller than cells[163].

Finally, the recent advancements in biomaterial science, biofabrication and microfluidics has facilitated the generation of more complex 3D models including 3D bioprinting, tumor-on-chip platforms and organoids (**Figure 6**). For example, 3D bioprinting allows to accurately control the arrangement of cells in three dimensions to mimic the native tissues, which can overcome the lack of architectural control found in scaffold-based 3D cultures[164]. Even more complex is the generation of microfluidic platforms, also called organ-on-chip systems. These platforms have been developed to

mimic physiological functions of an organ or tissue in a controlled environment (chip). This chip consists of engraved structures such as interconnected channels or chambers that allow cell growth in a very defined space. Moreover, chips are usually combined with a controlled fluid flow, which makes them a very appropriate system to mimic the systemic administration of therapeutics in the blood stream as well as the blood flow within organs. Finally, organoids have received a lot of attention due to their potential to develop 3D organ-like structures that resemble key biological features and relevant tissue development[164]. Tumor organoids are multicellular systems established from tissue-derived cells that are embedded into a 3D environment such as Matrigel[165]. It has been shown that long-term organoid cultures can be stablished from a variety of primary cancer biopsies such as colon, stomach, liver, breast and pancreas[166,167]. Significantly, tumor-derived organoids have shown to resemble the tumor epithelium they were derived from.
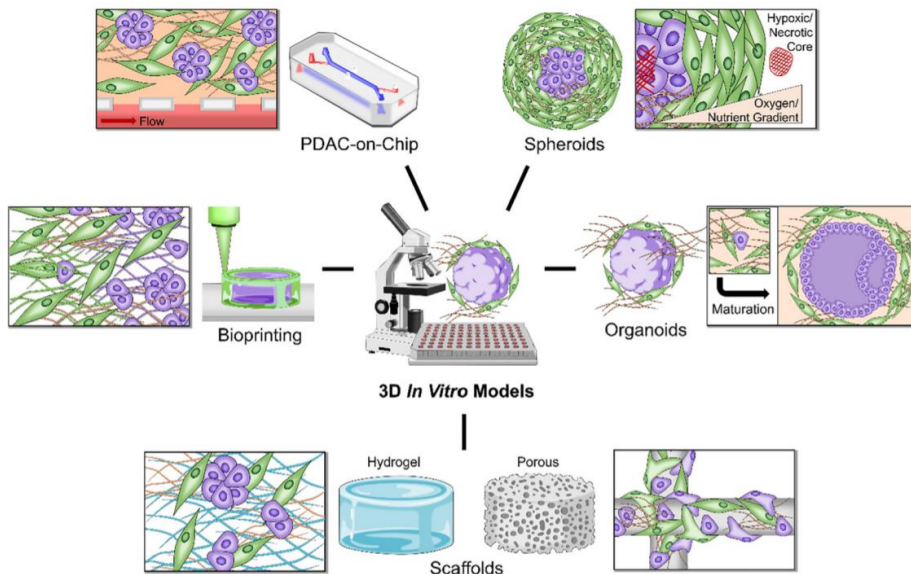
Figure 6. 3D in vitro models to mimic the tumor microenvironment. Different approaches to create 3D in vitro models can be classified in cell-based approaches (spheroids and organoids) and engineering-based approaches (organ-on-chip, bioprinting and scaffolds). Extracted from[164].

In summary, cancer cells, as well as normal cells, require cues from a 3D environment to form tissue structures *in vitro* that can more accurately resemble the *in vivo* environment. Three-dimensional cultures, and specially scaffold-based models, provide another dimension for external mechanical inputs, cell adhesion, and the generation of molecular gradients[168]. Therefore, cells grown in 3D cultures are in a more physiological environment compared to 2D cultures, excepting for epithelial cell cultures on appropriately designed 2D substrates that could mimic the basal membrane in terms of stiffness and signaling, among others.

1.4 Self-assembling peptides as scaffolds for 3D culture

In the last years, peptide nanofibers have emerged as a synthetic alternative to polymeric scaffolds for 3D cell culture. Synthetic peptide nanofibers are characterized by 10 nm fibers and 5-200 nm pores in diameter (1,000 times smaller than cells). Thus, the main advantage of culture cells in peptide scaffolds is that they experience a truly 3D environment. Moreover, the constituents of these biomaterials are well defined and do not present variations from batch-to-batch. Peptide nanofibers contain biologically inspired sequences, with the most relevant examples being peptide amphiphiles[169], β-hairpin peptides[170], and self-assembling peptides[163]. Inspired by tandem repeats found in natural proteins, such as the sequence EAK16 in the yeast protein Zuotin[171] or Lysβ-21 in the egg white Lysozyme[172], a new generation of self-assembling peptides such as DN1[172] RAD16-I[163] and KLD12[173] were rationally designed.

The self-assembling peptide RAD16-I has been used in this work as a scaffold for 3D cell culture. RAD16-I is a short peptide constituted by the sequence AcN-RADARADARADARADA-CONH$_2$ (R arginine, A alanine, D aspartic acid) which alternates hydrophilic and hydrophobic amino acids. The peptide undergoes self-assembly into a nanofiber network with antiparallel β-sheet configuration by increasing ionic strength or adjusting pH to neutrality (**Figure 7**).

The nanoscale architecture of the fiber network (around 10 nm diameter and 50-200 nm pore size, a thousand times smaller than mammalian cells) allows the cells to experiment a truly 3D environment. Besides, biomolecules in such nanoscale environment diffuse slowly and are likely to establish a local molecular gradient. Non-covalent interactions allow cell growth, migration, contact with other cells, shape changes and a properly exposition of membrane receptors. Moreover, since stiffness can be controlled by changing peptide concentration these hydrogels can be tuned up to embed cells but not to entrap them[174].

Since the peptide scaffold does not contain signaling motifs, the environment can be considered non-instructive, from the point of view of cell receptor recognition/activation. On the other hand, the self-assembling peptide can be modified with signaling motifs, such as ECM ligands for cell receptors. In fact, this peptide has been functionalized through solid-phase synthesis extension at the C-termini with short peptide sequences to trigger different cellular responses[158,175].

A) AcN-RADARADARADARADA-CONH$_2$

B)
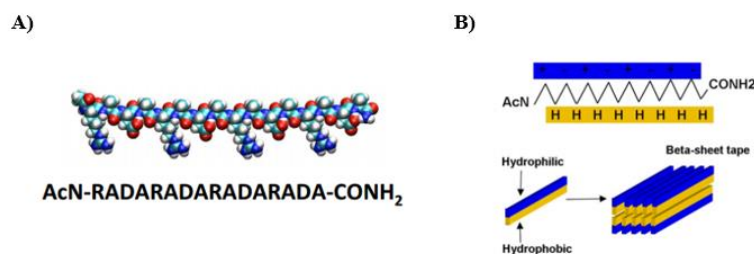
Figure 7. The peptide RAD16-I self-assembles into a network of nanofibers. (a) Molecular model of peptide RAD16-I. R= Arg; A=Ala; D=Asp; **(b)** Molecular model of the nanofiber developed by self-assembling RAD16-I molecules. The nanofiber is formed by a double tape of assembled RAD16-I molecules in antiparallel β-sheet configuration. Adapted from[176].

This peptide scaffold has been proved to promote cell adhesion[177], phenotype maintenance[178], differentiation[178,179] and proliferation[180,181] of a variety of mammalian cells. For example, RAD16-I has been used to promote chondrogenic[182], osteogenic[183], adipogenic[183] and cardiac[184] differentiation of adult stem cells. Also, culture of rat liver-derived progenitor cells in RAD16-I promoted its differentiation into functional hepatocytes[185]. Moreover this peptide scaffold has been modified by adding biologically active sequences from proteins of the extracellular matrix such as laminin and fibronectin to modulate cell response[158,178,186].

1.5 In vitro models to study the effect of matrix stiffness on cell behavior

Matrix stiffness influences cell fate and behavior, and therefore this parameter should be appropriately adjusted when performing experiments. For example, while soft substrates promote MSCs differentiation into neurons, stiffer ones support myogenic and osteogenic differentiation[85]. Stiffness plays a key role in tumor initiation and progression, and in the last years, scientists have started to incorporate and adjust this parameter when developing cancer models.
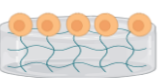
In vitro models to assess the influence of stiffness include both 2D and 3D culture systems (**Table 3**). 2D models include cell seeding on top of polyacrylamide (PA) gels of varying stiffness coated with different ECM proteins such as collagen[187], fibronectin[128,188,189] and reconstituted basal membrane (rBM)[190], or seeding directly on top of natural collagen matrices[191,192]. The principal advantage of using coated-PA gels is that they allow to increase the substrate stiffness without increasing the number of biological signals (e.g., adhesion sites), contrary to natural matrices such as collagen I and rBM. The stiffness of these natural matrices is usually increased by increasing concentration, which also increases ligand density.
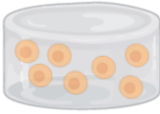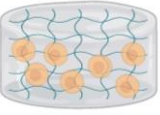
On the other hand, three-dimensional models include cell encapsulation within polymeric matrices, usually functionalized with RGD or MMP-cleavable motifs[193–196], or ECM-like matrices such as Collagen type I[191,197,198], basal membrane extracts[197,199] and alginate[200–202]. Moreover, spheroid embedment in 3D matrices are useful platforms to study cell migration and matrix invasion[203–206]. In these last ones, cell spheroids are made without any scaffold, using for example the hanging drop method, low-binding or agarose-coated well plates. Once stablished, spheroids are transferred to a 3D matrix.

Cancer models including stiffness as a parameter have demonstrated that it can regulate epithelial-to-mesenchymal transition (EMT)[128,188,190,200,207], resistance to chemotherapy[187,196,203], cell proliferation[187,191,195,196,200], migration[189,199,202] and invasion[203–206] (**Table 3**). Importantly, results should be interpreted in the context of each experimental design, considering not only the stiffness range but also other parameters such as the type of three-dimensional matrix used and temporality[208]. For example, increased stiffness have shown to promote proliferation in natural scaffolds such as collagen type I[191,198] and alginate/Matrigel[200], while it restricts proliferation in cells cultured in polymeric scaffolds[195,196]. Also, studies using synthetic matrices in a physiological stiffness

range (0 – 20 kPa) reported that invasion is mostly promoted with increased stiffness, but it is inhibited at nonphysiological higher stiffness (>20 kPa)[208]. Also, matrix stiffness has been shown to delay cell invasion[206], and therefore, studies with short endpoints[204] may not reflect the actual infiltration of cancer cells at later points, and therefore this studies likely not repot that stiffness promotes invasion[208].

Table 3. In vitro models to study the effect of matrix stiffness on cancer cells

Culture model	Biomaterial	Stiffness (Pa)	Tissue	Cell line	Main conclusions
2D on top of ECM protein-coated polyacrylamide	Collagen type I-coated PA	1,000 – 12,000 (Shear modulus)	HCC	Huh7, HepG2	Increasing stiffness promotes cell spreading, proliferation and chemotherapeutic resistance to cisplatin[187]
	Fibronectin fragment variants (FnIII9-10)-coated PA	2,000 – 32,000 (Elastic modulus)	Alveolar epithelium	RLE-6TN	Both the biochemical (fibronectin conformation) and mechanical (stiffness) signals from the microenvironment play a role in activating the EMT program. Either the ligand or the compliance can overcome the effect of the other[188]
	Fibronectin, rBM and Collagen type I-coated PA	400 – 60,000 (Elastic modulus)	Breast, kidney	NMuMG MDCK	Matrix rigidity regulates a PI3K/Akt-mediated switch in TGF-β–induced cell functions. TGF-β1 induces apoptosis of epithelial cells in compliant substrates, while promotes EMT in rigid substrates[190]
	Fibronectin-coated PA	1,100 – 33,700 (Young's modulus)	HCC	HCCLM3, L02	Migration of hepatocellular carcinoma cell line M3 and hepatic L02 cells was higher in intermediate stiffness (10.7 kPa) than in stiffer substrates (33.7 kPa)[189]
	Collagen type I-coated PA in a 3D Matrigel overlay[209,210]	150 – 5,700 (Elastic modulus)	Breast cancer	MCF10A, Eph4Ras	Increasing matrix stiffness activates EMT, tumor invasion, and metastasis through the EMT-inducing transcription factor TWIST1[207]
	Fibronectin-coated PA	1,000 – 25,000 (Young's modulus)	PDAC	BxPC-3, AsPC-1, Suit2-007	Matrix stiffness promotes elements of EMT such as increase in vimentin expression and nuclear localization of β-catenin and YAP/TAZ[128]
2D on top of ECM-like matrix	Collagen type I	4,000 – 17,000 (Shear modulus)	Breast	NMuMG	Cellular protrusions and pFAK^Y397-positive focal adhesions area increase as a function of substrate stiffness. Cells on soft substrates present cortical actin localization while stress fiber formation occurs on stiff

				substrates, suggesting a role for Rho in the cellular response to physical stimuli[191]
	Collagen type I	35 – 65 (Young's modulus)	Breast cancer	MDA-MB-231, MCF-7	Collagen fibril diameter and not pore size is shown to be the major determinant of cell morphology, cluster formation and invasion capacity. Increasing fibril diameter increases invasiveness and decreases cell clustering, independently of overall pore size[192]
3D cell embedment in polymeric matrix	PEG-RGDS PEG-PQ	21,000 – 55,000 (Elastic modulus)	Lung adenocarcinoma	344SQ	Epithelial structures were more organized (lumen formation, sphere development and polar organization) in stiff than soft matrices[193]
	PEG functionalized with CRGD, MMP-cleavable sequence and HA	1,000 – 26,000 (Elastic modulus)	Glioblastoma	U87	Matrix stiffness induces differential ECM deposition and remodeling though different HAS and MMPs[194]
	PEG	1,000 – 3,000 (Shear modulus)	PDAC	COLO-357	Cell proliferation and spheroid formation is restricted by increased stiffness[195]
	PEG/Gelatin IPNs	270 – 1,300 (Elastic modulus)	Fibrosarcoma	HT1080	Soft matrices enhanced cell proliferation and resistance to 5-FU compared to stiff environments[196]
3D cell embedment in ECM-like matrix	Matrigel	10 – 50 (Storage modulus)	Prostate carcinoma	DU-145	Cell migration speed in Matrigel is maximum at intermediate stiffness, but maximal cell movement shifts to low stiffness matrices when integrin-mediated cell-matrix interactions are blocked[199]
	Collagen type I	10,000 – 44,000 (Elastic modulus)	Breast cancer	NMuMG, MCF10A, T47D, MDA-MB-231	Stiff matrices promote proliferation in an Erk-dependent manner via FAK/Src activation[191]
	SAP RAD16-I/Laminin or rBM	120 – 1200 (Young's modulus)	Breast	MCF10A	Laminin-supplemented soft SAP gels support epithelial morphogenesis and direct apical-basal polarity. Increased stiffness perturbs epithelial morphogenesis, disrupts apical-basal polarity and induces the expression of genes involved in tumor progression and invasion[211]
	Type I oligomeric	100 – 1,000	PDAC	BxPC-3, PANC-1,	At matched stiffness, Oligomer promotes EMT and

24

	collagen (Oligomer), Matrigel	(Shear Storage modulus)		MiaPaCa-2	Matrigel MET. Increased Oligomer density induces confined clustered growth due to spatial constraints and stiffness[197]
	Collagen type I	120 – 590 (Elastic modulus)	Gastric cancer	AGS, MKN74	Integrin-mediated mechanotransduction pathways are activated by alterations in ECM density, thus increasing downstream FAK and ERK signaling[198]
	Alginate/Matrigel IPNs	30 – 310 (Young's modulus)	Lung adenocarcinoma	A549, Thp-1	Increased ECM stiffness promotes cell proliferation and invasiveness. The presence of tumour-associated macrophages and the ECM stiffness together contribute to an invasive phenotype, and modulate the expression of key EMT-related markers[200]
	Alginate/rBM IPNs	400 – 2,000 (Elastic modulus)	Breast cancer	MCF10A	YAP is responsible for mechanotransduction in stiff 2D cultures, but not in 3D cultures, regardless of the stiffness[201]
	Alginate/rBM IPNs	400 – 9,300 (Elastic modulus)	Breast cancer	MDA-MB-231	Increased matrix stiffness limits invadopodia formation and cell migration of invasive breast cancer cells[202]
3D spheroid embedment in ECM-like matrix	Collagen type I	300 – 6,000 (Shear modulus)	Breast cancer	MDA-MB-231	Increasing matrix stiffness results in greater resistance to paclitaxel treatment while decreases invasiveness[203]
	Collagen type I, BME	3 – 350 (Storage modulus)	Breast cancer	MDA-MB-231	Cell invasion decreases with increasing collagen concentration, while cells fail to invade BME matrices regardless of the stiffness[204]
	GelMA/Collagen IPNs	2,000 – 12,000 (Shear modulus)	Breast cancer	MDA-MB-231	Cells in GelMA require collagen fibers to invade the matrix regardless of the stiffness. Increased stiffness decreases cell invasion independently of collagen content[205]
	GelMA/Collagen IPNs	2,000– 12,000 (Shear modulus)	Breast cancer	MDA-MB-231	Stiffness delays cell invasion but at the same time activates intracellular signaling pathways by which tumor cells modify the microenvironment to a permissive state[206]

BME: Basal Membrane Extract, ECM: Extracellular Matrix, EMT: Epithelial-to-Mesenchymal Transition, GelMA: Gelatin-methacrylate, HA: Hyaluronic Acid, HAS: Hyaluronic Acid Synthase, HCC: Hepatocellular Carcinoma, IPNs: Interpenetrating Polymer Networks, MDCK: Madin–Darby canine kidney epithelial cells, MEC: Mammary Epithelial Cell, MMP: Matrix Metalloproteinase, NMuMG: Normally murine mammary gland cells, PA: polyacrylamide, PEG: Poly(ethylene glycol), rBM: reconstituted Basal Membrane, SAP: Self-Assembling Peptide.

1.6 Content of dissertation

This thesis has been executed in the context of a project granted to our group by the Programa Estatal de I+D+i Orientada a los Retos de la Sociedad "Dual Tyrosine Kinase Inhibitors in Pancreatic Cancer: Virtual Screening, Synthesis, *in vitro* (2D and 3D) and *in vivo* Biological Testing, (PANCTKI, RTI2018-096455-B-I00). The main objectives of this project were **(1)** to obtain multi-target inhibitors of kinases involved in pancreatic cancer (*Synthesis laboratory, Organic Chemistry Dept., IQS; headed by Dr José Ignacio Borrell*), **(2)** to synthesize novel multi-target tyrosine kinase inhibitors as drug candidates for the treatment of pancreatic cancer (*Synthesis laboratory, Organic Chemistry Dept., IQS*), **(3)** to develop a new *in vitro* 3D tumor model for the evaluation of the drug candidates (*Tissue Engineering laboratory, Bioengineering Dept., IQS; headed by Dr Carlos E. Semino*) and *in vivo* confirmation studies using preclinical orthoxenografts (*Group of Chemotherapy and Orthotopic xenografts, Institut Català d'Oncologia (ICO); Dr Alberto Villanueva*).

This thesis is framed in the context of the third objective of PANCTKI. In this work, 3D in vitro models to study different aspects of pancreatic ductal adenocarcinoma (PDAC) have been developed. In particular, we have deconstructed the extracellular milieu in three main parameters, being dimensionality (2D *vs* 3D), stiffness (soft *vs* stiff) and signaling (synthetic *vs* natural scaffolds), and we explored the contribution of each one in triggering different cell responses such as cell proliferation, drug resistance and signal mechanotransduction.

We first focused on developing a 3D model to test the anti-cancer activity of tyrosine kinase inhibitors (Chapter 3). With this model, we explored the contribution of the extracellular environment (dimensionality and stiffness) in activating drug resistance mechanisms. We selected the EGFR as a model of tyrosine kinase receptor (TKR) and the commercially available drug erlotinib as its specific inhibitor. The expression of the receptor was analyzed at a protein level in 3D cultures in the presence and absence of both ligand (EGF) and inhibitor, and compared to conventional 2D cultures. Results reflected the capacity of cancer -but not normal- cells to acquire molecular mechanisms which could help them to escape from drug action in 3D cultures. Importantly, this model could be used to test other experimental drugs targeting TKRs.

In the next chapter (Chapter 4), we studied the relationship between tumor cells and their biomechanical environment in terms of matrix stiffness. In this section of the thesis, we used both synthetic and natural 3D matrices, as the degradation that the latter ones may suffer during culture time could drastically affect the local stiffness, and therefore, cell response. In particular, we analyzed the effect of matrix stiffness in terms of focal adhesion kinase (FAK) activation, as this protein has been widely reported to sense the stiffness of the environment and participate in signal mechanotransduction pathways. We also tested the ability of RAD16-I, which provides a non-instructive environment, to allow FAK activation via integrin binding. Our results showed the ability of this synthetic matrix to promote signal transduction, probably through protein adsorption to RAD16-I fibers, which decorated the matrix and allowed cell adhesion and receptor activation.

1.7 Hypothesis and general aims

The main motivation of this thesis was to develop in vitro three-dimensional (3D) models to study different aspects of pancreatic ductal adenocarcinoma. Our hypothesis was that 3D cultures could recapitulate some aspects of PDAC better than conventional 2D cultures, and thus fulfill the need for more reliable in vitro approaches for cancer research. Thus, by using 3D matrices of different composition and stiffness values we were able to deconstruct the complex tumor microenvironment in three basic parameters: dimensionality, stiffness and biological signaling.

The general aims for this thesis were the following:

(1) To develop a 3D cell model to study drug resistance to tyrosine kinase inhibitors in PDAC cells (Chapter 3)

(2) To develop a 3D cell model to study the effect of matrix stiffness on PDAC cells (Chapter 4)

Chapter 2. Materials and Methods

2.1 Two-dimensional cell culture

The human pancreatic ductal adenocarcinoma cell lines BxPC-3 (EP-CL-0042, Elabscience), PANC-1 (CRL-1469, ATCC) and MiaPaCa-2 (85062806, ECAAC), the breast cancer cell line MCF-7 (EP-CL-0149, Elabscience) and primary human normal dermal fibroblasts (hNDF) (C-12302, Promocell), were cultured at 10,000 cells/cm^2 for no more than 15 passages in DMEM (DMEM-HXA, Capricorn) or RPMI (RPMI-XA, Capricorn) in the case of BxPC-3, supplemented with 10% Fetal Bovine Serum (FBS) (S1810; Biowest), L- glutamine (X055, Biowest) and Penicillin/Streptomycin (P/S) (L0022, Biowest). Cultures were maintained at 37 ºC and 5% CO_2 in a humidified atmosphere.

2.2 Three-dimensional cell culture in RAD16-I

Three-dimensional (3D) cell cultures were prepared using the synthetic self-assembling peptide scaffold RAD16-I[212], commercially available as PuraMatrix[TM] (354250, Corning). The peptide stock (1% in water) was diluted to a final concentration of 0.3% (v/v) in 10% (w/v) sucrose (S0389, Sigma) or maintained at 1% (stock), and sonicated for 30 min. Meanwhile, cells were harvested by trypsinization and resuspended to 4·10^6 cells/mL in 10% (w/v) sucrose, which is an isotonic and non-ionic medium that avoids peptide spontaneous assembly during the encapsulation process. The cell suspension was then mixed with an equal volume of 0.3% or 1% RAD16-I peptide solution to obtain a mixture of 2·10^6 cells/mL and 0.15% (soft) or 0.5% (stiff) RAD16-I. Next, 40 µL of cell/peptide suspension (80,000 cells) were loaded into wells of a 48-well plate previously filled with 500 µL of culture medium, which induced the peptide spontaneous self-assembly. The plate was left in the flow cabinet for 20 min to let the peptide gel and then placed in the incubator for 1 h. Medium was changed twice to favor the leaching of sucrose. 3D cultures were maintained in DMEM or RPMI supplemented with 10% FBS, L-glutamine and P/S at 37 ºC and 5% CO_2 in a humidified atmosphere and medium was changed three times per week. Cells were cultured for 6 days to ensure adaptation to the 3D environment before being incubated with drugs and/or processed for protein extraction and western blot, MTT assay or immunofluorescence staining.

2.3 Three-dimensional cell culture in Collagen type I

Three-dimensional cultures (3D) cultures were prepared using high concentration rat tail Collagen I (10 mg/mL, 354249, Corning) at a final concentration of 1.5 mg/mL or 5 mg/mL. Collagen I was mixed with Phenol red and PBS (**Table 4**), and brought to alkalinity using NaOH, maintaining the solution in ice to avoid collagen gelation. Cells were harvested by trypsinization and resuspended to 5·10^6 cells/mL in 1x PBS. Then, the cell suspension was mixed with the collagen solution (**Table 4**), and 40

µL of the mixture (80,000 cells) were loaded into 24-well plates. Collagen constructs were left gelling for 40 min in the incubator (37 ºC). Medium was then added to the wells, and cultures were placed in the incubator overnight. Next day, 3D constructs attached to the bottom of the well were released with a cell lifter. Medium was changed three times per week. Cells were cultured for 6 days to ensure adaptation to the 3D environment.

Table 4. Protocol for preparing collagen gels at different concentrations from a 10 mg/mL stock collagen

Final collagen concentration	Collagen	10x PBS	1x PBS	Phenol red	NaOH	Cells ($5·10^6$ cells/mL)	Final volume
1.5 mg/mL	75 µL	50 µL	125 µL	2 µL	2 µL	125 µL	500 µL
5 mg/mL	250 µL	50 µL	-	2 µL	2 µL	125 µL	500 µL

2.4 Protein binding to RAD16-I gels

To test protein binding to cell-free RAD16-I gels, 100 µL of a 0.3% solution were loaded into tissue culture inserts, gelled for 1 h with 10% FBS in PBS or PBS alone (negative control), and then washed with PBS overnight for several times. Gels were disrupted in RIPA buffer and bound protein content was quantified with a BCA assay (39228, Serva). To test collagen binding to RAD16-I gels, 10 µL of a 3 mg/mL collagen solution (A1048301, Gibco) were mixed with 90 µL of 10% sucrose and afterwards mixed with an equal volume of a 0.6% RAD16-I peptide solution. 40 µL of this solution were induced to self-assemble with PBS for 1 h, and then washed with PBS overnight for several times. Gels were disrupted by vortexing in 2x SDS sample loading buffer (LC2676, ThermoFisher), mixed with β-mercaptoethanol at 10% final concentration and boiled for 5 min at 95 ºC. Samples (20 µL) were loaded in 10% Tris-Glycine pre-cast protein gels (XP00105BOX, ThermoFisher) and run by applying 120 V for 90 min. Finally, gels were stained with Coomassie blue and distained overnight.

2.5 Drug incubation

For 2D assays, cells were seeded at 10,000 cells/cm^2 and drugs were added on the following day. For 3D assays, cells were cultured for 6 days before adding the drug. In both 2D and 3D conditions, cells were incubated with 50 µM erlotinib and 10 ng/mL EGF for 16 h. To inhibit lysosome and proteasome degradation, cells were pre-treated for 8 h before erlotinib treatment with 600 nM bafilomycin A1 (SML1661, Merck) or 10 µM MG-132 (M7449, Merck), respectively. To inhibit MMP activity, 10 µM GM6001 (sc-203979, scbt) was added to culture medium 24 h after cell embedding in collagen gels*.*

2.6 MTT assay

MTT [3-(4,5-dimethylthiazol-2-yl)-2,5-diphenyltetrazolium bromide] (M5655, Sigma) was used to assess cell viability in 2D and 3D cultures. Cell culture medium was aspirated and 200 μL (2D) or 500 μL (3D) of MTT reagent were added to a final concentration of 0.5 mg/mL in culture medium. Samples were incubated for 2 h (2D) or 3 h (3D) at 37 ºC and 5% CO_2 in a humidified atmosphere. MTT solution was then removed and cells were lysed with 200 μL of DMSO (D8418, Sigma). Absorbance was read at 570 nm using a microplate reader (Biotek Epoch™).

2.7 Immunofluorescence

Cells in 2D and 3D cultures were fixed with 3.7% formaldehyde in PBS containing tyrosine phosphatase inhibitor (ab201113, abcam) at 1:100 for 15 min and washed with 1x PBS. Cultures were blocked with 5% BSA/0.1% Triton X-100 in PBS for 1 h (2D cultures) or 2 h (3D cultures) and incubated overnight at 4ºC with the primary antibodies diluted in 1% BSA. Next, samples were extensively washed with 1% BSA and incubated for 2 h with secondary antibodies. Finally, samples were counterstained with Phalloidin-TRITC and DAPI for cytoskeleton and nuclei visualization. Pictures were acquired with Leica Thunder Imager widefield microscope coupled to a Leica DFC9000 GTC sCMOS camera, using an APO 63x objective. Images were processed and analyzed with ImageJ software[213].

2.8 Image analysis

For colocalization analysis, Manders' coefficients were calculated. Manders' coefficients are an overlapping parameter that describe the proportion of channel A signal coinciding with channel B over the total A intensity (M_1) and the proportion of channel B signal coinciding with channel A over the total B intensity (M_2)[214]. This coefficient ranges from 0 (no overlapping) to 1 (total overlapping). Manders' coefficients are very sensitive to noise, and for this reason, background needs to be set to zero. Moreover, to calculate Mander's coefficients it is important to establish a threshold for segmentation. The analysis was performed using ImageJ software[213]. Each channel was processed for background subtraction and filtered using Median and Gaussian Blur to reduce the presence of noise. Images were then segmented by thresholding using the Default option and the resulting binary images were cleaned with the Erode and Open functions. Binary images were then used as masks to sample the denoised images using the Image Calculator function with the Min operator, creating a background-less image for each channel[215]. Finally, Manders' colocalization coefficients were calculated using JACoP (Just Another Colocalization Plugin) version 2.0[216] setting the threshold values

to 1. Coefficients were obtained from at least 5 images (n>5) containing 5-10 cells per colony in the case of tumor cells or single cells in hNDF.

2.9 Western blot

2D cultures and 3D constructs were lysed with RIPA buffer (R0278, Sigma) containing protease inhibitor cocktail (11836153001, Roche) and phosphatase inhibitors (ab201113, abcam) at 1:100. Total protein content was quantified with a BCA protein assay kit (39228, Serva) and 5 µg of protein were loaded into polyacrylamide gels and run by applying 120 V for 90 min. Afterwards, proteins were transferred to a PVDF membrane (IPVH07850, Merck) by applying 40 V for 2 h. The membrane was then blocked for 1 h with 4% (w/v) nonfat powdered milk in 0.2% PBS-Tween (for non-phosphorylated proteins) or 5% BSA in 0.1% TBS-Tween (for phosphorylated proteins). Next, the membrane was incubated with primary antibodies for 1 h at room temperature or overnight at 4 ºC. The membrane was then washed and incubated with secondary antibodies for 1 h at RT. Finally, the membrane was revealed for HRP detection with a SuperSignal West Pico Chemiluminescent Substrate (34080, Thermo Scientific). Chemiluminescent images were taken in the ImageQuant™ LAS 4000 mini (GE HealthCare). Protein bands were quantified using ImageJ software and expressed as a ratio between the protein of interest and the loading control. Each blot was repeated three times (N=3).

2.10 Antibodies

The antibodies used in this work together with its respective dilution for each application (immunofluorescence or western blot) are described in **Table 5**.

Table 5. Antibodies and its respective dilution used for each application

Antibody	Dilution	Application	Company	Reference
rabbit α EGFR	1:1,000	IF	Invitrogen	700308
		WB		
mouse α integrin β1	1:500	IF	abcam	ab24693
mouse α LAMP1	1:150	IF	Invitrogen	14-1079-80
mouse α EEA1	1:500	IF	Invitrogen	14-9114-80
rabbit α pFAK^{Y397}	2:500	IF	Invitrogen	700255
	1:1,000	WB		
rabbit α pFAK^{Y861}	2:500	IF	Invitrogen	44-626G
rabbit α FAK	1:500	WB	Invitrogen	AHO0502
rabbit α vinculin	2:500	IF	Invitrogen	700062
	1:1,000	WB		
mouse α Fibronectin	1:500	IF	Invitrogen	14-9869-80
mouse α pErk1/2^{T202,Y204}	1:500	WB	Invitrogen	14-9109-80
rat α Erk1/2	1:1,000	WB	Biolegend	686902
mouse α GAPDH	1:2,000	WB	Biolegend	649201
Donkey α mouse-Alexa488	1:500	IF	abcam	ab150105
Goat α rabbit-Alexa647	1:500	IF	abcam	ab150079
Donkey α mouse-HRP	1:1,000	WB	abcam	ab6820
Goat α rabbit-HRP	1:1,000	WB	abcam	ab672a1
Goat α rat-HRP	1:1,000	WB	Biolegend	405405

2.11 Statistics

Data is presented as mean ± Standard Deviation. Conditions were tested in triplicate (n=3) in three independent experiments (N=3). Statistical differences were analyzed with GraphPad Prism 6 by one-way or two-way ANOVA followed by Tukey's multiple comparisons test. Statistical differences were indicated as * for $pv<0.05$, ** for $pv<0.01$, *** for $pv<0.001$ and **** for $pv<0.0001$.

Chapter 3. Development of 3D models to study drug resistance to tyrosine kinase inhibitors in PDAC

3.1 Background

The Epithelial Growth Factor Receptor (EGFR) is a tyrosine kinase receptor (TKR) that participates in many biological processes such as cell proliferation, differentiation and motility, under both physiological and pathological conditions. Overexpression and/or hyperactivation of the EGFR is a hallmark of many epithelial cancers such as breast, lung, colon and pancreatic cancer, and therefore EGFR is a target for cancer treatment. EGFR inhibitors can be classified as small molecules tyrosine kinase inhibitors (such as erlotinib, gefitinib and lapatinib) or monoclonal antibodies (such as cetuximab and panitumumab)[217].

Autophosphorylation and activation of the EGFR is triggered by ligand binding, which initiates signaling cascades at the plasma membrane. Complete activation of the EGFR as well as termination of its signaling depends on its internalization into endosomes and intracellular trafficking[218]. EGFR can also be internalized due to different stresses such as UV irradiation[219], hypoxia[220,221] and oxidative stress[222]. The internalization mechanism of EGFR as well as whether the receptor is subsequently degraded in lysosomes or recycled to the membrane will depend on the type of stimulus. For example, EGF binding induces ubiquitin-dependent lysosomal degradation of the receptor and a partial recycling to the membrane[223], while TGFα ligand induces endocytosis and a rapid recycling[223,224]. Other stresses such as UV radiation, serum starvation or cisplatin treatment trigger internalization and arrest in nondegradative endosomes [218]. Tyrosine kinase inhibitors (TKIs) have also been described to promote EGFR trafficking in cancer cells. For example, gefitinib induces EGFR endocytosis and non-degradative endosomal arrest[225] as well as mitochondrial translocation[226] in glioblastoma cell lines. However, EGFR internalization due to TKIs exposure may be cell type-dependent, since other works report that gefitinib inhibits endocytosis in non-small cell lung cancer cell lines[227]. In contrast, the monoclonal antibody cetuximab has been shown to induce EGFR degradation[228], its sorting to the endoplasmic reticulum and nucleus[229], and mitochondrial translocation of the truncated form EGFRvIII[228].

Two-dimensional cell cultures have been used for many years to study not only EGFR trafficking mechanisms in normal and cancer cells, but also as a model to study cell physiology and pathophysiology in general. However, it has been widely demonstrated that 2D cultures do not recreate the microenvironment in which normal cells exist, and neither the milieu of solid tumors. In such 2D conditions, cells are forced to adhere to a flat and stiff substrate which results in morphological changes that ultimately modify cellular function[149]. Moreover, molecular gradients are not reproduced and cells along the 2D surface are exposed to the same nutrient, oxygen and drug levels, while cells within a tumor are exposed to a large gradient of concentration as molecules diffuse from blood vessels[230]. It is also important to note that ECM composition and configuration are strongly modified in 2D cultures, and consequently cells do not receive the proper signals that a normal ECM configuration provides[149]. Three-dimensional (3D) cancer cell models allow to better mimic the tumor microenvironment and manipulate each component in order to study its implications in tumor

39

progression[231,232]. In this sense, extracellular matrix analogs, also called scaffolds, have become very popular among researchers[157]. Biomaterial scaffolds permit not only cell-cell but also ECM-cell interactions, and also provide the chemical, physical and mechanical cues needed for cells to form tissue structures *in vitro*[149].

The selection of the type of scaffold is a key point when planning experiments and different factors such as the application of the 3D model, the tumor etiology and the concrete step of tumor progression to be recreated should be considered. For example, scaffolds from natural origin such as collagen are typically used to study cancer cell migration and invasion[233–235]. On the other hand, polymeric scaffolds such as poly(vinyl alcohol), poly(ethylene oxide terephthalate) (PEOT) and poly(butylene terephthalate) (PBT) have been used to investigate the influence of the scaffold architecture on pancreatic cancer cell growth and behavior, permitting thus to create stage-specific pancreatic cancer models[236]. Moreover, when working with 3D cell culture, it is important to interpret the obtained results in the context of each experimental design. For example, culture of PDAC cells in collagen matrices promotes epithelial-to-mesenchymal transition (EMT), while culturing the same cells in basement membrane extract gels at matched stiffness promotes mesenchymal-to-epithelial transition (MET)[197] .Furthermore, not only the composition but also the stiffness of the matrix is an important parameter to be adjusted when culturing cells in three dimensions. Increased matrix stiffness is a hallmark of many cancers such as breast[69], colorectal[127] and pancreatic[237] cancers. PDAC is characterized by a dense and fibrotic stroma due to the production of abundant amounts of ECM (mostly collagens) by stromal pancreatic cells[20]. In consequence, PDAC tissue can be several folds stiffer than its healthy counterpart[143,237] and different 3D models using synthetic [195] and natural scaffolds have been developed in order to study the effect of matrix stiffness on PDAC cells.

In this chapter, we present a new 3D cell model of EGFR trafficking and degradation in pancreatic ductal adenocarcinoma (PDAC), based on the synthetic self-assembling peptide RAD16-I as a biomaterial for cell culture. In a neutral pH, this peptide self-assembles into a nanofiber network (around 10 nm diameter and 50-200 nm pore size) that allows the embedding of cells in a 3D environment[157]. The main advantage of self-assembling peptide scaffolds (SAPS) over natural matrices is that they do not suffer degradation *in vitro* and therefore allow the maintenance of the same mechanical conditions (matrix stiffness) along culture time. Moreover, it allows to establish both soft and stiff 3D environments by simply changing its final concentration. RAD16-I is a non-instructive matrix from the point of view of receptor recognition/activation and therefore, this synthetic matrix holds the cells in an inert 3D configuration until they produce ECM proteins and decorate their own physiological environment. RAD16-I has been widely used as a cell culture platform for different tissue engineering applications such as bone[238], cartilage[239], cardiac[184] and hair[183] tissue engineering, and it has also been used to develop 3D models of ovarian[240], breast[211] and pancreatic[180] cancers.

3.2 Motivation and aims

The main motivation of this chapter was to develop an in vitro three-dimensional (3D) cancer model to study drug resistance to tyrosine kinase inhibitors (TKI). For that, we selected the EGFR as a prototype of receptor tyrosine kinase, and the small molecule Erlotinib as a TKI. Our working hypothesis was that 3D cultures would allow us to study the role of different extracellular cues, specifically dimensionality (2D *vs* 3D cultures) and stiffness (soft *vs* stiff), in triggering survival strategies for cancer cells after drug treatment. The specific aims for this chapter were the following:

(1) To develop a 3D cancer cell model to study the effect of drug treatment on cell viability

(2) To characterize the effect of erlotinib treatment on the expression and location of the EGFR in 2D and 3D cultures

(3) To study EGFR intracellular trafficking in 2D and 3D cultures of normal and PDAC cells

3.3 Results

3.3.1 Cell culture in self-assembling peptide scaffold RAD16-I

In the present chapter, two pancreatic cancer cell lines (BxPC-3 and PANC-1) have been used, as well as primary human dermal fibroblasts (hNDF), as a control of healthy, non-tumor cells, to study the effect of the tyrosine kinase inhibitor (TKI) erlotinib on EGFR internalization and degradation in a three-dimensional (3D) environment. These two PDAC cell lines were chosen for three main reasons. First, they represent a model of epithelial phenotype (BxPC-3) and an intermediate epithelial-mesenchymal phenotype (PANC-1)[197]. Second, they present with differences regarding erlotinib sensitivity, BxPC-3 being considered an erlotinib-sensitive line and PANC-1 an insensitive one[241]. Third, they present with different KRAS genetic signature, an important gene involved in PDAC progression. BxPC-3 cells have wild type KRAS, while PANC-1 cells present with a G12C mutation that produces its constitutive activation. This is of vital importance since 95% of primary pancreatic tumors show mutations in the KRAS gene[242]. For three-dimensional cell culture, we used the self-assembling peptide scaffold RAD16-I, which has been previously used for different cancer cell line cultures[180,211,240]. Moreover, cultures in RAD16-I were prepared at two different peptide concentrations: 0.15% and 0.5%, which correspond approximately to a stiffness of 120 Pa (namely soft matrix) and 2,500 Pa (namely stiff matrix), respectively, previously measured by rheometry[243]. Results show that both pancreatic cancer cell lines presented good viability regardless of matrix stiffness (**Figure 8a**). Moreover, growth rate in 3D cultures decreased for both cell lines compared to 2D, partially recapitulating the growth behavior of in vivo cancer cells (**Table 6**). Dermal fibroblasts did not show proliferation in the soft RAD16-I matrix, as previously reported[180], but did proliferate in the stiff matrix (**Table 6**). This behavior was previously shown for fibroblasts cultured in 3D collagen gels[244]. We also determined cell viability after a 72 h incubation with the TKI erlotinib. Under our culture conditions, we determined an IC_{50} of 10 µM for the erlotinib-sensitive cell line BxPC-3 and also for normal fibroblasts, in both 2D and 3D cultures. For the erlotinib-insensitive cell line PANC-1 we determined an IC_{50} of 45 µM for 2D cultures and 100 µM for 3D cultures, in both matrix stiffness conditions (**Table 6**). Therefore, the 3D environment promoted these cells to be even more resistant to erlotinib treatment.

Table 6. Doubling time (h) and erlotinib sensitivity in 2D and 3D cultures.

	Condition	BxPC-3	PANC-1	hNDF
	2D	39	30	24.3
Doubling time (h)	0.15% RAD	ND	63.6	No proliferation
	0.5% RAD	95	62.3	65.3
Erlotinib IC_{50} (µM)	2D	10	45	10
	3D	10	100	10

ND: Not determined

Regarding cell phenotype, the epithelial cell line BxPC-3 grew forming round or oval clusters (**Figure 8b, left**) while PANC-1 cells formed more grape-like spheres (**Figure 8b, middle**). We did not find a correlation between matrix stiffness and cell phenotype or colony size in the tumor cells analyzed. Matrix stiffness had a great effect on dermal fibroblasts which formed a highly interconnected network in the soft matrix, contracting the hydrogel and notably reducing its dimension in a few days (**Figure 8d**). In the stiff matrix, fibroblasts managed to interconnect to each other as well (**Figure 8b, right**), but required more time in culture to do so, and contracted the matrix to a lesser extent (**Figure 8d**). This hydrogel-contraction behavior (also called matrix condensation) is characteristic of primary mesenchymal cells cultured in this kind of scaffold[183] but did not happen in tumor cells (**Figure 8c**).

Figure 8. Cell culture in RAD16-I scaffold. (a) Viability of BxPC-3, PANC-1 and hNDF cultured in 0.15% and 0.5% RAD16-I scaffold measured by MTT assay at day 1 and day 7 of culture. Statistical differences are indicated as * for pv<0.05, ** for pv<0.01, *** for pv<0.001 and **** for pv<0.0001, Two-way ANOVA, N=2, n=3); **(b)** Z-projection pictures of BxPC-3, PANC-1 and hNDF cells at day 6 of culture stained with Phalloidin (pseudo-colored in yellow) and DAPI (blue). Scale bars represent 20 μm; **(c)** Macroscopic view of PANC-1 and **(d)** hNDF 3D constructs in 0.15% and 0.5% RAD16-I scaffolds at different time points. Scale bars represent 1 mm.

3.3.2 EGFR expression in 2D and 3D cultures

We next analyzed the location and expression levels of the EGFR by immunofluorescence and western blot in both culture types. In 2D cultures of BxPC-3 cells, the EGFR displayed a strong staining in the cell periphery, colocalizing with β1-integrin, as well as a diffused cytoplasmatic staining (**Figure 9a, top**). In PANC-1 cells, the EGFR was found mainly in the cell periphery, presenting a strong staining that overlapped with β1-integrin (**Figure 9a, middle**). In fibroblasts instead, the EGFR showed a dotted staining all over the cell (**Figure 9a, bottom**). Similar to 2D cultures, BxPC-3 and PANC-1 in 3D cultures showed a peripheral staining of the EGFR, while hNDF displayed a dotted staining (**Figure 9b**). Western blot analysis revealed that total EGFR was downregulated in 3D cultures compared to 2D monolayer cultures in the three types of cells analyzed (**Figure 9c**) especially in dermal fibroblasts. Moreover, matrix stiffness in 3D cultures also influenced EGFR expression, being downregulated in stiff conditions compared to soft cultures in hNDF cells, but not in BxPC-3 and PANC-1, which presented similar EGFR levels regardless of the stiffness (**Figure 9d**).
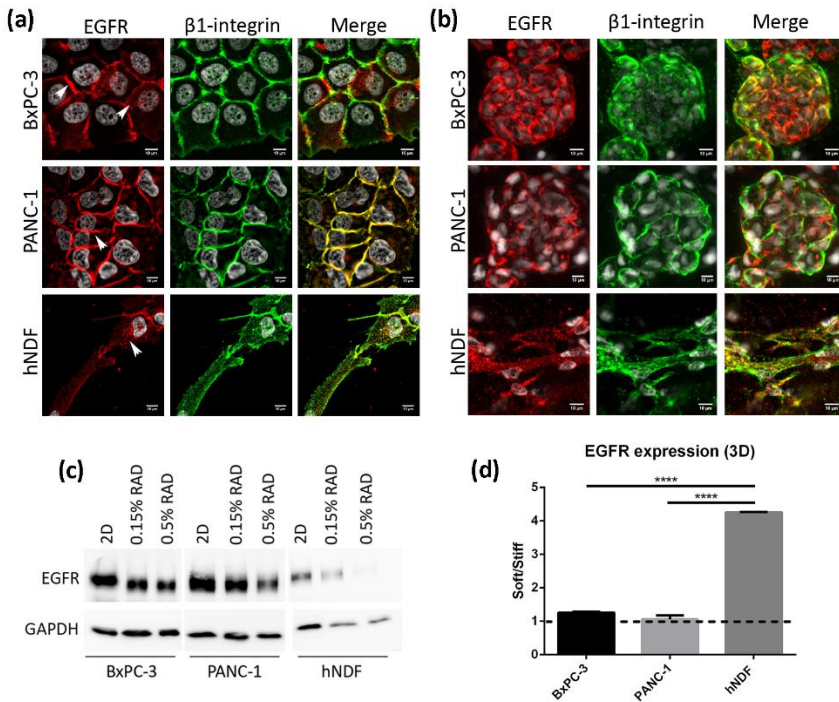
Figure 9. EGFR expression in 2D and 3D cultures. **(a)** EGFR (red) and β1-integrin (green) immunofluorescence counterstained with DAPI (grey) in BxPC-3, PANC-1 and hNDF cells cultured in 2D monolayer and **(b)** Z-projection of EGFR and β1-integrin immunofluorescence in BxPC-3, PANC-1 and hNDF cells in 3D RAD16-I scaffold at 0.15% peptide concentration. Scale bars represent 10 μm; **(c)** Western blot bands of EGFR in 2D and 3D cultures; **(d)** Quantification of EGFR in 3D cultures represented as the ratio between soft and stiff cultures. GAPDH was used as loading control. One representative blot is shown. Experiments were repeated three times (N=3) and statistical differences are indicated as **** for pv<0.0001.

3.3.3 Effect of EGF and Erlotinib on the location of the EGFR

We next analyzed the effect of EGF and acute erlotinib treatment on cells in 2D and 3D cultures. For that, cells were incubated with 10 ng/mL EGF or 50 μM erlotinib or the combination of both during 16 h. Under control conditions, EGFR in 2D-cultured PANC-1 cells was found predominantly in the cell membrane, showing a strong peripheral staining (**Figure 10a, b**) and colocalizing with β1-integrin (**Figure 10c**). The presence of EGF triggered ligand-induced endocytosis of the EGFR, as previously described[223], thus being internalized from the cell periphery (**Figure 10a**, white arrows) into the cytoplasm (**Figure 10a**, empty arrows), accumulating perinuclearly (**Figure 10a, b**). Treatment of cells with erlotinib did not induce EGFR internalization, as demonstrated by its peripheral staining (**Figure 10a, b**) and high colocalization degree with β1-integrin, similar to control conditions (**Figure 10c**). However, when we incubated the cells with erlotinib in combination with EGF, we detected both membrane and perinuclear EGFR staining (**Figure 10a, b**).

Figure 10. Immunofluorescence analysis of the EGFR in PANC-1 cells incubated with EGF, erlotinib or both in 2D cultures. (a) EGFR (red) and β1-integrin (green) immunofluorescence counterstained with DAPI (grey) in the presence of EGF, erlotinib or both in PANC-1 and close-up sections (gray pictures) of the cell periphery and the perinuclear area labeled with white and empty arrows, respectively. Scale bars represent 10 μm; **(b)** Fluorescence intensity profiles corresponding to the white line in pictures from (a). Different cell regions are indicated as: P for cell periphery, N for nucleus and PN for perinuclear area; **(c)** Manders' colocalization coefficients.

The location of EGFR in 2D cultures of BxPC-3 under control conditions was mainly peripheral, associated with β1-integrin staining, but also diffused expression was detected in the cytoplasm (**Figure 11a**). The presence of EGF induced a strong accumulation of the receptor in the cytoplasm and the perinuclear area (**Figure 11a, b**). In the presence of erlotinib, EGFR displayed a similar location as in the control (**Figure 11a**), but the fraction of β1-integrin colocalizing with EGFR increased compared to the control (**Figure 11c**). Finally, when BxPC-3 cells were incubated with erlotinib in combination with EGF, we detected a strong perinuclear staining (**Figure 11a, b**), but also an increased colocalization degree with the membrane marker β1-integrin compared to EGF-incubated cells (**Figure 11c**), similar to what happened in PANC-1 cells. The cytoplasmatic staining of EGFR in BxPC-3 under control conditions suggests that basal levels of EGFR trafficking may exist, which could be due to different reasons. First, even though EGFR mainly resides in the plasmatic membrane, it constantly undergoes trafficking through the endocytic system[218]. Second, it is important to note that in order to keep culture conditions between 2D and 3D as similar as possible, cells were not serum-starved prior to the experiments. In 2D cultures, FBS proteins are removed by simply changing the culture medium. However, protein release from RAD16-I hydrogels can take more than 50 h[179,182], and therefore complete serum depletion is not possible in the short term in our 3D culture system.
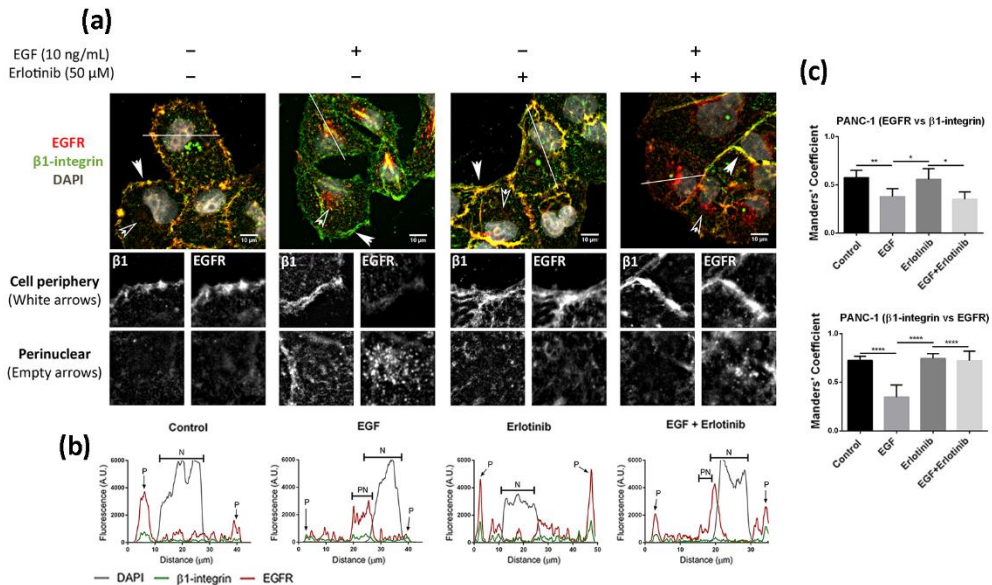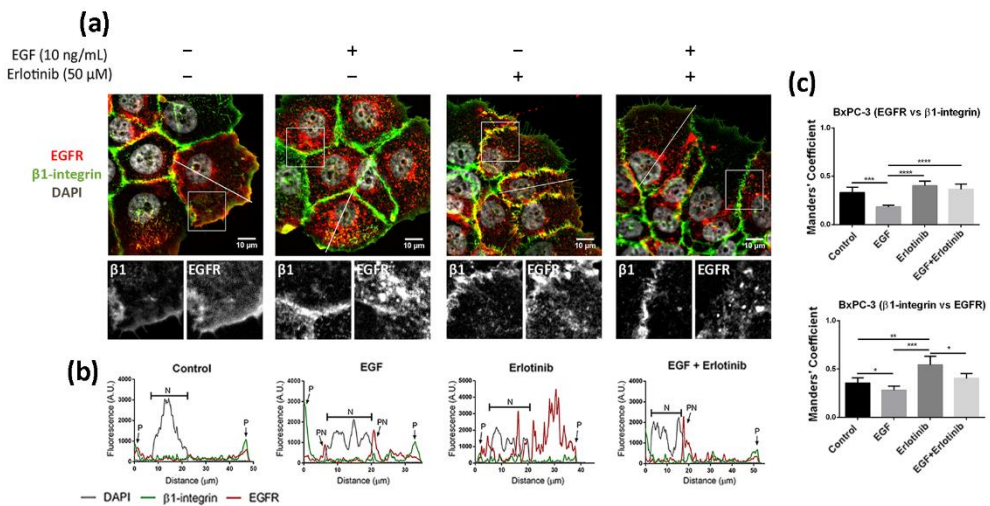

Figure 11. Immunofluorescence analysis of the EGFR in BxPC-3 cells incubated with EGF, erlotinib or both in 2D cultures. **(a)** EGFR (red) and β1-integrin (green) immunofluorescence counterstained with DAPI (grey) in the presence of EGF, erlotinib or both and close-up sections (gray pictures). Scale bars represent 10 μm; **(b)** Fluorescence intensity profiles corresponding to the white line in pictures from (a). Different cell regions are indicated as: P for cell periphery, N for nucleus and PN for perinuclear area; **(c)** Manders' colocalization coefficients.

Finally, we analyzed the effect of EGF and erlotinib in 2D cultures of human normal dermal fibroblasts (hNDF). In this case, cells under control conditions showed a punctate staining of the EGFR distributed all over the cell and also some pericellular staining (**Figure 12**). The presence of EGF alone or combined with erlotinib induced the accumulation of the receptor mainly in the perinuclear area, probably in endosomal compartments, while erlotinib alone promoted the accumulation of the receptor along all the cell surface and pericellularly (**Figure 12**). Altogether, these results suggest that erlotinib partially prevents EGFR internalization and trafficking to endosomal compartments upon EGF binding in 2D cultures, retaining part of the receptor in the plasmatic membrane, as previously described[245].
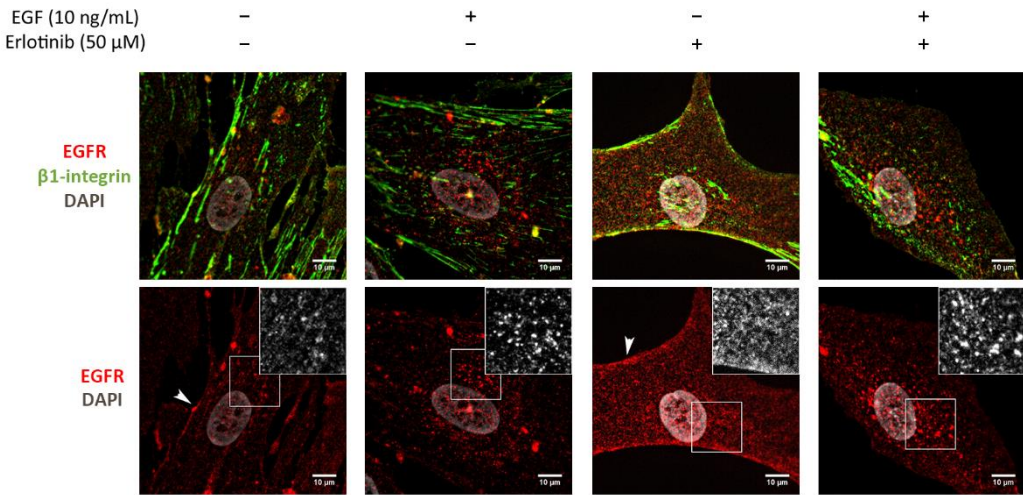
Figure 12. Immunofluorescence analysis of the EGFR in hNDF cells incubated with EGF, erlotinib or both in 2D cultures. Scale bars represent 10 µm. Insets represent high magnification images of the region indicated by a white square.

In 3D cultures both tumor cell lines displayed peripheral staining of the EGFR, as happened in 2D cultures (**Figure 13, top and middle**). Under control conditions and in the presence of erlotinib alone, EGFR staining was peripheral and well-defined but when EGF or EGF and erlotinib were added, EGFR signal in the membrane became more diffused and both pericellular and cytoplasmic punctate staining were detected, which showed evidence of the internalization of the receptor (**Figure 13,** see arrows). In hNDF under control conditions the EGFR displayed a punctate staining all over the cell, while accumulating perinuclearly after EGF exposure (**Figure 13, bottom**, see arrows). In erlotinib-treated hNDF, the dotted EGFR expression found in the control was lost, becoming strongly concentrated all over the cell. When combining EGF and erlotinib treatment, both phenotypes could be detected.
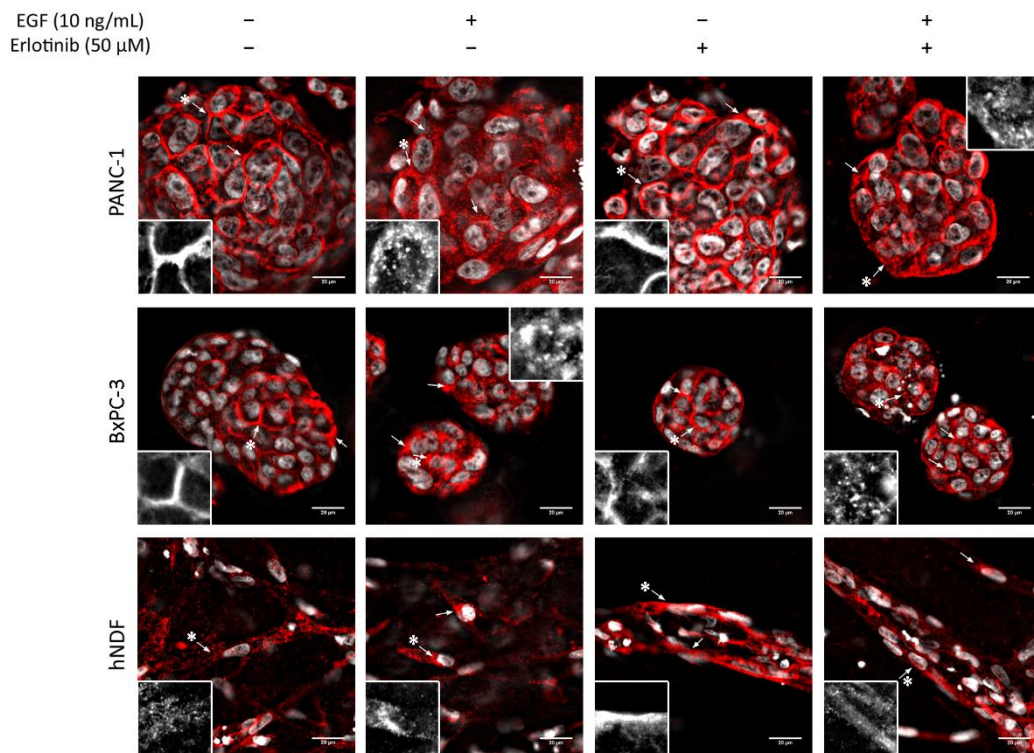
Figure 13. EGFR immunofluorescence in PANC-1, BxPC-3 and hNDF cells incubated with EGF, erlotinib or both in 0.15% RAD16-I 3D cultures. One representative Z plane is shown. Scale bars represent 20 μm. Insets represent high magnification images of the region indicated by an asterisk (*).

3.3.4 Effect of EGF and Erlotinib on EGFR degradation

It has been previously shown using 2D cultures that treatment of cells with monoclonal antibodies targeting the EGFR such as cetuximab[228] and Sym004[245,246] resulted in overall decrease of EGFR levels due to protein degradation. In contrast, TKI treatment has not shown to induce significant EGFR degradation in different 2D-cultured cancer cell lines[247–250]. Consistent with these studies we did not detect a relevant decrease in EGFR levels after 16 h erlotinib treatment (neither alone nor in combination with EGF) in any of the cells analyzed (**Figure 14a, c, lanes 3-4**). On the other hand, EGF treatment alone induced strong EGFR degradation in hNDF but not in tumor cells (**Figure 14a, c, lane 2**), which express much higher EGFR levels than hNDF. Therefore, it is likely that the EGF dose used (10 ng/mL) is insufficient to promote EGFR degradation in these PDAC cell lines. Remarkably, the presence of erlotinib in hNDF treated with EGF rescued EGFR levels similar to those in untreated cells **Figure 14a, c, lane 4**), reinforcing the hypothesis that erlotinib prevents EGFR internalization in 2D-cultered cells.

Similar to 2D cultures, EGF did not induce significant EGFR degradation in 3D-cultured tumor cells. On the contrary, EGF induced a dramatic EGFR degradation in 3D cultures of fibroblasts regardless of matrix stiffness (**Figure 14b, d, lanes 1-4**). Interestingly, and contrary to what was found in 2D cultures, erlotinib promoted EGFR degradation when combined with EGF, but not alone, in PANC-1 and BxPC-3 cells cultured in 3D scaffolds under both stiffness conditions (**Figure 14b, d, lanes 5-8**). Moreover, the extent of EGFR degradation was erlotinib dose-dependent (**Figure 15**).

Contrary to tumor cells, the presence of erlotinib in EGF-incubated fibroblasts in 3D, not only did not induce the degradation of the receptor but prevented it (**Figure 14b, d, lanes 5-8**), as happened in 2D cultures. In conclusion, erlotinib treatment (combined with EGF) had a contrary effect depending on cell type and dimensionality, promoting EGFR degradation in PDAC cell lines cultured in 3D but preventing it in normal fibroblasts in both 2D and 3D cultures.
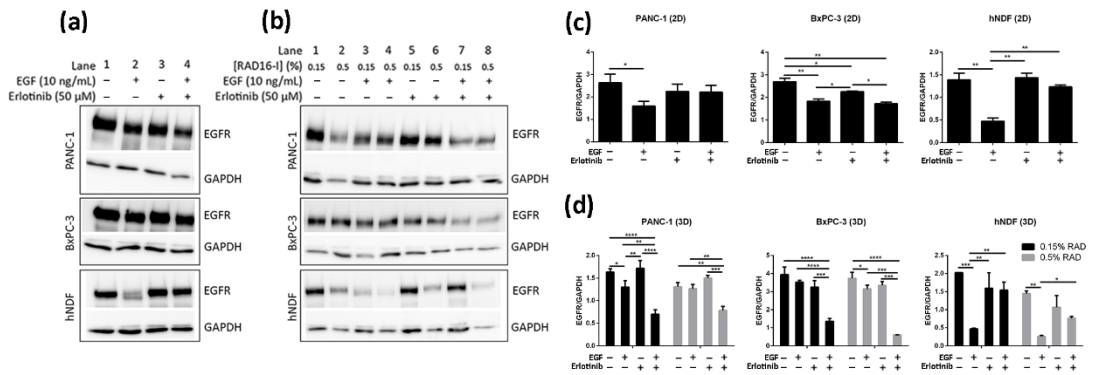
Figure 14. Western blot analysis of the EGFR in BxPC-3, PANC-1 and hNDF cells incubated with EGF or erlotinib or both in 2D cultures and soft and stiff 3D cultures. (a) Western blot bands of EGFR in 2D cultures; **(b)** Western blot bands of EGFR in 0.15% and 0.5% RAD16-I 3D cultures; **(c)** Densitometry of bands shown in (a) for 2D cultures; **(d)** Densitometry of bands shown in (b) for 3D cultures. GAPDH was used as an internal control. One representative blot is shown. Experiments were repeated three times (N=3) and statistical differences are indicated as * for pv<0.05, ** for pv<0.01, *** for pv<0.001 and **** for pv<0.0001.
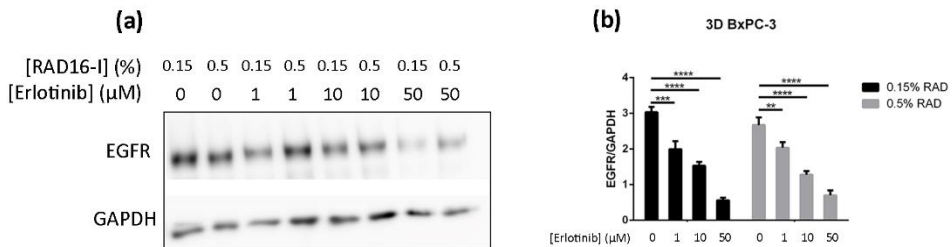
Figure 15. EGFR degradation with increasing concentrations of erlotinib in EGF-incubated BxPC-3 cells in 3D RAD16-I scaffolds. (a) Western blot bands of EGFR in BxPC-3 cultured in soft and stiff RAD16-I scaffold with different erlotinib concentrations; **(b)** Densitometry of bands showed in (a). GAPDH was used as an internal control. Statistical differences are indicated as ** for pv<0.01, *** for pv<0.001 and **** for pv<0.0001.

To confirm that the decrease of EGFR levels in 3D cultures of PANC-1 and BxPC-3 cells treated with EGF and erlotinib was actually due to protein degradation, we inhibited proteasomal and lysosomal degradation by pre-incubating the cells with MG-132 (proteasome inhibitor) and bafilomycin A1 (lysosome inhibitor). It has been extensively reported that EGF-induced degradation occurs via lysosomes[223], and therefore we questioned whether EGFR downregulation in erlotinib-treated tumor cells (**Figure 14b, d**) was also due to lysosomal degradation.

Results show that lysosome inhibition in cells treated with erlotinib and EGF led to a notable increase in EGFR levels due to protein accumulation (**Figure 16, lane 8**). Bafilomycin A1 inhibits fusion between endosomes and lysosomes, which causes the accumulation of cargo unable to suffer degradation[251,252]. Moreover, MG-132 also led to EGFR accumulation upon EGF and erlotinib treatment, but to a lesser extent than bafilomycin A1 (**Figure 16, lane 7**). Proteasomal inhibition has been reported to deplete the free ubiquitin pool within the cell, thus interfering with protein degradation[253]. Moreover, combinatorial treatment with both inhibitors (MG-132 and bafilomycin A1) also led to protein accumulation in PANC-1, but not in BxPC-3 cells, which presented with reduced EGFR levels compared to its respective control (**Figure 16, lane 5 and 9**). This could be explained by the fact that proteasome disruption leads to endoplasmic reticulum stress to which the cell responds by attenuating protein translation, and therefore inhibiting global protein synthesis[254]. Altogether, these results confirm that EGFR degradation due to erlotinib and EGF treatment in our 3D cancer cell culture system occurs via lysosomes.
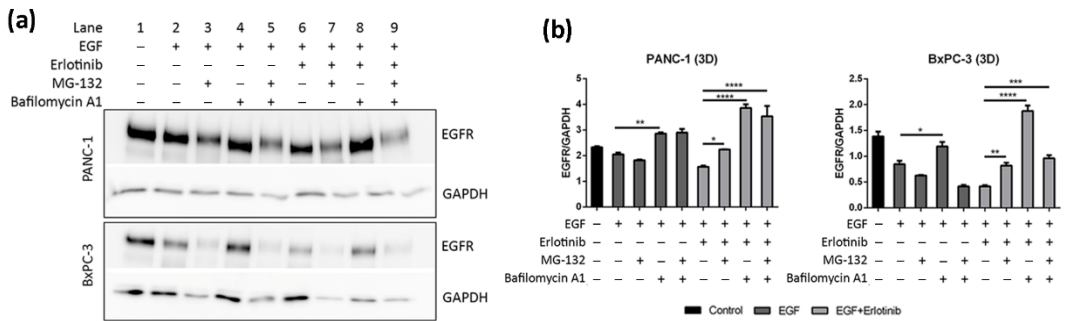
Figure 16. Western blot analysis of the EGFR in PANC-1 and BxPC-3 cells incubated with EGF and erlotinib in the presence of the proteasome (MG-132) and lysosomes (Bafilomycin A1) inhibitors in 0.15% RAD16-I 3D cultures. **(a)** Western blot bands of EGFR; **(b)** Densitometry of bands shown in (a). GAPDH was used as an internal control. One representative blot is shown. Experiments were repeated three times (N=3) and statistical differences are indicated as * for pv<0.05, ** for pv<0.01, *** for pv<0.001 and **** for pv<0.0001.

3.3.5 EGFR trafficking to early endosomes and lysosomes in 2D cultures

It is well established that after stimulation with EGF, the EGFR is activated, internalized and sorted into endosomal compartments. Once in EEA1-positive early endosomes, a small fraction of the receptor is recycled to the plasmatic membrane, while most of it is sorted into late endosomes and subsequently degraded in lysosomes[223]**.** In 2D cultures, we found a low EGFR fraction colocalizing with EEA1-positive early endosomes in PANC-1 (**Figure 17a, d**) and BxPC-3 tumor cells (**Figure 17b, d**). After EGF exposure, the fraction of EGFR colocalizing with EEA1 increased for both tumor cell lines (**Figure 17d**).

Figure 17. Colocalization analysis of the EGFR and EEA1 (early endosomes) in cells incubated with EGF, erlotinib or both in 2D cultures. EGFR (red) and EEA1 (green) immunofluorescence counterstained with DAPI (grey) in **(a)** PANC-1; **(b)** BxPC-3 and **(c)** hNDF cells. Scale bars represent 10 μm; **(d)** Manders' colocalization coefficients showing the proportion of EGFR overlapping with EEA1; **(e)** Manders' colocalization coefficients showing the proportion of EEA1 overlapping with EGFR. Statistical differences are indicated as * for pv<0.05, ** for pv<0.01 and *** for pv<0.001, **** for pv<0.0001.

Moreover, and in concordance with the hypothesis that erlotinib partially prevents EGFR internalization, erlotinib-treated cells presented with the lowest colocalization values between EGFR and EEA1. Additionally, we found that in hNDF (**Figure 17c**) the EGFR fraction colocalizing with EEA1 was extremely low for all the conditions tested (**Figure 17d**), but on the contrary, Manders' coefficients obtained for the proportion of EEA1-positive early endosomes containing EGFR signal were almost 1 (**Figure 17e**), meaning that almost all EEA1-positive endosomes were carrying EGFR. These differences between both Manders' coefficients in hNDF exist because these are very large cells expressing EGFR all over the cellular milieu, while early endosomes are located mainly perinuclearly. Therefore, the EGFR signal coinciding with EEA1 signal over the total EGFR intensity (EGFR vs EEA1) is much lower than the EEA1 signal coinciding with EGFR signal over the total EEA1 intensity (EEA1 vs EGFR). Moreover, even colocalization between EEA1 and EGFR (**Figure 17e**) was similar between the

control and the EGF-incubated cells, it significantly decreased in the presence of erlotinib alone, indicating a basal EGFR trafficking that was prevented by the presence of erlotinib.

We next analyzed colocalization between EGFR and LAMP1 (lysosomal-associated membrane protein 1), a well-known lysosomal marker. Lysosome distribution was mainly perinuclear in BxPC-1 and hNDF cells under all conditions tested (**Figure 18b, c**). However, in PANC-1 cells, lysosomes were distributed all over the cytoplasm in control conditions as well as when incubated with erlotinib, but accumulated perinuclearly after EGF treatment (**Figure 18a**). LAMP1 staining showed significantly higher colocalization coefficients between lysosomes and the EGFR in cells treated with EGF compared to control in all the cell types analyzed (**Figure 18d, e**). Moreover, the presence of erlotinib alone produced significant differences only in BxPC-3 cells, in which Manders' coefficients (LAMP1 vs EGFR) (**Figure 18e**) increased compared to the control.
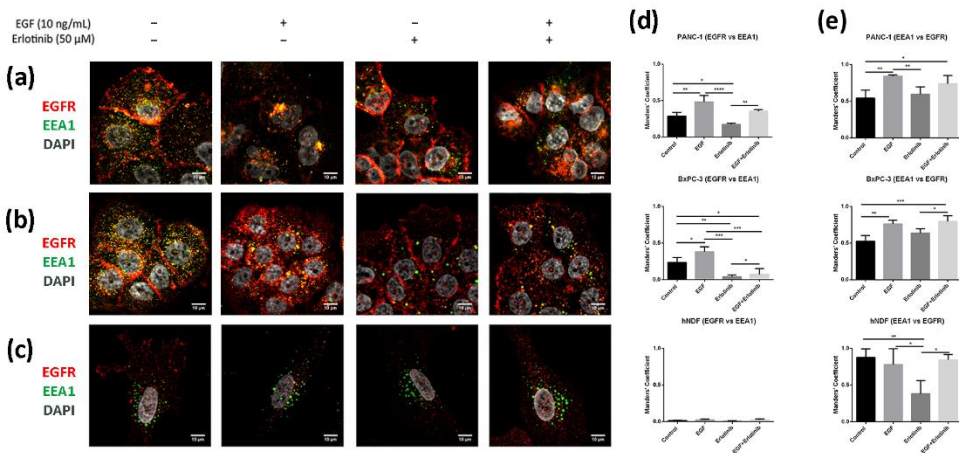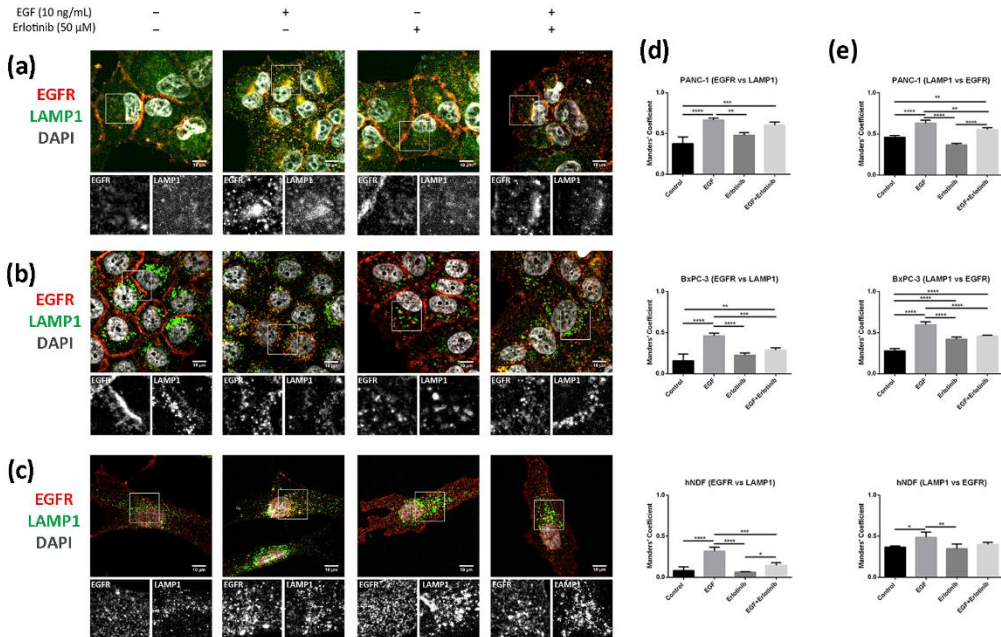

Figure 18. Colocalization analysis of the EGFR and LAMP1 (lysosomes) in cells incubated with EGF, erlotinib or both in 2D cultures. EGFR (red) and LAMP1 (green) immunofluorescence counterstained with DAPI (grey) in **(a)** PANC-1; **(b)** BxPC-3 and **(c)** hNDF cells. Scale bars represent 10 μm. Gray pictures show close-up sections of each marker; **(d)** Manders' colocalization coefficients showing the proportion of EGFR overlapping with LAMP1; **(e)** Manders' colocalization coefficients showing the proportion of LAMP1 overlapping with EGFR. Statistical differences are indicated as * for pv<0.05, ** for pv<0.01, *** for pv<0.001, **** for pv<0.0001.

3.3.6 EGFR trafficking to early endosomes and lysosomes in 3D cultures

Finally, we analyzed EGFR sorting into early endosomes and lysosomes in 3D cultures. In BxPC-3 tumor cells we detected EGFR trafficking to EEA1-positive early endosomes in all conditions tested, but colocalization was much more evident in cells treated with EGF or EGF and erlotinib (**Figure 19a**, see arrows), in which EGFR was undergoing endocytosis. A similar pattern was found in hNDF (**Figure 19b**, see arrows). Regarding EGFR sorting into lysosomes, we found that in PANC-1 (**Figure 20a**) and BxPC-3 cells (**Figure 20b**) colocalization between EGFR and LAMP1 was mostly detected in cells treated with EGF or EGF and erlotinib. Even though we detected certain colocalization between EGFR and LAMP1-positive lysosomes in 3D-cultured tumor cells incubated with EGF, degradation under these conditions was undetectable at a western blot level (**Figure 14**), suggesting that the presence of erlotinib exacerbated this degradation in EGF-treated cells.
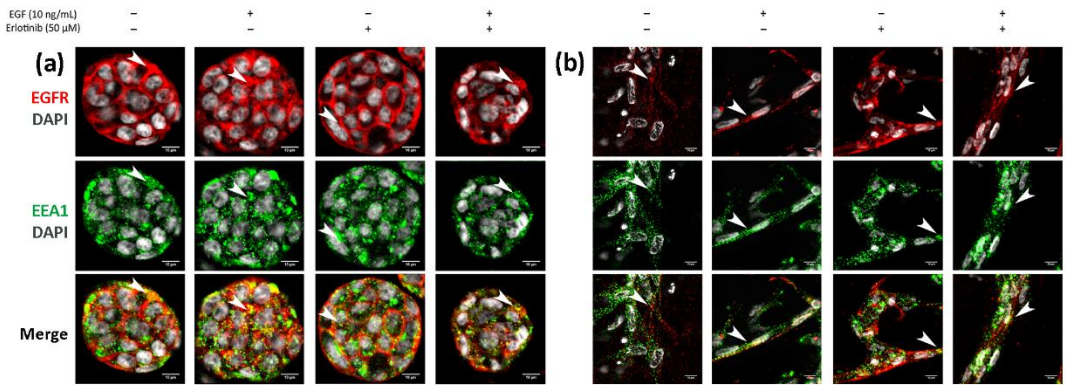
Figure 19. Immunofluorescence of EGFR and EEA1 in 3D cultures. (a) BxPC-3 cells and **(b)** hNDF incubated with EGF, erlotinib or both in 0.15% RAD16-I 3D cultures. One representative Z plane is shown. Scale bars represent 10 μm. White arrows show EGFR colocalizing with early endosomes.
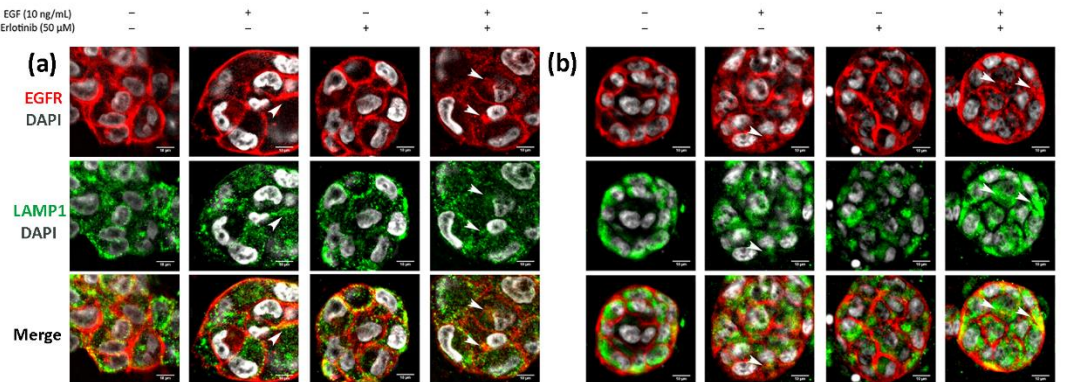
Figure 20. Immunofluorescence of EGFR and LAMP1 in 3D cultures. (a) PANC-1 and **(b)** BxPC-3 cells incubated with EGF, erlotinib or both in 0.15% RAD16-I 3D cultures. One representative Z plane is shown. Scale bars represent 10 μm. White arrows show EGFR colocalizing with lysosomes.

3.4 Discussion

The EGFR is the only TKR reported to respond to multiple stimuli by internalizing into endosomal compartments. Moreover, different stressors induce different trafficking pathways that can end in endosomal accumulation and recycling to the membrane or degradation. Two-dimensional cell cultures are generally used to study EGFR trafficking mechanisms because they are economically affordable and easier to handle as well as to analyze than 3D cultures. However, it is widely accepted that 2D cultures do not recreate the microenvironment of in vivo tissue cells nor can they predict therapy outcome as precisely as 3D cultures do. Growing cells in a 3D environment reveals a more realistic drug response, being that 3D-cultured cells are more resistant to chemotherapy when compared to the same cells grown in 2D monolayer[240,255,256]. Different mechanisms have been attributed to this enhanced drug resistance, but the most straightforward explanation is that the microenvironment provided by the 3D system protects the cells from drug penetration[151]. Besides, most drugs have rapidly dividing cells as a target, and 3D cultures have been described to decrease the proliferation rate of cancer cells compared to 2D cultures[180]. Moreover, quiescent cells that exist in the inner part of the 3D culture remain protected from drug effect[152]. In addition, some pancreatic cancer cell lines have shown an increased expression of diverse drug resistance genes in 3D culture compared to 2D culture[153]. For example, PDAC cells in 3D collagen hydrogels but not in 2D cultures present with gemcitabine resistance through the upregulation of the membrane type-I matrix metalloprotease (MT1-MMP)[257]. Therefore, 3D-cultured cells can recapitulate mechanisms of drug resistance found in tumors, thus offering the opportunity to analyze these mechanisms and test multidrug therapies *in vitro* in order to reduce animal experimentation.

In this chapter we report a new model for EGFR internalization and degradation due to tyrosine-kinase inhibitor treatment in a 3D cell culture of pancreatic ductal adenocarcinoma cells. Using the synthetic self-assembling peptide RAD16-I as a platform for 3D culture, we found that erlotinib treatment combined with EGF, but not alone, promoted EGFR degradation in 3D, but not 2D cultures of both PDAC cell lines (**Figure 14**). These results suggest that in 3D culture, EGF is necessary to promote EGFR endocytosis in PDAC cell lines, and that upon internalization, erlotinib promotes its lysosomal degradation (**Figure 16**). Interestingly, this behavior was not detected in normal fibroblasts, in which erlotinib prevented EGF-induced EGFR internalization and degradation in both 2D and 3D cultures (**Figure 12, Figure 13, Figure 14**). In this sense, results can be controversial since previous in vitro studies demonstrate that TKI inhibitors such as erlotinib and gefitinib induce EGFR internalization and accumulation in non-degradative endosomes in different cell types [225], while others describe that the same TKI suppresses ligand-stimulated endocytosis[227]. Another work in which the authors develop an in vivo tumor model of human oral squamous carcinoma using xenografts reports that gefitinib treatment inhibits EGFR endocytosis[258], suggesting that receptor kinase activity is required for receptor internalization[259]. We indeed detected this kinase activity-dependence to internalize the receptor in fibroblasts (**Figure 12**) and also in tumor cells, but to a lesser extent (**Figure 10, Figure 11**). One explanation could be that PDAC cell lines are more resistant to erlotinib and therefore the dose used could be not enough to inhibit the kinase activity of the receptor. However, we used an acute

dose of 50 µM, corresponding to the IC_{50} of the erlotinib-resistant cell line PANC-1, and therefore, it should be enough to inhibit the EGFR in the erlotinib-sensitive BxPC-3 cell line and in hNDF, which both presented an IC_{50} of 10 µM.

It is well established that receptor recycling to the plasmatic membrane after endocytosis leads to continuous signaling. By contrast, degradation in lysosomes is associated with signaling attenuation and therefore, endocytic downregulation could be associated with TKIs sensitization. For example, it has been reported that mutant-EGFR forms are internalized via clathrin-mediated endocytosis and sorted into endosomal compartments, where they continue signaling[260]. Instead, clathrin inhibition in mutant-EGFR-expressing cells induces a micropinocytosis-dependent EGFR internalization followed by degradation in lysosomes which results in signal extinction and apoptosis, and thus overcoming resistance to TKI[260]. Another recent study reports that TKI treatment induces intracellular accumulation of mutated-EGFR. The authors found a positive correlation between EGFR accumulation and clinical benefit in patients presenting with tumors harboring these EGFR mutations, suggesting that blocked EGFR-membrane recycling contributes to TKI sensitivity and a positive therapy outcome[261]. Our results demonstrate not only that erlotinib has a different effect on tumor and normal cells, but also that PDAC cells respond differently to erlotinib treatment when cultured in a 3D microenvironment. In fact, PANC-1 cells increased their erlotinib resistance from 45 to 100 µM when cultured in 2D vs 3D (**Table 6**), even though under these 3D conditions the EGFR was undergoing degradation. On the other hand, BxPC-3 cells did not show increased erlotinib resistance when cultured in 3D, but did also show EGFR degradation. Therefore, under our experimental conditions, EGFR degradation did not sensitize the cells to erlotinib treatment. Given that this EGFR degradation was only detected in 3D cultures, it is possible that in this 3D environment PDAC cells acquire additional resistance mechanisms that allow them to survive independently of the EGFR signaling pathway.

Importantly, EGFR degradation in 3D cultures due to TKI was only detected in the presence of EGF, suggesting that ligand binding is necessary for endocytosis, and that once the receptor is internalized, erlotinib treatment promotes its degradation. EGF can reach very high concentrations in different body fluids such as bile, urine and milk[262,263], and a normal epithelium avoids these fluids to reach EGF receptors which are expressed basolaterally. However, as a result of a premalignant neoplasia, in which the tight junctions of the epithelium become leaky, high concentrations of EGF can reach and activate EGFRs[264]. Moreover, since EGFR ligands have been found in several tumors[265–267] it is likely that our 3D model could closely mimic the tumor in vivo scenario during erlotinib therapy.

3.5 Concluding remarks

In this chapter we have developed a 3D cancer cell culture system to study EGFR trafficking and degradation due to TKI treatment. This study highlights not only that erlotinib had a distinct effect on tumor and normal cells but also that pancreatic ductal adenocarcinoma cells responded differently to erlotinib treatment when cultured in a 3D microenvironment. In particular, treatment with erlotinib, together with EGF, promoted EGFR degradation in 3D cultures but not in 2D cultures of PDAC cell lines. Moreover, we showed that EGFR degradation due to erlotinib treatment did not occur in normal fibroblast cells, probably because erlotinib prevented receptor internalization. To our knowledge, this is the first time that EGFR trafficking is explored in a three-dimensional environment, and it is our hope that this new 3D cell model may introduce new perspectives in the study of EGFR degradation and its implications in cancer therapy, in an environment that more accurately reproduces the in vivo conditions found in a tumor. Moreover, future research might be focused in studying the effect that ECM components present in PDAC, such as collagens and hyaluronic acid, could have on EGFR trafficking.

Chapter 4. Development of 3D in vitro models to study the effect of matrix stiffness on PDAC cells

4.1 Background

Pancreatic ductal adenocarcinoma (PDAC) is the most relevant pancreatic disease, accounting for more than 90% of all pancreatic malignancies. PDAC is the fourth most common cause of cancer-related death in Europe and US, with an extremely low five-year survival rate of around 10%[268] even though its occurrence is very low (around 13 per 100,000 habitants), representing only 3% of all diagnosed cancers[268]. The high mortality of PDAC has been associated in part with its asymptomatic nature at early stages, non-specific symptoms[2] and limited response to therapy[269]. The most common driver gene mutations found in PDAC are KRAS (88-100% of cases), CDKN2A (90% of cases), TP53 (85% of cases) and SMAD4 (55% of cases), which all fulfill key roles in pancreatic tumorigenesis[12]. Apart from this genetic landscape, PDAC also has a unique tumor microenvironment (TME), which favors malignant progression as well. One of the hallmarks of PDAC, and probably the most important, is the presence of high amounts of extracellular matrix (ECM) proteins, specially type I collagen, fibronectin, laminin and hyaluronic acid, which are produced by stromal cells[11]. Interestingly, ECM production in PDAC is so large, that stromal components can account for up to 90% of the tumor mass[16]. This stromal reaction causes tissue stiffening, that in turn also accelerates PDAC progression via changes in integrin-mediated signal mechano-transduction as well as producing a feedback loop that sustains the fibrotic activity of stromal cells. Therefore, one of the principal features of PDAC and probably one of the main properties of the malignant phenotype, is the presence of a dense and remarkably stiff ECM surrounding the tumor, which generates a unique microenvironment that fosters sustained cancer cell proliferation and resistance to drug-induced apoptosis[17–24]. Indeed, PDAC tissue can be several folds stiffer than its normal counterpart, as determined by both ex vivo and in vivo methods[270]. For example, ex vivo studies measuring tissue stiffness by mesoscale indentation, reported values of 1, 2 and 5.5 kPa (steady-state-modulus) for normal pancreas, pancreatitis and PDAC tissues, respectively[144]. In vivo studies using magnetic resonance imaging (MRE) showed that while normal pancreas presented with an average stiffness of 2.5 kPa, tissue stiffness increased to 6 kPa for PDAC[143].

Given the significance that not only the biochemical signals but also the biomechanics have in cancer initiation and progression, researchers are progressively considering and adjusting this parameter when developing in vitro models. The classic example of a first cancer model to incorporate matrix stiffness as a parameter was breast cancer. Since it was described 40 years ago that high breast density was associated to 4–6 times higher risk of developing breast cancer many in vitro models have been developed. Typically, these models involve the culture of cells in natural 3D matrices formed by collagen[191,203–206] or reconstituted basal membrane extract (rBM)[69,201,202] either alone or in combination with other constituents such as alginate and gelatin. Biomechanics focused on PDAC are currently attracting the attention of more researchers[270,271] and in vitro models to assess the influence of stiffness in PDAC cells include both 2D and 3D culture systems. 2D models include mainly cell seeding on top of polyacrylamide (PA) gels of varying stiffness coated with different ECM proteins. For example, it was reported using fibronectin-coated polyacrylamide (1–25 kPa) that increased stiffness promotes elements of epithelial-to-mesenchymal transition (EMT) such as higher vimentin

expression and nuclear localization of β-catenin and YAP/TAZ in PDAC cell lines[128]. The main advantage of using coated-PA gels is that they allow the increase of substrate stiffness without increasing the number of biological signals (e.g., adhesion sites), contrary to natural matrices such as collagen I and rBM. On the other hand, three-dimensional models include cell embedding within polymeric matrices, usually functionalized with RGD or MMP-cleavable motifs[193–196], or within ECM-like matrices such as Collagen type I and basal membrane extracts[197].

Natural matrices such as collagen allow the modulation of stiffness by simply changing the concentration of the gel, but they also suffer degradation *in vitro* due to MMPs activity[235,272], which may induce changes in fiber orientation and thickness[235]. In fact, collagen degradation by cells can start as early as 6 h in culture on polymerized collagen substrate[273]. Therefore, global measures of stiffness values in collagen gels do not necessarily represent the real local value around cells due to the potential degradation of nanofibers. Finally, the stiffness of these natural matrices is usually increased by increasing concentration, which also increases ligand density. By contrast, synthetic biomaterials promise better control of mechanical properties, as they do not contain MMP-cleavable motifs *per se*. In particular, self-assembling peptide scaffolds (SAPS) are an attractive synthetic option for 3D cell culture. Unlike synthetic polymer scaffolds, SAPS mimic the fiber architecture found in some natural matrices such as collagen type I gels[243]. Our group has a vast experience working with the self-assembling peptide RAD16-I (AcN-RADARADARADARADA-CONH$_2$, R arginine, A alanine, D aspartic acid)[212,274]. This synthetic peptide self-assembles into a network of interweaving nanofibers of ~10 nm diameter forming hydrogel scaffolds with 99% water content and 50-200 nm pore size, which allow to culture cells in a truly 3D environment. Importantly, stiffness can be controlled by simply adjusting peptide concentration, and it is likely to be maintained along culture time due to the low biodegradability of the peptide in vitro. This peptide scaffold has been demonstrated to promote adhesion[177], maintenance[178], differentiation[178,179,182–184] and proliferation[180,181] in a variety of mammalian cells.

In this chapter, we have used RAD16-I as a 3D cell culture platform to study the effect of matrix stiffness on PDAC cells in terms of focal adhesion kinase (FAK) expression and activity. We demonstrate that, even being a non-instructive milieu, RAD16-I allows integrin-mediated signal mechanotransduction, probably due to its capacity to adsorb proteins contained in fetal bovine serum (FBS) used to supplement cell culture medium. Moreover, its low biodegradability in vitro makes it an ideal platform to assess the effect of matrix stiffness *per se*, without increasing the number of biological signals. Our results show that increased matrix stiffness in 3D cultures of RAD16-I promotes downregulation of total FAK at a protein level in all cell types analyzed, while the extent of FAK activation in terms of phosphorylation at position Y397 is cell-type dependent. Moreover, we found that the increased stiffness of 3D collagen gels did not affect the extent of FAK phosphorylation, nor promoted the total FAK downregulation found in RAD16-I cultures. Altogether, our results demonstrate that cell response to matrix stiffness depends on the cell type as well as the kind of matrix used for 3D culture.

4.2 Motivation and aims

The main motivation of this chapter was to develop an in vitro three-dimensional (3D) cancer model to study the effect of matrix stiffness on pancreatic cancer cells. For that, we have used both synthetic (RAD16-I) and natural (Collagen I) matrices. Our working hypothesis was that synthetic RAD16-I matrix would represent a better option than natural matrices such as collagen I to perform studies where the effect of matrix stiffness is tested. These synthetic matrices have similar nanostructured network to the natural ECM but at the same time are able to better maintain mechanical and structural properties for long culture time compared to natural matrices.

The specific aims for this chapter were the following:

(1) To develop a 3D biomechanical cancer cell model to study the effect of matrix stiffness on cell phenotype

(2) To characterize signal mechanotransduction pathways in 2D and 3D cultures

(3) To study FAK expression and activation in RAD16-I and Collagen 3D cultures of different stiffnesses

4.3 Results

4.3.1 Cell culture in self-assembling peptide scaffold RAD16-I

Three-dimensional cell cultures were prepared using the self-assembling peptide scaffold RAD16-I as a synthetic matrix for cell embedding. We stablished both soft and stiff 3D environments by changing the peptide final concentration: peptide hydrogels at 0.15% would have a storage modulus (G´) of approximately 100 Pa, while hydrogels at 0.5% have a stiffness of ≈2,500 Pa, previously measured by rheometry (**Table 7**)[243].

Table 7. Approximate stiffness of RAD16-I hydrogels (Pa) depending on peptide concentration, measured by rheometry[243]

Peptide concentration (%, w/v)	G' hydrogel (Pa)
0.15	125
0.25	450
0.3	725
0.5	2,500
0.8	8,500
1	15,000

Cells in 2D cultures were harvested and mixed with the peptide solution, which self-assembles into a nanofiber network upon contact with the cell culture medium, resulting into cells embedding in a truly 3D environment (**Figure 21a**) in macroscopic size constructs of around 5 mm diameter and 0.5 mm thickness (**Figure 21b**). Even though RAD16-I is a non-instructive matrix from the point of view of receptor recognition/activation, cells under both 3D environments (0.15% and 0.5% RAD16-I) were able to spread and interact with each other and with their surrounding matrix (**Figure 21a**). Moreover, tumor cells cultured in 3D were able to proliferate at the same rate regardless of matrix stiffness (**Figure 21c**).

This self-assembling peptide is also protein adsorbent[177]. Although it does not contain integrin-binding sites, and cannot therefore mediate ligand-dependent ECM receptor signaling *per se*, it can adsorb ECM proteins such as laminin[211], reconstituted basal membrane (rBM)[211] and fibronectin[177]. Moreover, the proteins contained in the fetal bovine serum (FBS) (most probably vitronectin and fibronectin[275]) used to supplement cell culture medium may also be responsible for cell adhesion to the peptide nanofibers[177]. We also hypothesized that cells in RAD16-I matrices could decorate their own environment by synthesizing their own extracellular matrix proteins. To confirm that proteins contained in the serum remained attached to the hydrogel we assessed protein content in cell-free RAD16-I gels incubated with 10% FBS (**Figure 22a**). We also performed fibronectin immunostaining of pancreatic cancer cells cultured in RAD16-I matrices (**Figure 22b**). We found that PANC-1 and MiaPaCa-2 cells in 3D RAD16-I hydrogels were also able to deposit and decorate their cellular environment with fibronectin (**Figure 22b**). Moreover, we detected the presence of fibronectin in cell-free regions of the 3D matrix, further confirming that fibronectin in the FBS was adsorbed into the hydrogel.
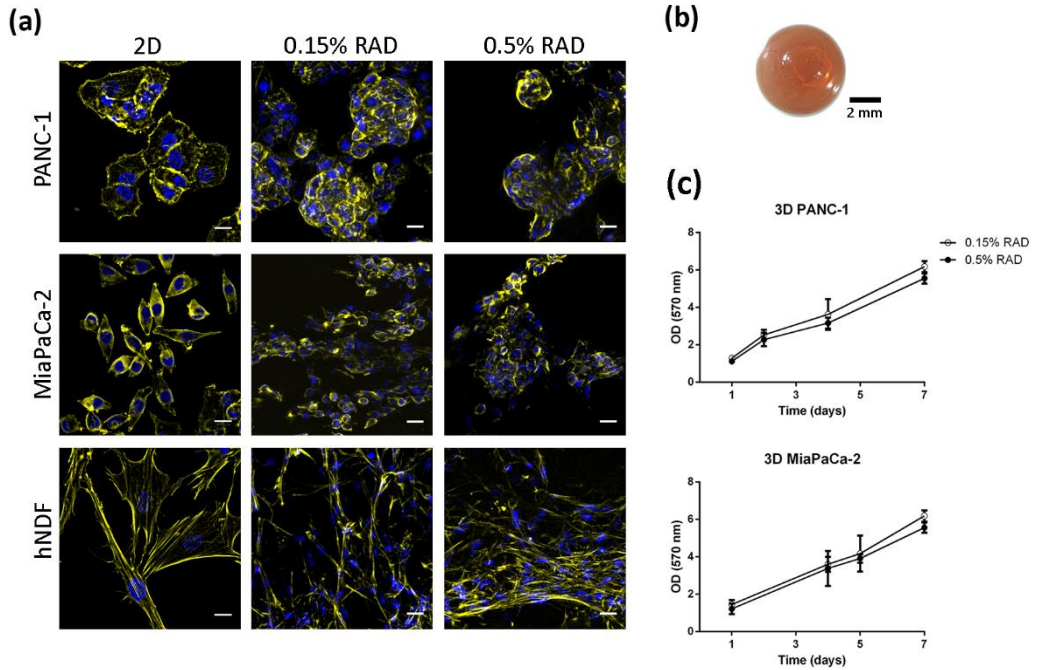
Figure 21. Cell culture in 3D RAD16-I scaffolds. (a) Cell morphology in 2D and 3D cultures. Actin (Phalloidin, pseudo-colored in yellow) and nuclei (DAPI, blue) staining of PANC-1, MiaPaCa-2 and hNDF cells cultured in classic 2D dishes and RAD16-I 3D scaffolds at two different peptide concentrations. Scale bars represent 20 µm; **(b)** Macroscopic view of 3D constructs stained with congo red for clearer visualization; **(c)** Growth curves of PANC-1 and MiaPaCa-2 cells in 0.15% and 0.5% RAD16-I.
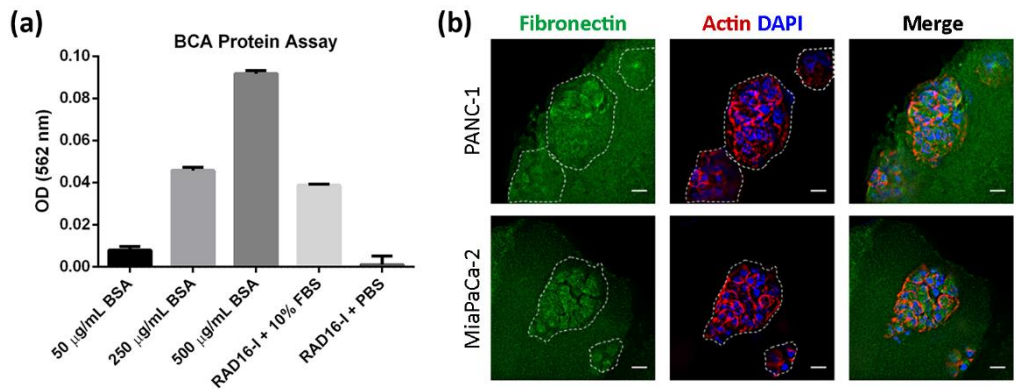
Figure 22. Protein adsorbing to RAD16-I hydrogels. (a) BCA protein assay of RAD16-I gels. The graph shows the OD values obtained for known concentrations of protein (50 µg/mL–500 µg/mL BSA) and RAD16-I hydrogels assembled with 10% FBS or PBS; **(b)** Fibronectin (green) immunofluorescence of PANC-1 and MiaPaCa-2 cells in RAD16-I 3D culture counterstained with phalloidin (red) and DAPI (blue). Scale bars represent 20 µm.

4.3.2 FAK activation analysis in RAD16-I by confocal microscopy

At a cellular level, matrix recognition and stiffness is sensed through integrins, which after engagement with the ECM, activate different downstream signaling pathways such as the focal adhesion kinase (FAK) and the extracellular-signal-regulated kinase/mitogen-activated protein kinase (ERK/MAPK)[276]. Moreover, proteins involved in signal mechanotransduction such as β1-integrin and its downstream effector FAK have been known to be more active in stiff matrices compared to soft ones in a variety of cancer cells such as gastric cancer cells and hepatocellular carcinoma cells[187,198]. Cells cultured in 2D plastic dishes, which are extremely stiff (G' ≈2.5 GPa) have been described to recruit vinculin to integrins and phosphorylate FAK at position Y397, as well as to present with actin stress fibers[69]. In accordance with previous studies[69], we found that cells in classic 2D monolayer culture on plastic dishes phosphorylated FAK at positions Y397 and Y861 (**Figure 23a, b**). Moreover β1-integrin colocalized with vinculin and actin, confirming that under stiff 2D culture conditions, integrins are active and engaged with ECM proteins (**Figure 23c, d**).
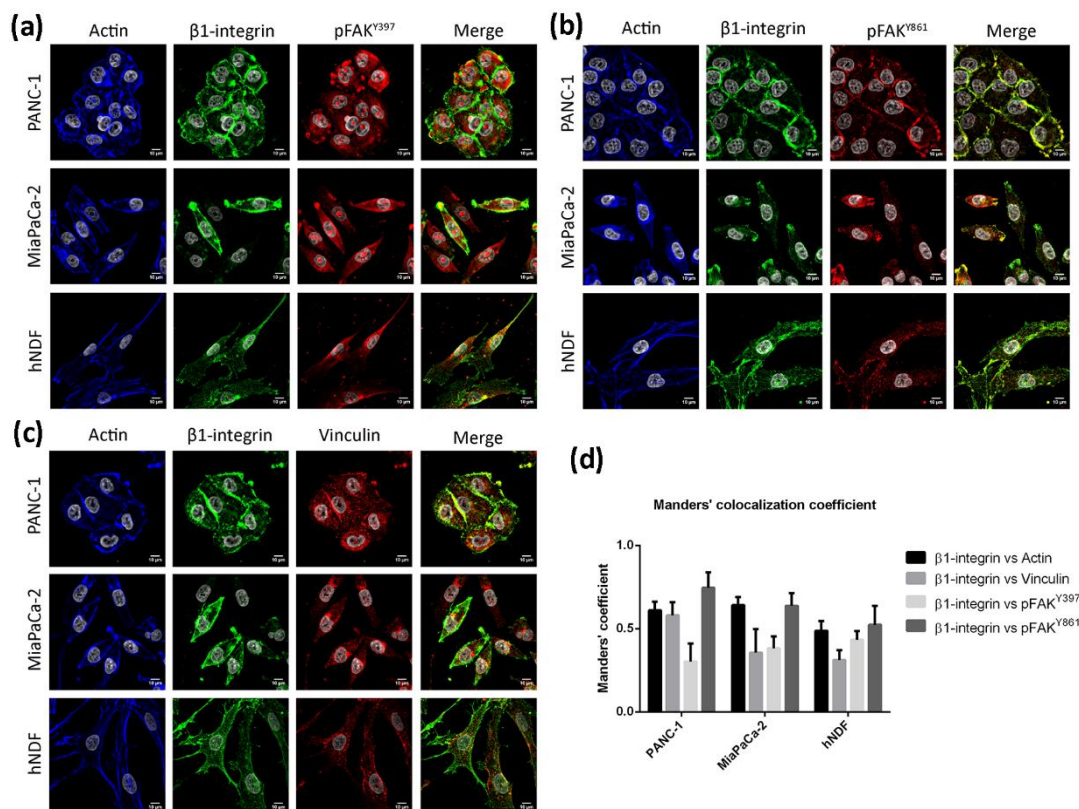
Figure 23. Immunofluorescence analysis of signal mechanotransduction proteins in 2D cultures of PANC-1, MiaPaCa-2 and hNDF cells. **(a)** Actin, β1-integrin and pFAK[Y397] staining; **(b)** Actin, β1-integrin and pFAK[Y861] staining; **(c)** Actin, β1-integrin and vinculin staining; **(d)** Manders' colocalization coefficients. Scale bars represent 10 μm.

To confirm that even being a non-instructive milieu, RAD16-I was able to trigger integrin-mediated signal transduction we performed immunofluorescence and co-localization analysis of β1-integrin and FAK in soft (0.15% RAD) and stiff (0.5% RAD) 3D matrices. We hypothesized that the fibronectin adsorbed into the hydrogel (containing RGD motif) would be enough to activate integrins and promote FAK activation. Indeed, we could detect the active form of FAK (pFAK^{Y397}) in 3D cultures in both soft and stiff matrices as well as pFAK^{Y861} (**Figure 24**). Moreover, in both 3D cultures, vinculin was detected co-localizing with β1-integrin and actin in both stiffness conditions, similar to 2D cultures. Interestingly, in PANC-1 cells, the colocalization degree of pFAK^{Y861} with β1-integrin was higher in 3D stiff and 2D cultures than 3D soft cultures, while pFAK^{Y397} in soft 3D cultures co-localized more with β1-integrin than in stiff conditions. On the other hand, no statistical differences were found in MiaPaCa-2 cells between 3D and 2D cultures.
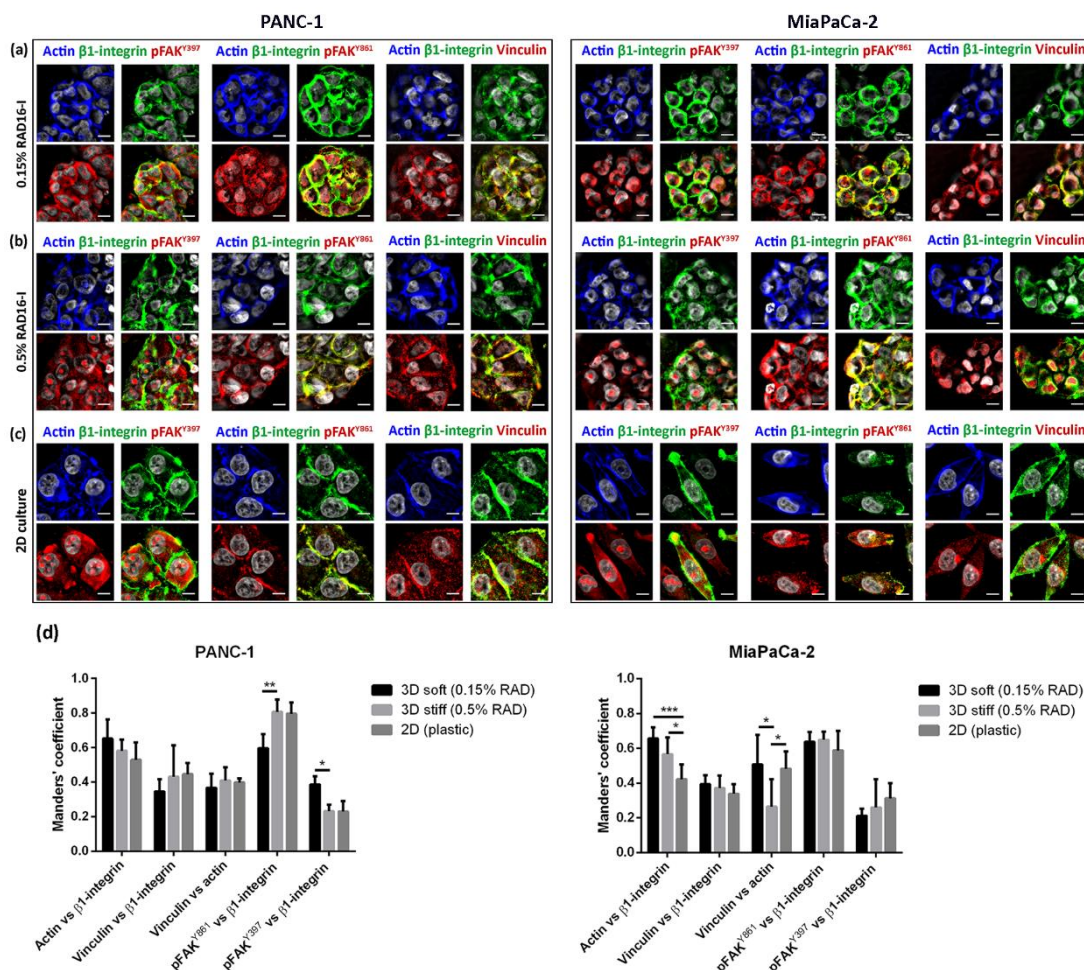
Figure 24. Immunofluorescence analysis of signal mechanotransduction proteins in 3D cultures. Actin (blue) β1-integrin (green), pFAK^{Y397} (red), pFAK^{Y861} (red) and vinculin (red) staining in PANC-1 (left) and MiaPaCa-2 (right) cells in **(a)** 0.15% RAD16-I; **(b)** 0.5% RAD16-I and; **(c)** 2D cultures. Merge of green and red channels is also shown. Scale bars represent 10 μm; **(d)** Mander's colocalization coefficients of PANC-1 and MiaPaCa-2 cells (n=5).

4.3.3 FAK activation analysis in RAD16-I by western blot

We next analyzed the expression of FAK and its active form (pFAK^{Y397}) in 2D cultures and 3D soft and stiff RAD16-I matrices by western blot (**Figure 25**). We performed these experiments with the PDAC cell lines PANC-1 (epithelial/mesenchymal phenotype) and MiaPaCa-2 (mesenchymal phenotype)[197] as well as non-tumoral human dermal fibroblasts (hNDF, mesenchymal phenotype). Results show that 2D cultures, which are extremely stiff and out of the pathophysiological range (G'≈2.5 GPa) promoted the highest total and active FAK expression. Surprisingly, stiff RAD16-I 3D cultures (≈2,500 Pa) promoted total FAK downregulation in the 3 cell types analyzed (PANC-1, MiaPaCa-2 and hNDF) (**Figure 25a, b**). However, the phosphorylation pattern of FAK was different for the two PDAC cell lines. In particular, PANC-1 cells in soft 3D matrices (100 Pa) had higher levels of both total and phosphorylated FAK, and therefore, when representing the ratio pFAK^{Y397}/FAK we found approximately a ≈2-fold downregulation in stiff matrices compared to soft ones (Figure 4b, black bars). This pattern was reversed in MiaPaCa-2 cells. In this case, cells showed similar levels of pFAK^{Y397} in both soft and stiff 3D matrices, and higher levels of total FAK in soft matrices. Therefore, when representing the ratio pFAK^{Y397}/FAK, we found that proportionally, MiaPaCa-2 in stiff matrices phosphorylated to a higher extent the FAK (Figure 4b, gray bars). Fibroblasts in 2D cultures and soft 3D cultures showed a similar pattern as PANC-1 cells, but in stiff 3D cultures both FAK and its phosphorylated form were almost undetectable (**Figure 25a**). In view of the unexpected results obtained when working with the two stiffnesses of ≈100 Pa (0.15% RAD) and ≈2,500 Pa (0.5% RAD), we also analyzed an intermediate (0.3% RAD, 700 Pa) and a higher stiffness (0.8% RAD, 8,500 Pa) in PANC-1 cells (**Table 7**). Under these conditions, western blot bands further confirmed that total FAK expression and its activated form (pFAK^{Y397}) proportionally decreased with increased matrix stiffness (**Figure 25c, d**). Finally, increased stiffness in RAD16-I 3D cultures also promoted total FAK downregulation in another PDAC cell line (BxPC-3) and in another well-known epithelial breast cancer cell line, MCF-7 (**Figure 26**).
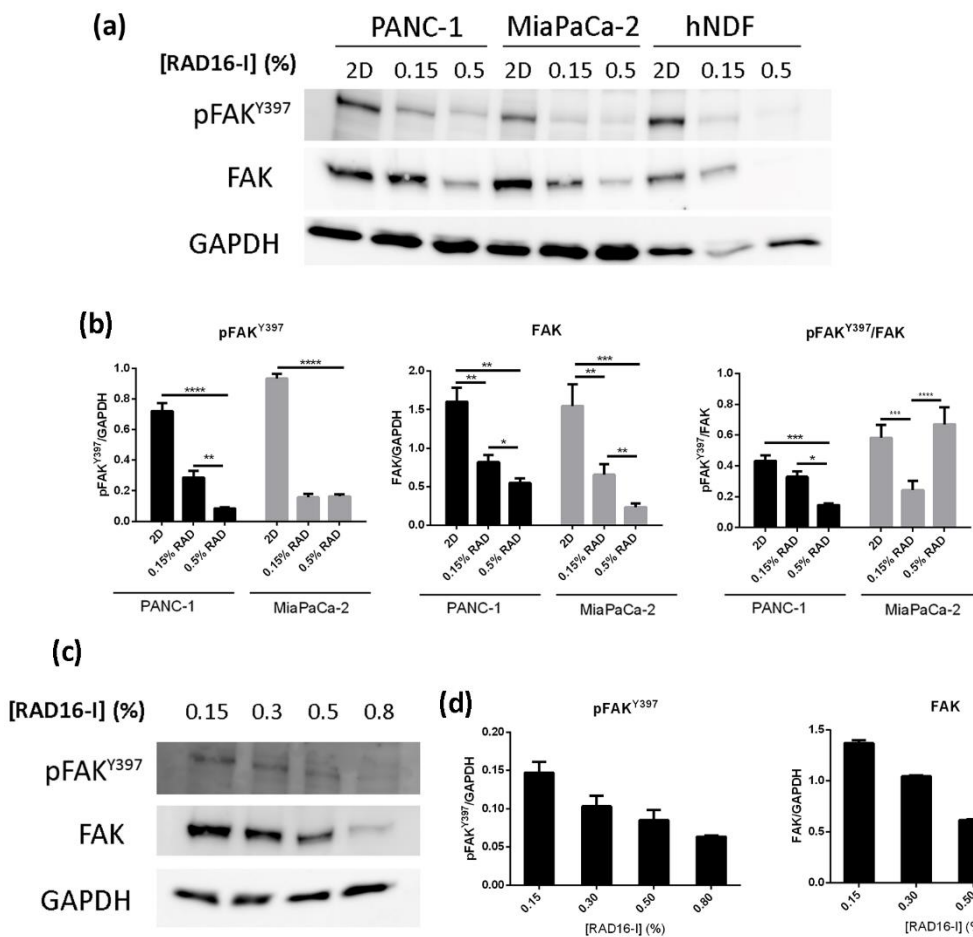
Figure 25. pFAK^Y397 and FAK expression in cancer cells lines and normal fibroblasts cultured in RAD16-I hydrogels. (a) Western blot bands of pFAK^Y397 and total FAK in PANC-1, MiaPaCa-2 and hNDF cells cultured in 2D and 0.15% (soft) and 0.5% (stiff) RAD16-I gels; **(b)** Densitometry of bands shown in **(a)**; **(c)** Western blot bands of pFAK^Y397 and total FAK in PANC-1 cells cultured in 3D RAD16-I hydrogels of increased stiffness (from 0.15% to 0.8% RAD16-I representing a stiffness range of 100 – 8,500 Pa); **(d)** Densitometry of bands shown in **(c)**. GAPDH was used as loading control.
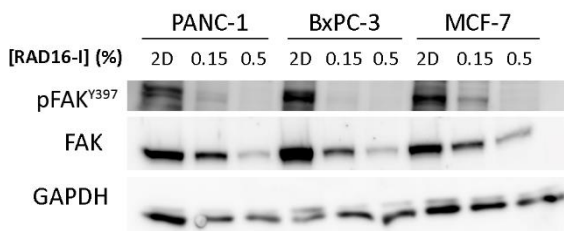
Figure 26. Western blot bands of pFAK^Y397 and FAK in PDAC cell lines (PANC-1 and BxPC-3) and the breast cancer cell line MCF-7 cultured in 2D and in RAD16-I hydrogels at 0.15% and 0.5% peptide concentration. GAPDH was used as loading control.

To determine the effect of biological signaling on FAK expression, we also functionalized RAD16-I matrices with small amounts of collagen type I, named RAD/COL gels. Collagen was successfully incorporated into RAD16-I matrices by simply mixing, and has retained after several overnight washes, as demonstrated by SDS-PAGE of cell-free gels (**Figure 27a**), which revealed the typical pattern for type I collagen with bands at approximately 215 kDa (β-chain), 130 kDa (α1 chain) and 115 kDa (α2 chain). We also detected an intense band in the bottom of the gel, corresponding to the RAD16-I peptide, with a molecular weight of approximately 2 kDa[274]. Moreover, fibroblasts in RAD/COL gels could detect the presence of collagen therefore spreading and interconnecting to each other faster than those in RAD cultures (**Figure 27b**). Western blot analysis of PANC-1 cells in functionalized matrices showed that the addition of collagen into RAD16-I gels did not induce significant differences in protein expression nor reversed the soft/stiff pattern for FAK and pFAK^{Y397} found in the non-functionalized RAD16-I matrix (**Figure 27c, d**). Moreover, Erk1/2 was found active in both stiffness conditions and no difference in their expression was found between non-instructive and collagen-functionalized matrices (**Figure 27c, d**).
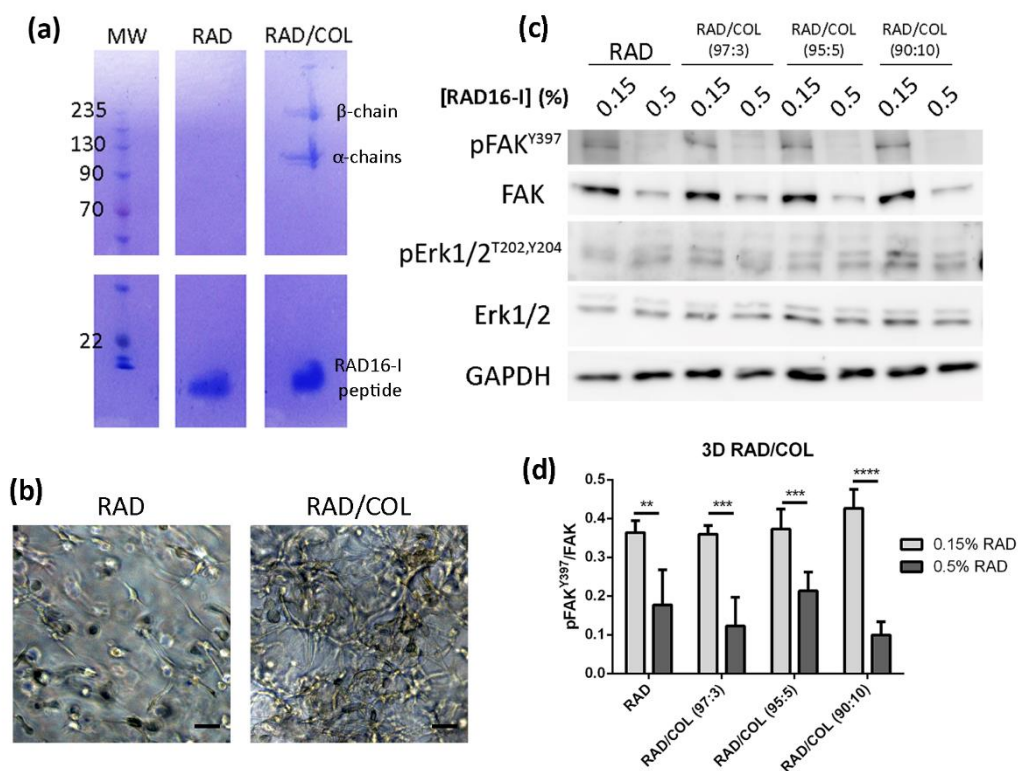
Figure 27. Cell culture in RAD16-I matrix functionalized with collagen type I. (a) SDS-PAGE of RAD or RAD/COL cell-free gels; **(b)** Phase-contrast microscopy images of fibroblast 24 h after cell embedding within 0.15% RAD or RAD/COL gels. Scale bars represent 50 μm; **(c)** Western blot bands of FAK and Erk1/2 and its phosphorylated forms in PANC-1 cells cultured in 0.15% (soft) and 0.5% (stiff) RAD16-I gels mixed with increasing amounts of collagen I; **(d)** Densitometry of pFAK^{Y397}/FAK shown in **(c)**. GAPDH was used as loading control.

The same pattern was maintained when co-culturing PANC-1 cells with dermal fibroblasts in RAD16-I 3D matrices (**Figure 28**). Therefore, we hypothesized that the effect which addition of small amounts of collagen could have on cell phenotype was probably overlapped by the proteins present in the FBS or the ones produced by the own cells (**Figure 22**).
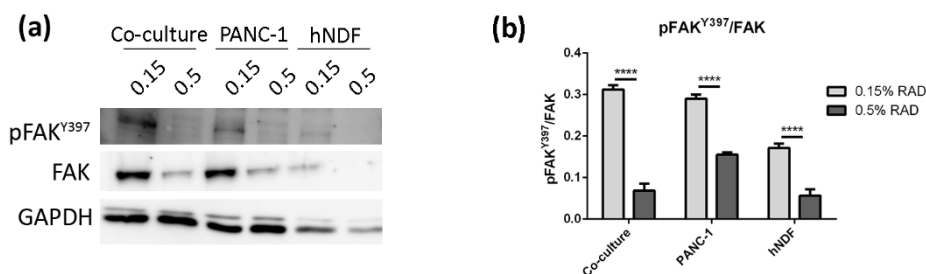
Figure 28. Analysis of FAK activation in RAD16-I 3D co-cultures and mono-cultures of PANC-1 and hNDF. **(a)** Western blot bands of FAK and pFAK[Y397]; **(b)** Densitometry of bands shown in **(a)**.

4.3.4 FAK expression in 3D collagen type I cultures

We next wanted to determine whether FAK downregulation found in 0.5% RAD16-I matrices was also observed in a classic gold standard 3D culture system such as collagen type I gels. For that, we cultured the same cells in 3D collagen gels with concentrations of 0.15% and 0.5% concentration, which have an associated stiffness of approximately 100 Pa and 3,000 Pa, respectively, determined by dynamic mechanical analysis (DMA)[277]. Spontaneous contraction of the 3D matrix was detected in soft (0.15%) collagen gels due to the strong interaction of cells with collagen fibrils through integrins[278], most probably $\alpha 2\beta 1$[278], which enabled the cells to drag the hydrogel (**Figure 29a**). This phenomenon was not observed in stiff (0.5%) collagen gels, probably because the cells could not overcome the surrounding resistance to drag the hydrogel with them, which proved the dependence between matrix contraction and stiffness. Surprisingly, we found that in this case, PDAC cells did not respond to the increased matrix stiffness, as no differences in total or active FAK expression were found (**Figure 29b, c**). This phenomenon was also reproduced in MCF-7 breast cancer cell line (**Figure 29b, c**).

Even though matrix stiffness was maintained along culture time[277], global measures of stiffness values did not necessarily represent the real local value around cells due to the potential degradation of nanofibers by cells. We hypothesized that if cells could not degrade the collagen fibers, the downregulation pattern previously observed for RAD16-I would be reproduced in collagen gels. To address this, we incubated the cells with the MMP inhibitor GM6001, but it did not cause any effect on the pattern of FAK expression or phosphorylation (**Figure 29d**), suggesting that potential collagen degradation was not affecting FAK expression or phosphorylation.
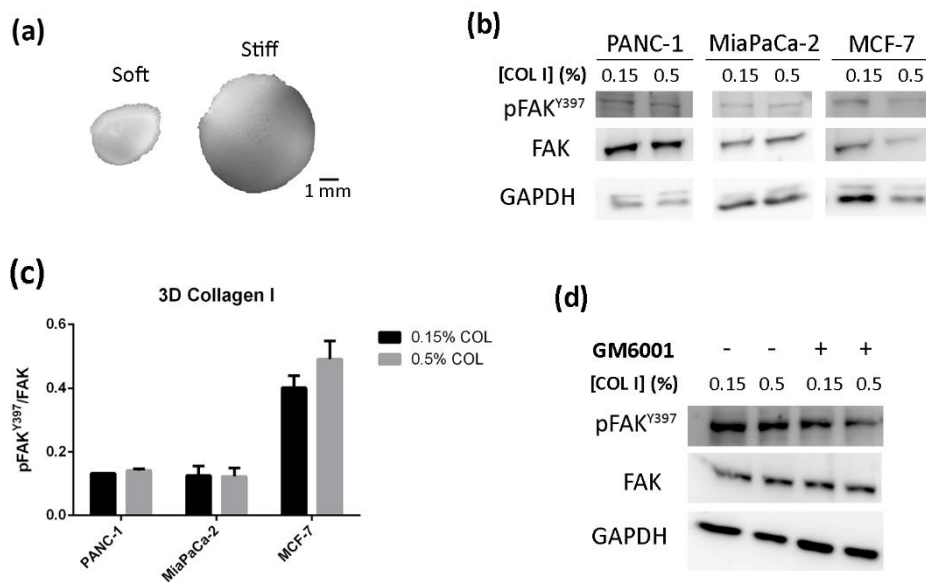
Figure 29. Cell culture in 3D collagen type I gels. (a) Macroscopic view of collagen 3D constructs containing PANC-1 cells **(b)** Western blot bands of pFAK[Y397] and total FAK in PANC-1, MiaPaCa-2 and MCF-7 cells cultured in 0.15% (soft) and 0.5% (stiff) collagen gels; **(c)** Densitometry of bands shown in **(b)** represented as pFAK[Y397]/FAK; **(d)** Western blot bands of pFAK[Y397] and total FAK in PANC-1 cells cultured in 0.15% (soft) and 0.5% (stiff) collagen gels in the presence of GM6001.

4.4 Discussion

A common feature in some cancers is an increased deposition of ECM components, mainly collagen I, which is in part responsible for the increased stiffness in these tumors. Indeed, tumor tissues such as breast cancer[69], colorectal cancer[127], pancreatic ductal adenocarcinoma (PDAC)[128] and hepatocellular carcinoma (HCC)[129] can be several folds stiffer than their healthy counterparts. Matrix stiffness influences cell fate and behavior, and therefore researchers are progressively adjusting this parameter when performing experiments. Cancer models that include stiffness as a parameter have demonstrated that it can regulate epithelial-to-mesenchymal transition (EMT)[128,188,190,200,207], resistance to chemotherapy[187,196,203], cell proliferation[187,191,195,196,200], migration[189,199,202] and invasion[203–206]. However, the use of different matrices or the experimental temporality can yield contradicting results. For example, increased stiffness has shown to promote proliferation in natural scaffolds such as collagen type I[191,198] and alginate/Matrigel[200], while restricting proliferation in cells cultured in polymeric scaffolds[195,196]. Studies using synthetic matrices in a physiological stiffness range (0 – 20 kPa) reported that invasion is mostly promoted with increased stiffness, but it is inhibited at nonphysiological higher stiffness (>20 kPa)[208]. Also, matrix stiffness has been shown to delay cell invasion[206], and therefore, studies with short endpoints[204] may not reflect the actual infiltration of cancer cells at later points, and therefore these studies likely do not report that stiffness promotes invasion[208]. Therefore, results should be interpreted in the context of each experimental design, considering not only the stiffness range but also other parameters such as the type of three-dimensional matrix used and experimental temporality[208].

Focal adhesion kinase (FAK) is a nonreceptor protein tyrosine kinase that plays a key role in tumor invasion and metastasis. FAK is a key component present in focal adhesion[92], and it is known to be sensitive to stiffness, becoming activated when recruited to focal adhesions after integrin engagement with the ECM in stiff environments. FAK is hyperactivated in several cancers, including PDAC, and it is correlated with high levels of fibrosis[279]. In vitro models to study the effect of matrix stiffness in terms of FAK activation have been developed mainly in the context of breast cancer, as mammographically dense breast tissue is one of the greatest risk factors for developing breast carcinoma. In the present chapter we were committed to develop a 3D in vitro model to study the effect of matrix stiffness in PDAC cells mainly in terms of FAK expression, as such models do not exist up to date. For that, we used a synthetic nanofiber matrix, RAD16-I, which, importantly, does not suffer a significative degradation *in vitro* in contrast to matrices from natural origin such as collagen type I[273]. For example, pancreatic cancer cell lines cultured in 3D collagen gels upregulate MT1-MMP expression, which produces changes in collagen fiber orientation and thickness as a consequence of local collagen degradation around the cells[235], therefore compromising the maintenance of the same mechanical properties along culture time. Synthetic hydrogels such as the ones formed by self-assembling peptides allow one to maintain the same experimental conditions in terms of matrix stiffness, which is vital to study signal mechanotransduction pathways in a 3D context.

RAD16-I matrix does not contain biological motifs and therefore it is non-instructive from the point of view of receptor recognition/activation. However, RAD16-I has been proven to be protein adsorbent (**Figure 22a**). In particular, we detected the presence of fibronectin, which could be both soluble fibronectin from the FBS used for medium supplementation and/or fibronectin secreted by the cells (**Figure 22b**). Fibronectin, as well as other ECM proteins, is usually secreted by resident cells in stromal compartments, such as pancreatic stellate cells (PSCs)[24]. However, pancreatic epithelial cells have also been described to synthesize and secret fibronectin as part of their malignant transformation during tumor initiation and progression[211]. Consistent with previous results reporting fibronectin synthesis in pancreatic cancer cells cultured in 3D collagen and Matrigel hydrogels[197,235], PDAC cells in RAD16-I were also able to decorate their environment with fibronectin (**Figure 22**). Therefore, it is likely that fibronectin or other RGD-containing proteins present in the FBS or synthesized by the cells and adsorbed into the RAD16-I hydrogel are mediating integrin signaling in said 3D system. In fact, our results show that vinculin and actin are recruited to β1 integrin adhesions in both soft and stiff 3D environments similar to 2D cultures, and also that FAK activation occurs in both stiffness conditions (**Figure 24**). This contradicts previous studies that show that only mammary epithelial cells (MECs) within a stiff matrix can phosphorylate FAK[Y397] and recruit vinculin to β1 integrin adhesions[69]. Interestingly, the same study reports that MECs in a soft matrix express higher amounts of total and active Src family kinases (Src, Lyn and Lck)[69] compared to stiff matrices, while others propose the contrary[191]. In our case, cells in a soft synthetic matrix expressed higher amounts of total FAK than in stiff matrices in all cell types analyzed, while phosphorylation at position Y397 and the resulting pFAK[Y397]/FAK ratio was cell-type dependent (**Figure 25**).

We next wanted to test if the binding of distinct specific integrins to different ECM proteins could be the reason for these results. For that, we functionalized RAD16-I with small amounts of collagen type I. Collagen has previously been incorporated into Fmoc-based self-assembling peptide hydrogels by simple diffusion[280], and has been shown to interact with the hydrogel fibers without affecting the overall mechanical properties. Moreover, collagen molecules incorporated into the hydrogels were biologically active and provided sites for adhesion through interaction with the α2β1 integrin[280]. We have successfully incorporated collagen type I into RAD16-I hydrogels by simply mixing the collagen solution with the peptide before inducing the self-assembling. Collagen was retained in the hydrogel after several washes, as demonstrated by SDS-PAGE (**Figure 27a**). Moreover, fibroblasts spreading in RAD/COL gels demonstrates that collagen was still biologically active and provided sites for cell adhesion (**Figure 27b**). However, the addition of collagen into RAD16-I hydrogels had no effect on FAK expression, as the same downregulation pattern with increased stiffness obtained for only RAD16-I hydrogels was observed (**Figure 27c, d**).

To address these unexpected results, we cultured the cells in classic 3D full collagen type I hydrogels. Surprisingly, we found that neither PDAC cells nor breast cancer cells responded to the increased matrix stiffness, as total and active FAK levels were maintained constant between both conditions (**Figure 29**). Importantly, while PANC-1 cells express the collagen-recognizing integrin α2β1, MiaPaCa-2 cells lack both integrins that bind to collagen (α1β1 and α2β1) and did not attach or proliferate when cultured on top of type I collagen gels[281]. However, both cell lines were able to phosphorylate

FAK at Y397, independently of their integrin expression pattern. Therefore, it is probable that serum proteins such as fibronectin are also adsorbed into collagen fibers[282,283], and cells are actually recognizing and binding through RGD-containing proteins and not directly to collagen fibers.

It has recently been proposed that more confining matrix architectures reduce cell adhesions to the matrix and decrease pFAK^{Y397} levels[284]. Increasing peptide concentration significantly affects the stiffness of the resulting self-assembling peptide gel, however the geometry of the nanofibers, such as pore size, may also be changing[211,243], and therefore, cells in stiffer hydrogels are under more constraining conditions. While cells in such synthetic environments cannot degrade the nanofibers due to the absence of degradation sites, cells within 3D collagen gels can rely on enzymatic proteolysis to remodel their surrounding matrix and relieve constraints[235]. We hypothesized that because cells in collagen matrices could be locally degrading the collagen fibers, cells in stiffer matrices may sense the same stiffness that exists in softer matrices as a result of matrix degradation, and for this reason no changes were detected at the level of FAK phosphorylation or expression. To address this, we incubated PANC-1 cells with a broad-spectrum MMP inhibitor (**Figure 29d**), expecting an increase in pFAK^{Y397} expression in stiff collagen gels, but not differences were detected. Therefore, collagen degradation by cell-secreted MMPs was probably not the reason that FAK downregulation found in stiff RAD16-I cultures was not being reproduced in stiff collagen gels. Other hypothesis that could explain these differences between synthetic and natural 3D matrices could be integrin co-signaling competition events between fibronectin and collagen, as well as differences in hydrogel nanostructure features between collagen type I nanofibers and self-assembling peptide scaffold networks. In fact, it has been reported that RAD16-I gels self-assembled in longer nanofibers and formed an increased amount of cross-links and fibril entanglements compared to collagen type[285].

4.5 Concluding remarks

In this chapter we have developed a 3D cancer cell culture system to study the effect of matrix stiffness on PDAC cells. Even though being a non-instructive milieu, RAD16-I allowed FAK activation in both stiffness conditions, probably via integrin binding to ECM proteins adsorbed to the hydrogel nanofibers, which decorated the matrix and allowed cell adhesion and receptor activation. We also found that cells responded differently to matrix stiffness when cultured in synthetic (RAD16-I) or in natural (Collagen I) matrices. In particular, stiff RAD16-I gels induced a downregulation of total FAK protein, while cells in collagen I maintained similar levels of total and phosphorylated FAK regardless of matrix stiffness. Moreover, changes in the ratio $pFAK^{Y397}$/FAK due to increased stiffness in 3D RAD16-I cultures were cell type-dependent. Even though self-assembling peptide scaffolds closely mimic the fiber architecture found in some natural matrices such as collagen type I gels, cell response to increased stiffness strongly differed in both types of matrices.

CONCLUSIONS

Three-dimensional cell culture models for pancreatic ductal adenocarcinoma were developed by deconstructing the complex tumor microenvironment into three basic parameters: dimensionality, stiffness and biological signaling.

The contribution of the microenvironment on drug resistance to tyrosine kinase inhibitors was studied using synthetic RAD16-I matrices. A new model for EGFR trafficking and degradation due to EGF and erlotinib treatment was developed:

- Cell viability after erlotinib treatment was evaluated in 2D and 3D cultures. Erlotinib IC_{50} doubled in the erlotinib-insensitive PANC-1 cells cultured in RAD16-I 3D cultures compared to 2D cultures. In erlotinib-sensitive BxPC-3 cells and in normal fibroblasts the IC_{50} remained constant regardless of culture dimensionality.

- Treatment with erlotinib combined with EGF, but not alone, promoted strong EGFR degradation via lysosomes in 3D cultures but not in 2D cultures of PDAC cell lines. These results suggest that in 3D culture, ligand binding is necessary for receptor endocytosis, and that upon internalization, erlotinib promotes its lysosomal degradation.

- EGFR degradation due to erlotinib treatment did not occur in normal fibroblast cells regardless of culture dimensionality, probably because erlotinib prevented EGF-induced receptor internalization.

- EGFR degradation in 3D cultures did not sensitize the cells to erlotinib treatment, suggesting that in this 3D environment PDAC cells acquired additional resistance mechanisms that allowed them to survive independently of the EGFR signaling pathway.

The contribution of the microenvironment on triggering signal mechanotransduction pathways and focal adhesion kinase (FAK) activation was studied using synthetic RAD16-I matrices and natural collagen I matrices of different stiffnesses:

- Even though being a non-instructive milieu, RAD16-I promoted FAK activation in both stiffness conditions, probably via integrin binding to ECM proteins adsorbed to the hydrogel nanofibers, which decorated the matrix and allowed cell adhesion and receptor activation.

- Increased stiffness promoted total FAK downregulation in 3D cultures of RAD16-I but not in collagen I hydrogels.

- Changes in the ratio $pFAK^{Y397}/FAK$ due to increased stiffness in 3D RAD16-I cultures were found to be cell type-dependent. In 3D collagen cultures, the ratio $pFAK^{Y397}/FAK$ remained constant regardless of the increased stiffness within the stiffness range analyzed.

- RAD16-I was successfully functionalized with small amounts of collagen I, which was still biologically active and provided sites for cell adhesion. However, the addition of collagen into RAD16-I hydrogels had no effect on FAK expression compared to non-functionalized RAD16-I scaffolds.

CONCLUSIONS

S'han desenvolupat models de cultiu cel·lular en 3D d'adenocarcinoma ductal pancreàtic deconstruïnt el complex microambient tumoral en tres paràmetres bàsics: dimensió, duresa i senyals biològiques.

S'ha estudiat la contribució del microambient en la resistència a fàrmacs inhibidors de tirosina quinasa utilitzant la matriu sintètica RAD16-I. S'ha desenvolupat un nou model per estudiar el tràfic intracel·lular i la degradació del EGFR degut al tractament amb EGF i erlotinib:

- S'ha avaluat la viabilitat cel·lular després del tractament amb erlotinib en cultius 2D i 3D. La CI_{50} de l'erlotinib en la línia cel·lular insensible PANC-1 es va doblar en cultius 3D en RAD16-I comparat amb els cultius en 2D. En la línia cel·lular sensible a l'erlotinib BxPC-3 i en fibroblasts normals, la CI_{50} es va mantenir constant independentment de la dimensió del cultiu.

- El tractament amb erlotinib combinat amb EGF, però no tot sol, va promoure una forta degradació del EGFR via lisosomes en cultius 3D però no en cultius 2D de línies cel·lulars de càncer pancreàtic. Aquests resultats suggereixen que en cultius 3D, la unió del lligand és necessària per a l'endocitosi del receptor, i que un cop internalitzat, l'erlotinib promou la seva degradació en lisosomes.

- La degradació del EGFR deguda al tractament amb erlotinib no va succeir en fibroblasts, independentment de la dimensió del cultiu, probablement degut a que l'erlotinib evitava la internalització del receptor induïda per EGF.

- La degradació del EGFR en cultius 3D no va sensibilitzar les cèl·lules al tractament amb erlotinib, suggerint que en aquest ambient 3D, les cèl·lules de càncer pancreàtic adquirien mecanismes de resistència addicionals que els hi permetien sobreviure independentment de la senyalització del EGFR.

S'ha estudiat la contribució del microambient en desencadenar vies de mecanotransducció de senyals i l'activació de la quinasa d'adhesions focals (FAK) utilitzant matrius d'origen sintètic (RAD16-I) i natural (Col·lagen tipus I) de diferents dureses:

- Tot i ser un ambient no instructiu, RAD16-I va promoure l'activació de FAK en les dues condiciones de duresa testades, probablement via unió d'integrines a proteïnes de la matriu extracel·lular adsorbides a les nanofibres de l'hidrogel, que decoraven la matriu i van permetre l'adhesió cel·lular i l'activació de receptors.

- L'augment de duresa va promoure la regulació negativa de FAK en cultius 3D de RAD16-I però no en col·lagen tipus I.

- Els canvis en el ratio pFAK^{Y397}/FAK associats a l'augment de duresa en cultius 3D de RAD16-I eren dependents del tipus de cèl·lula. En cultius 3D de col·lagen, el ratio pFAK^{Y397}/FAK es mantenia constant independentment de l'augment de duresa, dins del rang analitzat.

- La matriu RAD16-I es va funcionalitzar amb petites quantitats de col·lagen, que es va mantenir biològicament actiu i proporcionava llocs d'adhesió cel·lular. No obstant, l'addició de col·lagen a hidrogels de RAD16-I no va tenir cap efecte en l'expressió de FAK comparat amb hidrogels de RAD16-I no modificats.

CONCLUSIONES

Se han desarrollado modelos de cultivo celular en 3D de adenocarcinoma ductal pancreático deconstruyendo el complejo microambiente tumoral en tres parámetros básicos: dimensionalidad, dureza i señales biológicas.

Se ha estudiado la contribución del microambiente en la resistencia a fármacos inhibidores de tirosina quinasa utilizando la matriz sintética RAD16-I. Se ha desarrollado un nuevo modelo para estudiar el tráfico intracelular y la degradación del EGFR debida al tratamiento con EGF y erlotinib:

- Se ha evaluado la viabilidad celular después del tratamiento con erlotinib en cultivos 2D y 3D. La CI_{50} del erlotinib en la línea celular insensible PANC-1 se dobló en cultivos 3D en RAD16-I comparado con los cultivos en 2D. En la línea celular sensible al erlotinib BxPC-3 y en fibroblastos normales, la CI_{50} se mantuvo constante independientemente de la dimensionalidad del cultivo.

- El tratamiento con erlotinib combinado con EGF, pero no por sí solo, promovió una fuerte degradación del EGFR vía lisosomas en cultivos 3D, pero no en cultivos 2D, de líneas celulares de cáncer pancreático. Estos resultados sugieren que en cultivos 3D, la unión del ligando es necesaria para la endocitosis del receptor, y que una vez internalizado, el erlotinib promueve su degradación en lisosomas.

- La degradación del EGFR debida al tratamiento con erlotinib no sucedió en fibroblastos, independientemente de la dimensionalidad del cultivo, probablemente debido a que el erlotinib evitaba la internalización del receptor inducida por EGF.

- La degradación del EGFR en cultivos 3D no sensibilizó las células al tratamiento con erlotinib, sugiriendo que en este ambiente 3D, las células de cáncer pancreático adquieren mecanismos de resistencia adicionales que les permiten sobrevivir independientemente de la señalización del EGFR.

Se ha estudiado la contribución del microambiente en desencadenar vías de mecanotransducción de señales y la activación de la quinasa de adhesiones focales (FAK) utilizando matrices de origen sintético (RAD16-I) y natural (Colágeno tipo I) de diferentes durezas:

- Aunque es un ambiente no instructivo, RAD16-I promovió la activación de FAK en las dos condiciones de dureza testadas, probablemente vía unión de integrinas a proteínas de la matriz extracelular adsorbidas a las nanofibras del hidrogel, que decoraban la matriz y permitieron la adhesión celular y la activación de receptores.

- El augmento de dureza promovió la regulación negativa de FAK en cultivos 3D de RAD16-I pero no en colágeno tipo I.

- Los cambios en el ratio pFAK^{Y397}/FAK asociados al augmento de dureza en cultivos 3D de RAD16-I fueron dependientes del tipo de célula. En cultivos 3D de colágeno, el ratio pFAK^{Y397}/FAK se mantuvo constante independientemente del aumento de dureza, dentro del rango analizado.

- La matriz RAD16-I se modificó con pequeñas cantidades de colágeno, que se mantuvo biológicamente activo y proporcionaba sitios de adhesión celular. No obstante, la adición de colágeno a hidrogeles de RAD16-I no tuvo ningún efecto en la expresión de FAK comparado con hidrogeles de RAD16-I no modificados.

PUBLICATIONS

ARTICLES PUBLISHED FROM THIS THESIS

- **Betriu, N.**, Andreeva, A., & Semino, C.E. (2021). Erlotinib Promotes Ligand-Induced EGFR Degradation in 3D but Not 2D Cultures of Pancreatic Ductal Adenocarcinoma Cells. *Cancers*, *13*(18), 4504.

- **Betriu, N.**, Andreeva, A., Alonso, A., & Semino, C.E. (2022). Increased stiffness downregulates focal adhesion kinase expression in pancreatic cancer cells cultured in 3D self-assembling peptide scaffolds. *Biomedicines*, *10*(8), 1835.

OTHER ARTICLES PUBLISHED DURING THE COURSE OF THIS THESIS

RESEARCH ARTICLES

- **Betriu, N**., Jarrosson-Moral, C., Semino, C.E. (2020). Culture and Differentiation of Human Hair Follicle Dermal Papilla Cells in a Soft 3D Self-assembling Peptide Scaffold. *Biomolecules*, *10*(5), 684

- Genové, E., **Betriu, N.,** Semino, C.E. (2022). β-Sheet to Random Coil Transition in Self-assembling Peptide Scaffolds Promotes Proteolytic Degradation. *Biomolecules*, *12*(3), 411.

REVIEW ARTICLES

- **Betriu, N.,** Bertran-Mas, J., Andreeva, A., Semino, C.E. (2021). Syndecans and Pancreatic Ductal Adenocarcinoma. *Biomolecules*, *11*(3), 349

REFERENCES

1. Siegel, R. L., Miller, K. D. & Jemal, A. Cancer statistics, 2019. *CA. Cancer J. Clin.* **69**, 7–34 (2019).

2. Rawla, P., Sunkara, T. & Gaduputi, V. Epidemiology of Pancreatic Cancer: Global Trends, Etiology and Risk Factors. *World J. Oncol.* **10**, 10–27 (2019).

3. Yuan, C. *et al.* Cigarette smoking and pancreatic cancer survival. *J. Clin. Oncol.* **35**, 1822–1828 (2017).

4. Goral, V. Pancreatic cancer: Pathogenesis and diagnosis. *Asian Pacific J. Cancer Prev.* **16**, 5619–5624 (2015).

5. Grant, T. J., Hua, K. & Singh, A. Molecular Pathogenesis of Pancreatic Cancer. *Prog. Mol. Biol. Transl. Sci.* **144**, 241–275 (2016).

6. Lemmon, M. A. & Schlessinger, J. Cell signaling by receptor-tyrosine kinases. *Cell* **141**, 1117–1134 (2010).

7. Alberts, B. *et al.* Molecular biology of the cell. 3rd. *New York Garl. Pub* **43**, 67 (1994).

8. Hynes, R. O. The Extracellular Matrix: Not Just Pretty Fibrils. *Science* **326**, 1216–1219 (2009).

9. Klein, G., Vellenga, E., Fraaije, M. W., Kamps, W. A. & de Bont, E. S. J. M. The possible role of matrix metalloproteinase (MMP)-2 and MMP-9 in cancer, e.g. acute leukemia. *Crit. Rev. Oncol. Hematol.* **50**, 87–100 (2004).

10. Laklai, H. *et al.* Genotype tunes pancreatic ductal adenocarcinoma tissue tension to induce matricellular-fibrosis and tumor progression. *Nat. med.* **22**, 497–505 (2016).

11. Weniger, M., Honselmann, K. C. & Liss, A. S. The extracellular matrix and pancreatic cancer: A complex relationship. *Cancers* **10**, 316 (2018).

12. Makohon-Moore, A. & Iacobuzio-Donahue, C. A. Pancreatic cancer biology and genetics from an evolutionary perspective. *Nat. Rev. Cancer* **16**, 553–565 (2016).

13. Gao, H. L., Wang, W. Q., Yu, X. J. & Liu, L. Molecular drivers and cells of origin in pancreatic ductal adenocarcinoma and pancreatic neuroendocrine carcinoma. *Exp. Hematol. Oncol.* **9**, 1–10 (2020).

14. Chaipinyo, K., Oakes, B. W. & Van Damme, M. P. I. Effects of growth factors on cell proliferation and matrix synthesis of low-density, primary bovine chondrocytes cultured in collagen I gels. *J. Orthop. Res.* **20**, 1070–1078 (2002).

15. Roth, M. T., Cardin, D. B. & Berlin, J. D. Recent advances in the treatment of pancreatic cancer. *F1000Research* **9**, 1–7 (2020).

16. Kota, J., Hancock, J., Kwon, J. & Korc, M. Pancreatic cancer: Stroma and its current and emerging targeted therapies. *Cancer Lett.* **391**, 38–49 (2017).

17. Koikawa, K. *et al.* Basement membrane destruction by pancreatic stellate cells leads to local invasion in pancreatic ductal adenocarcinoma. *Cancer Lett.* **425**, 65–77 (2018).

18. Zhan, H. xiang *et al.* Crosstalk between stromal cells and cancer cells in pancreatic cancer: New insights into stromal biology. *Cancer Lett.* **392**, 83–93 (2017).

19. Fujita, H. *et al.* Tumor-stromal interactions with direct cell contacts enhance proliferation of human pancreatic carcinoma cells. *Cancer Sci.* **100**, 2309–2317 (2009).

20. Apte, M. V *et al.* Desmoplastic Reaction in Pancreatic Cancer: Role of Pancreatic Stellate Cells. *Pancreas* **29**, 179–187 (2004).

21. Kikuta, K. *et al.* Pancreatic stellate cells promote epithelial-mesenchymal transition in pancreatic cancer cells. *Biochem. Biophys. Res. Commun.* **403**, 380–384 (2010).

22. Pothula, S. P. *et al.* Key role of pancreatic stellate cells in pancreatic cancer. *Cancer Lett.* **381**, 194–200 (2016).

23. Lachowski, D. *et al.* Substrate Rigidity Controls Activation and Durotaxis in Pancreatic Stellate Cells. *Sci. Rep.* **7**, 1–12 (2017).

24. Amrutkar, M., Aasrum, M., Verbeke, C. S. & Gladhaug, I. P. Secretion of fibronectin by human pancreatic stellate cells promotes chemoresistance to gemcitabine in pancreatic cancer cells. *BMC Cancer* **19**, 1–16 (2019).

25. Conroy, T. *et al.* FOLFIRINOX or Gemcitabine as Adjuvant Therapy for Pancreatic Cancer. *N. Engl. J. Med.* **379**, 2395–2406 (2018).

26. Tempero, M. A. *et al.* APACT: phase III, multicenter, international, open-label, randomized trial of adjuvant nab-paclitaxel plus gemcitabine (nab-P/G) vs gemcitabine (G) for surgically resected pancreatic adenocarcinoma. *J. Clin. Oncol.* **37**, 4000 (2019).

27. Hingorani, S. R. *et al.* HALO 202: Randomized Phase II Study of PEGPH20 Plus Nab-Paclitaxel/Gemcitabine Versus Nab-Paclitaxel/Gemcitabine in Patients With Untreated, Metastatic Pancreatic Ductal Adenocarcinoma. *J. Clin. Oncol.* **36**, 359–366 (2018).

28. Meng, H. *et al.* Two-Wave Nanotherapy To Target the Stroma and Optimize Gemcitabine Delivery To a Human Pancreatic Cancer Model in Mice. *ACS Nano* **7**, 10048–10065 (2013).

29. Han, H. *et al.* Metformin-Induced Stromal Depletion to Enhance the Penetration of Gemcitabine-Loaded Magnetic Nanoparticles for Pancreatic Cancer Targeted Therapy. *J. Am. Chem. Soc.* **142**, 4944–4954 (2020).

30. Apte, M. V, Pirola, R. C. & Wilson, J. S. Pancreatic stellate cells: a starring role in normal and diseased pancreas. *Front. Physiol.* **3**, 344 (2012).

31. Phillips, P. A. *et al.* Rat pancreatic stellate cells secrete matrix metalloproteinases: implications for extracellular matrix turnover. *Gut* **52**, 275–282 (2003).

32. Bachem, M. G. *et al.* Pancreatic carcinoma cells induce fibrosis by stimulating proliferation and matrix synthesis of stellate cells. *Gastroenterology* **128**, 907–921 (2005).

33. Löhr, M. *et al.* Transforming growth factor-beta1 induces desmoplasia in an experimental model of human pancreatic carcinoma. *Cancer Res.* **61**, 550–555 (2001).

34. Bailey, J. M. *et al.* Sonic hedgehog promotes desmoplasia in pancreatic cancer. *Clin. cancer Res. an Off. J. Am. Assoc. Cancer Res.* **14**, 5995–6004 (2008).

35. Thayer, S. P. *et al.* Hedgehog is an early and late mediator of pancreatic cancer tumorigenesis. *Nature* **425**, 851–856 (2003).

36. Imamura, T. *et al.* Quantitative analysis of collagen and collagen subtypes I, III, and V in human pancreatic cancer, tumor-associated chronic pancreatitis, and alcoholic chronic pancreatitis. *Pancreas* **11**, 357–364 (1995).

37. Mollenhauer, J., Roether, I. & Kern, H. F. Distribution of extracellular matrix proteins in pancreatic ductal

adenocarcinoma and its influence on tumor cell proliferation in vitro. *Pancreas* **2**, 14–24 (1987).

38. Linder, S., Castaños-Velez, E., von Rosen, A. & Biberfeld, P. Immunohistochemical expression of extracellular matrix proteins and adhesion molecules in pancreatic carcinoma. *Hepatogastroenterology.* **48**, 1321–1327 (2001).

39. Olivares, O. *et al.* Collagen-derived proline promotes pancreatic ductal adenocarcinoma cell survival under nutrient limited conditions. *Nat. Commun.* **8**, 16031 (2017).

40. Lu, J. *et al.* Pancreatic stellate cells promote hapto-migration of cancer cells through collagen I-mediated signalling pathway. *Br. J. Cancer* **110**, 409–420 (2014).

41. Koenig, A., Mueller, C., Hasel, C., Adler, G. & Menke, A. Collagen type I induces disruption of E-cadherin-mediated cell-cell contacts and promotes proliferation of pancreatic carcinoma cells. *Cancer Res.* **66**, 4662–4671 (2006).

42. Menke, A. *et al.* Down-regulation of E-cadherin gene expression by collagen type I and type III in pancreatic cancer cell lines. *Cancer Res.* **61**, 3508–3517 (2001).

43. Perl, A. K., Wilgenbus, P., Dahl, U., Semb, H. & Christofori, G. A causal role for E-cadherin in the transition from adenoma to carcinoma. *Nature* **392**, 190–193 (1998).

44. Nakajima, S. *et al.* N-cadherin expression and epithelial-mesenchymal transition in pancreatic carcinoma. *Clin. cancer Res. an Off. J. Am. Assoc. Cancer Res.* **10**, 4125–4133 (2004).

45. Shintani, Y. *et al.* Collagen I-mediated up-regulation of N-cadherin requires cooperative signals from integrins and discoidin domain receptor 1. *J. Cell Biol.* **180**, 1277–1289 (2008).

46. Miller, B. W. *et al.* Targeting the LOX/hypoxia axis reverses many of the features that make pancreatic cancer deadly: inhibition of LOX abrogates metastasis and enhances drug efficacy. *EMBO Mol. Med.* **7**, 1063–1076 (2015).

47. Cox, T. R. *et al.* LOX-mediated collagen crosslinking is responsible for fibrosis-enhanced metastasis. *Cancer Res.* **73**, 1721–1732 (2013).

48. Lee, J. *et al.* Tissue Transglutaminase Mediated Tumor-Stroma Interaction Promotes Pancreatic Cancer Progression. *Clin. cancer Res. an Off. J. Am. Assoc. Cancer Res.* **21**, 4482–4493 (2015).

49. Giancotti, F. G. & Ruoslahti, E. Integrin signaling. *Science* **285**, 1028–1032 (1999).

50. Yao, H. *et al.* Role of α(5)β(1) Integrin Up-regulation in Radiation-Induced Invasion by Human Pancreatic Cancer Cells. *Transl. Oncol.* **4**, 282–292 (2011).

51. Miyamoto, H. *et al.* Tumor-stroma interaction of human pancreatic cancer: acquired resistance to anticancer drugs and proliferation regulation is dependent on extracellular matrix proteins. *Pancreas* **28**, 38–44 (2004).

52. Edderkaoui, M. *et al.* Extracellular matrix stimulates reactive oxygen species production and increases pancreatic cancer cell survival through 5-lipoxygenase and NADPH oxidase. *Am. J. Physiol. Gastrointest. Liver Physiol.* **289**, G1137-47 (2005).

53. Dallas, S. L. *et al.* Fibronectin regulates latent transforming growth factor-beta (TGF beta) by controlling matrix assembly of latent TGF beta-binding protein-1. *J. Biol. Chem.* **280**, 18871–18880 (2005).

54. Theocharis, A. D., Tsara, M. E., Papageorgacopoulou, N., Karavias, D. D. & Theocharis, D. A. Pancreatic carcinoma is characterized by elevated content of hyaluronan and chondroitin sulfate with altered disaccharide composition. *Biochim. Biophys. Acta - Mol. Basis Dis.* **1502**, 201–206 (2000).

55. Thompson, C. B. *et al.* Enzymatic depletion of tumor hyaluronan induces antitumor responses in preclinical animal models. *Mol. Cancer Ther.* **9**, 3052–3064 (2010).

56. Provenzano, P. P. *et al.* Enzymatic targeting of the stroma ablates physical barriers to treatment of pancreatic ductal adenocarcinoma. *Cancer Cell* **21**, 418–429 (2012).

57. Cheng, X.-B., Kohi, S., Koga, A., Hirata, K. & Sato, N. Hyaluronan stimulates pancreatic cancer cell motility. *Oncotarget* **7**, 4829–4840 (2016).

58. Kohi, S. *et al.* Hyaluromycin, a Novel Hyaluronidase Inhibitor, Attenuates Pancreatic Cancer Cell Migration and Proliferation. *J. Oncol.* **2016**, 9063087 (2016).

59. Lu, P., Takai, K., Weaver, V. M. & Werb, Z. Extracellular Matrix degradation and remodeling in development and disease. *Cold Spring Harb. Perspect. Biol.* **3**, 1–24 (2011).

60. Camelliti, P., Borg, T. K. & Kohl, P. Structural and functional characterisation of cardiac fibroblasts. *Cardiovasc. Res.* **65**, 40–51 (2005).

61. Ramos, C. *et al.* Fibroblasts from idiopathic pulmonary fibrosis and normal lungs differ in growth rate, apoptosis, and tissue inhibitor of metalloproteinases expression. *Am. J. Respir. Cell Mol. Biol.* **24**, 591–598 (2001).

62. Kühl, U. *et al.* Role of muscle fibroblasts in the deposition of type-IV collagen in the basal lamina of myotubes. *Differentiation* **28**, 164–172 (1984).

63. Nagase, H., Visse, R. & Murphy, G. Structure and function of matrix metalloproteinases and TIMPs. *Cardiovasc. Res.* **69**, 562–573 (2006).

64. Kielty, C. M. Elastic fibres in health and disease. *Expert Rev. Mol. Med.* **8**, 1–23 (2006).

65. Humphrey, J. D., Dufresne, E. R. & Schwartz, M. A. Mechanotransduction and extracellular matrix homeostasis. *Nat. Rev. Mol. Cell Biol.* **15**, 802–812 (2014).

66. Cox, T. R. & Erler, J. T. Remodeling and homeostasis of the extracellular matrix: Implications for fibrotic diseases and cancer. *Dis. Model. Mech.* **4**, 165–178 (2011).

67. Guimarães, C. F., Gasperini, L., Marques, A. P. & Reis, R. L. The stiffness of living tissues and its implications for tissue engineering. *Nat. Rev. Mater.* **5**, 351–370 (2020).

68. Humphrey, J. D. & Rajagopal, K. R. A constrained mixture model for growth and remodeling of soft tissues. *Math. Model. Methods Appl. Sci.* **12**, 407–430 (2002).

69. Paszek, M. J. *et al.* Tensional homeostasis and the malignant phenotype. *Cancer Cell* **8**, 241–254 (2005).

70. Cook, J. R. *et al.* Abnormal muscle mechanosignaling triggers cardiomyopathy in mice with Marfan syndrome. *J. Clin. Invest.* **124**, 1329–1339 (2014).

71. Ganesh, S. K. *et al.* Clinical and biochemical profiles suggest fibromuscular dysplasia is a systemic disease with altered TGF-β expression and connective tissue features. *FASEB J.* **28**, 3313–3324 (2014).

72. Humphrey, J. D., Milewicz, D. M., Tellides, G. & Schwartz, M. A. Dysfunctional mechanosensing in aneurysms. *Science* **344**, 477–479 (2014).

73. Eyckmans, J., Boudou, T., Yu, X. & Chen, C. S. A hitchhiker's guide to mechanobiology. *Dev Cell.* **21**, 35–47 (2011).

74. Banes, A. J. *et al.* Mechanoreception at the cellular level: the detection, interpretation, and diversity of responses to mechanical signals. *Biochem. Cell Biol.* **73**, 349–365 (1995).

75. Brown, R. A., Prajapati, R., McGrouther, D. A., Yannas, I. V. & Eastwood, M. Tensional homeostasis in dermal fibroblasts: Mechanical responses to mechanical loading in three-dimensional substrates. *J. Cell. Physiol.* **175**, 323–332 (1998).

76. Delvoye, P., Wiliquet, P., Leveque, J.-L., Nusgens, B. V. & Lapière, C. M. Measurement of mechanical forces generated by skin fibroblasts embedded in a three- dimensional collagen gel. *J. Invest. Dermatol*. **97**, 898–902 (1991).

77. Burridge, K. & Chrzanowska-Wodnicka, M. Focal adhesions, contractility, and signaling. *J. Cell Sci.* **12**, 463–518 (1996).

78. Zaidel-Bar, R., Itzkovitz, S., Ma'ayan, A., Iyengar, R. & Geiger, B. Functional atlas of the integrin adhesome. *Nat. Cell Biol.* **9**, 858–867 (2007).

79. Zaidel-Bar, R. & Geiger, B. The switchable integrin adhesome. *J. Cell Sci.* **123**, 1385–1388 (2010).

80. del Rio, A. *et al.* Stretching Single Talin Rod Molecules Activates Vinculin Binding. *Science* **323**, 638–641 (2009).

81. Carragher, N. O., Levkau, B., Ross, R. & Raines, E. W. Degraded collagen fragments promote rapid disassembly of smooth muscle focal adhesions that correlates with cleavage of pp125(FAK), paxillin, and talin. *J. Cell Biol.* **147**, 619–630 (2009).

82. Moser, M., Legate, K. R., Zent, R. & Fässler, R. The Tail of Integrins, Talin, and Kindlins. *Science* **324**, 895–899 (2009).

83. Provenzano, P. P. & Keely, P. J. Mechanical signaling through the cytoskeleton regulates cell proliferation by coordinated focal adhesion and Rho GTPase signaling. *J. Cell Sci.* **124**, 1195–1205 (2011).

84. Maheshwari, G., Brown, G., Lauffenburger, D. A., Wells, A. & Griffith, L. G. Cell adhesion and motility depend on nanoscale RGD clustering. *J. Cell Sci.* **113**, 1677–1686 (2000).

85. Engler, A. J., Sen, S., Sweeney, H. L. & Discher, D. E. Matrix Elasticity Directs Stem Cell Lineage Specification. *Cell* **126**, 677–689 (2006).

86. Chrzanowska-Wodnicka, M. & Burridge, K. Rho-stimulated contractility drives the formation of stress fibers and focal adhesions. *J. Cell Biol.* **133**, 1403–1415 (1996).

87. Balaban, N. Q. *et al.* Force and focal adhesion assembly: a close relationship studied using elastic micropatterned substrates. *Nat. Cell Biol.* **3**, 466–472 (2001).

88. Lele, T. P. *et al.* Mechanical forces alter zyxin unbinding kinetics within focal adhesions of living cells. *J. Cell. Physiol.* **207**, 187–194 (2006).

89. Zaidel-Bar, R., Ballestrem, C., Kam, Z. & Geiger, B. Early molecular events in the assembly of matrix adhesions at the leading edge of migrating cells. *J. Cell Sci.* **116**, 4605–4613 (2003).

90. Hirata, H., Sokabe, M. & Lim, C. T. *Molecular mechanisms underlying the force-dependent regulation of actin-to-ECM linkage at the focal adhesions*. *Progress in Molecular Biology and Translational Science* **126**, (Elsevier Inc., 2014).

91. Pasapera, A. M., Schneider, I. C., Rericha, E., Schlaepfer, D. D. & Waterman, C. M. Myosin II activity regulates vinculin recruitment to focal adhesions through FAK-mediated paxillin phosphorylation. *J. Cell Biol.* **188**, 877–890 (2010).

92. Mitra, S. K., Hanson, D. A. & Schlaepfer, D. D. Focal adhesion kinase: In command and control of cell motility. *Nat. Rev. Mol. Cell Biol.* **6**, 56–68 (2005).

93. Burridge, K. & Wennerberg, K. Rho and Rac Take Center Stage. *Cell* **116**, 167–179 (2004).

94. Sadok, A. & Marshall, C. J. Rho GTPases. *Small GTPases* **5**, e983878 (2014).

95. Riento, K. & Ridley, A. J. ROCKs: multifunctional kinases in cell behaviour. *Nat. Rev. Mol. Cell Biol.* **4**, 446–456 (2003).

96. Maekawa, M. *et al.* Signaling from Rho to the Actin Cytoskeleton Through Protein Kinases ROCK and LIM-kinase. *Science* **285**, 895–898 (1999).

97. Nikolopoulos, S. N. *et al.* Targeted Deletion of the Integrin β4 Signaling Domain Suppresses Laminin-5-Dependent Nuclear Entry of Mitogen-Activated Protein Kinases and NF-κB, Causing Defects in Epidermal Growth and Migration. *Mol. Cell. Biol.* **25**, 6090–6102 (2005).

98. Walker, J. L. & Assoian, R. K. Integrin-dependent signal transduction regulating cyclin D1 expression and G1 phase cell cycle progression. *Cancer Metastasis Rev.* **24**, 383–393 (2005).

99. Streuli, C. H. & Akhtar, N. Signal co-operation between integrins and other receptor systems. *Biochem. J.* **418**, 491–506 (2009).

100. Jeanes, A. I. *et al.* Specific β-containing Integrins Exert Differential Control on Proliferation and Two-dimensional Collective Cell Migration in Mammary Epithelial Cells. *J. Biol. Chem.* **287**, 24103–24112 (2012).

101. Dong, J.-M., Lau, L.-S., Ng, Y.-W., Lim, L. & Manser, E. Paxillin nuclear-cytoplasmic localization is regulated by phosphorylation of the LD4 motif: evidence that nuclear paxillin promotes cell proliferation. *Biochem. J.* **418**, 173–184 (2009).

102. Sen, A. *et al.* Paxillin mediates extranuclear and intranuclear signaling in prostate cancer proliferation. *J. Clin. Invest.* **122**, 2469–2481 (2012).

103. Reif, S. *et al.* The role of focal adhesion kinase-phosphatidylinositol 3-kinase-Akt signaling in hepatic stellate cell proliferation and type I collagen expression. *J. Biol. Chem.* **278**, 8083–8090 (2003).

104. Li, Y., Dowbenko, D. & Lasky, L. A. AKT/PKB Phosphorylation of p21Cip/WAF1 Enhances Protein Stability of p21Cip/WAF1 and Promotes Cell Survival . *J. Biol. Chem.* **277**, 11352–11361 (2002).

105. Diehl, J. A., Cheng, M., Roussel, M. F. & Sherr, C. J. Glycogen synthase kinase-3β regulates cyclin D1 proteolysis and subcellular localization. *Genes Dev.* **12**, 3499–3511 (1998).

106. Xue, G. & Hemmings, B. A. PKB/Akt–Dependent Regulation of Cell Motility. *JNCI J. Natl. Cancer Inst.* **105**, 393–404 (2013).

107. Humphries, J. D., Byron, A. & Humphries, M. J. Integrin ligands at a glance. *J. Cell Sci.* **119**, 3901–3903 (2006).

108. Geiger, B., Bershadsky, A., Pankov, R. & Yamada, K. M. Transmembrane crosstalk between the extracellular matrix and the cytoskeleton. *Nat. Rev. Mol. Cell Biol.* **2**, 793–805 (2001).

109. Humphries, J. D. *et al.* Proteomic analysis of integrin-associated complexes identifies RCC2 as a dual regulator of Rac1 and Arf6. *Sci. Signal.* **2**, ra51–ra51 (2009).

110. Massia, S. P. & Hubbell, J. A. An RGD spacing of 440 nm is sufficient for integrin alpha V beta 3-mediated fibroblast spreading and 140 nm for focal contact and stress fiber formation. *J. Cell Biol.* **114**, 1089–1100 (1991).

111. Le Saux, G. *et al.* Spacing of Integrin Ligands Influences Signal Transduction in Endothelial Cells. *Biophys. J.* **101**, 764–773 (2011).

112.   Kilian, K. A., Bugarija, B., Lahn, B. T. & Mrksich, M. Geometric cues for directing the differentiation of mesenchymal stem cells. *Proc. Natl. Acad. Sci.* **107**, 4872–4877 (2010).

113.   Rumpler, M., Woesz, A., Dunlop, J. W. C., Van Dongen, J. T. & Fratzl, P. The effect of geometry on three-dimensional tissue growth. *J. R. Soc. Interface* **5**, 1173–1180 (2008).

114.   Benoit, D. S. W. & Anseth, K. S. The effect on osteoblast function of colocalized RGD and PHSRN epitopes on PEG surfaces. *Biomaterials* **26**, 5209–5220 (2005).

115.   Shu, X. Z. *et al.* Attachment and spreading of fibroblasts on an RGD peptide–modified injectable hyaluronan hydrogel. *J. Biomed. Mater. Res. Part A* **68A**, 365–375 (2004).

116.   Chen, C. S., Mrksich, M., Huang, S., Whitesides, G. M. & Ingber, D. E. Geometric Control of Cell Life and Death. *Science* **276**, 1425–1428 (1997).

117.   Théry, M., Pépin, A., Dressaire, E., Chen, Y. & Bornens, M. Cell distribution of stress fibres in response to the geometry of the adhesive environment. *Cell Motil.* **63**, 341–355 (2006).

118.   McBeath, R., Pirone, D. M., Nelson, C. M., Bhadriraju, K. & Chen, C. S. Cell Shape, Cytoskeletal Tension, and RhoA Regulate Stem Cell Lineage Commitment. *Dev. Cell* **6**, 483–495 (2004).

119.   Forner, A., Llovet, J. M. & Bruix, J. Hepatocellular carcinoma. *Lancet* **379**, 1245–1255 (2012).

120.   Kwak, N. *et al.* Lung cancer risk among patients with combined pulmonary fibrosis and emphysema. *Respir. Med.* **108**, 524–530 (2014).

121.   Aaron, B. B. & Gosline, J. M. Elastin as a random-network elastomer: A mechanical and optical analysis of single elastin fibers. *Biopolymers* **20**, 1247–1260 (1981).

122.   Gosline, J. *et al.* Elastic proteins: biological roles and mechanical properties. *Philos. Trans. R. Soc. Lond. B. Biol. Sci.* **357**, 121–132 (2002).

123.   Dutov, P., Antipova, O., Varma, S., Orgel, J. P. R. O. & Schieber, J. D. Measurement of Elastic Modulus of Collagen Type I Single Fiber. *PLoS One* **11**, e0145711 (2016).

124.   Sherratt, M. J. *et al.* Fibrillin Microfibrils are Stiff Reinforcing Fibres in Compliant Tissues. *J. Mol. Biol.* **332**, 183–193 (2003).

125.   Suki, B. & Bates, J. H. T. Extracellular matrix mechanics in lung parenchymal diseases. *Respir. Physiol. Neurobiol.* **163**, 33–43 (2008).

126.   Akhtar, R., Sherratt, M. J., Watson, R. E. B., Kundu, T. & Derby, B. Mapping the Micromechanical Properties of Cryo-sectioned Aortic Tissue with Scanning Acoustic Microscopy. *Mater. Res. Soc. Symp. Proc.* **1132**E, (2009).

127.   Kawano, S. *et al.* Assessment of elasticity of colorectal cancer tissue, clinical utility, pathological and phenotypical relevance. *Cancer Sci.* **106**, 1232–1239 (2015).

128.   Rice, A. J. *et al.* Matrix stiffness induces epithelial – mesenchymal transition and promotes chemoresistance in pancreatic cancer cells. *Oncogenesis* **6**, 1–9 (2017).

129.   Gordic, S. *et al.* Value of tumor stiffness measured with MR elastography for assessment of response of hepatocellular carcinoma to locoregional therapy. *Abdom. Radiol.* **42**, 1685–1694 (2017).

130.   Zhou, Z. H. *et al.* Reorganized collagen in the tumor microenvironment of gastric cancer and its association with prognosis. *J. Cancer* **8**, 1466–1476 (2017).

131.   Pelham, R. J. & Wang, Y. Cell locomotion and focal adhesions are regulated by substrate flexibility. *Proc.*

Natl. Acad. Sci. **94**, 13661–13665 (1997).

132.   Lo, C. M., Wang, H. B., Dembo, M. & Wang, Y. L. Cell movement is guided by the rigidity of the substrate. *Biophys. J.* **79**, 144–152 (2000).

133.   Menon, S. & Beningo, K. A. Cancer cell invasion is enhanced by applied mechanical stimulation. *PLoS One* **6**, e17277–e17277 (2011).

134.   Provenzano, P. P. *et al.* Collagen reorganization at the tumor-stromal interface facilitates local invasion. *BMC Med.* **4**, 38 (2006).

135.   Acerbi, I. *et al.* Human breast cancer invasion and aggression correlates with ECM stiffening and immune cell infiltration. *Integr. Biol.* **7**, 1120–1134 (2015).

136.   Brauchle, E. *et al.* Biomechanical and biomolecular characterization of extracellular matrix structures in human colon carcinomas. *Matrix Biol.* **68**–**69**, 180–193 (2018).

137.   Riching, K. M. *et al.* 3D collagen alignment limits protrusions to enhance breast cancer cell persistence. *Biophys. J.* **107**, 2546–2558 (2014).

138.   Samani, A., Zubovits, J. & Plewes, D. Elastic moduli of normal and pathological human breast tissues: An inversion-technique-based investigation of 169 samples. *Phys. Med. Biol.* **52**, 1565–1576 (2007).

139.   Sinkus, R. *et al.* Viscoelastic shear properties of in vivo breast lesions measured by MR elastography. *Magn. Reson. Imaging* **23**, 159–165 (2005).

140.   Lyshchik, A. *et al.* Elastic Moduli Of Thyroid Tissues Under Compression. **110**, 101–110 (2005).

141.   Venkatesh, S. K. *et al.* MR elastography of liver tumors: Preliminary results. *Am. J. Roentgenol.* **190**, 1534–1540 (2008).

142.   Ling, W. *et al.* Effects of vascularity and differentiation of hepatocellular carcinoma on tumor and liver stiffness: In vivo and in vitro studies. *Ultrasound Med. Biol.* **40**, 739–746 (2014).

143.   Itoh, Y. *et al.* Feasibility of magnetic resonance elastography for the pancreas at 3T. *J. Magn. Reson. Imaging* **43**, 384–390 (2016).

144.   Rubiano, A. *et al.* Viscoelastic properties of human pancreatic tumors and in vitro constructs to mimic mechanical properties. *Acta Biomater.* **67**, 331–340 (2017).

145.   Shoji, S. *et al.* Novel application of three-dimensional shear wave elastography in the detection of clinically significant prostate cancer. *Biomed. Reports* **8**, 373–377 (2018).

146.   Ruei-Zeng, L. & Hwan-You, C. Recent advances in three-dimensional multicellular spheroid culture for biomedical research. *Biotechnol. J.* **3**, 1285 (2008).

147.   Baker, B. M. & Chen, C. S. Deconstructing the third dimension – how 3D culture microenvironments alter cellular cues. *J. Cell Sci.* **125**, 3015–3024 (2012).

148.   Cukierman, E., Pankov, R., Stevens, D. R. & Yamada, K. M. Taking Cell-Matrix Adhesions to the Third Dimension. *Science* **294**, 1708 LP – 1712 (2001).

149.   Griffith, L. G. & Swartz, M. A. Capturing complex 3D tissue physiology in vitro. *Nat. Rev. Mol. Cell Biol.* **7**, 211–224 (2006).

150.   Birgersdotter, A., Sandberg, R. & Ernberg, I. Gene expression perturbation in vitro - A growing case for three-dimensional (3D) culture systems. *Semin. Cancer Biol.* **15**, 405–412 (2005).

151. Perche, F. & Torchilin, V. P. Cancer cell spheroids as a model to evaluate chemotherapy protocols. *Cancer Biol. Ther.* **13**, 1205–1213 (2012).

152. Chitcholtan, K., Asselin, E., Parent, S., Sykes, P. H. & Evans, J. J. Differences in growth properties of endometrial cancer in three dimensional (3D) culture and 2D cell monolayer. *Exp. Cell Res.* **319**, 75–87 (2013).

153. Longati, P. *et al.* 3D pancreatic carcinoma spheroids induce a matrix-rich, chemoresistant phenotype offering a better model for drug testing. *BMC Cancer* **13**, 1–13 (2013).

154. Mueller-Klieser, W. Tumor biology and experimental therapeutics. *Crit. Rev. Oncol. / Hematol.* **36**, 123–139 (2018).

155. Hutmacher, D. W. *et al.* Translating tissue engineering technology platforms into cancer research. *J. Cell. Mol. Med.* **13**, 1417–1427 (2009).

156. Loessner, D. *et al.* Bioengineered 3D platform to explore cell–ECM interactions and drug resistance of epithelial ovarian cancer cells. *Biomaterials* **31**, 8494–8506 (2010).

157. Alemany-Ribes, M. & Semino, C. E. Bioengineering 3D environments for cancer models. *Adv. Drug Deliv. Rev.* **79**, 40–49 (2014).

158. Genové, E., Shen, C., Zhang, S. & Semino, C. E. The effect of functionalized self-assembling peptide scaffolds on human aortic endothelial cell function. *Biomaterials* **26**, 3341–3351 (2005).

159. Fischbach, C. *et al.* Engineering tumors with 3D scaffolds. *Nat. Methods* **4**, 855–860 (2007).

160. Horning, J. L. *et al.* 3-D Tumor Model for In Vitro Evaluation of Anticancer Drugs. *Mol. Pharm.* **5**, 849–862 (2008).

161. Sahoo, S. K., Panda, A. K. & Labhasetwar, V. Characterization of Porous PLGA/PLA Microparticles as a Scaffold for Three Dimensional Growth of Breast Cancer Cells. *Biomacromolecules* **6**, 1132–1139 (2005).

162. Rizzi, S. C. *et al.* Recombinant Protein-co-PEG Networks as Cell-Adhesive and Proteolytically Degradable Hydrogel Matrixes. Part II: Biofunctional Characteristics. *Biomacromolecules* **7**, 3019–3029 (2006).

163. Zhang, S., Gelain, F. & Zhao, X. Designer self-assembling peptide nanofiber scaffolds for 3D tissue cell cultures. *Semin. Cancer Biol.* **15**, 413–420 (2005).

164. Heinrich, M. A., Mostafa, A. M. R. H., Morton, J. P., Hawinkels, L. J. A. C. & Prakash, J. Translating complexity and heterogeneity of pancreatic tumor: 3D in vitro to in vivo models. *Adv. Drug Deliv. Rev.* **174**, 265–293 (2021).

165. Drost, J. & Clevers, H. Organoids in cancer research. *Nat. Rev. Cancer* **18**, 407–418 (2018).

166. Huang, L. *et al.* Ductal pancreatic cancer modeling and drug screening using human pluripotent stem cell- and patient-derived tumor organoids. *Nat. Med.* **21**, 1364–1371 (2015).

167. Boj, S. F. *et al.* Organoid models of human and mouse ductal pancreatic cancer. *Cell* **160**, 324–338 (2015).

168. Cukierman, E., Pankov, R. & Yamada, K. M. Cell interactions with three-dimensional matrices. *Curr. Opin. Cell Biol.* **14**, 633–639 (2002).

169. Hartgerink, J. D., Beniash, E. & Stupp, S. I. Self-Assembly and Mineralization of Peptide-Amphiphile Nanofibers. *Science (80-.).* **294**, 1684 LP – 1688 (2001).

170. Schneider, J. P. *et al.* Responsive Hydrogels from the Intramolecular Folding and Self-Assembly of a Designed Peptide. *J. Am. Chem. Soc.* **124**, 15030–15037 (2002).

171. Zhang, S., Holmes, T., Lockshin, C. & Rich, A. Spontaneous assembly of a self-complementary oligopeptide to form a stable macroscopic membrane. *Proc. Natl. Acad. Sci* **90**, 3334–3338 (1993).

172. Aggeli, A. *et al.* Responsive gels formed by the spontaneous self-assembly of peptides into polymeric β-sheet tapes. *Letters to nature* **386**, 259–262 (1997).

173. Kisiday, J. *et al.* Self-assembling peptide hydrogel fosters chondrocyte extracellular matrix production and cell division: Implications for cartilage tissue repair. *PNAS* **99**, 9996–10001 (2002).

174. Semino, C. E. Can We Build Artificial Stem Cell Compartments ? **3**, 164–169 (2003).

175. Elsa, G. *et al.* Functionalized self-assembling peptide hydrogel enhance maintenance of hepatocyte activity in vitro. *J. Cell. Mol. Med.* **13**, 3387–3397 (2009).

176. Semino, C. E. Self-assembling Peptides: From Bio-inspired Materials to Bone Regeneration. *J. Dent. Res.* **87**, 606–616 (2008).

177. Sieminski, A. L., Semino, C. E., Gong, H. & Kamm, R. D. Primary sequence of ionic self-assembling peptide gels affects endothelial cell adhesion and capillary morphogenesis. *J. Biomed. Mater. Res. - Part A* **87**, 494–504 (2008).

178. Genové, E. *et al.* Functionalized self-assembling peptide hydrogel enhance maintenance of hepatocyte activity in vitro. *J. Cell. Mol. Med.* **13**, 3387–3397 (2009).

179. Fernández-Muiños, T. *et al.* Bimolecular based heparin and self-assembling hydrogel for tissue engineering applications. *Acta Biomater.* **16**, 35–48 (2015).

180. Betriu, N. & Semino, C. E. Development of a 3D Co-Culture System as a Cancer Model Using a Self-Assembling Peptide Scaffold. *Gels* **4**, 65 (2018).

181. Betriu, N., Andreeva, A. & Semino, C. E. Erlotinib Promotes Ligand-Induced EGFR Degradation in 3D but Not 2D Cultures of Pancreatic Ductal Adenocarcinoma Cells. *Cancers* **13**, 4504 (2021).

182. Recha-Sancho, L. & Semino, C. E. Chondroitin sulfate- and decorin-based self-Assembling scaffolds for cartilage tissue engineering. *PLoS One* **11**, 1–23 (2016).

183. Betriu, N., Jarrosson-Moral, C. & Semino, C. E. Culture and Differentiation of Human Hair Follicle Dermal Papilla Cells in a Soft 3D Self-Assembling Peptide Scaffold. *Biomolecules* **10**, 684 (2020).

184. Castells-Sala, C. *et al.* Three-Dimensional Cultures of Human Subcutaneous Adipose Tissue-Derived Progenitor Cells Based on RAD16-I Self-Assembling Peptide. *Tissue Eng. Part C Methods* **22**, ten.tec.2015.0270 (2016).

185. Semino, C. E., Merok, J. R., Crane, G. G., Panagiotakos, G. & Zhang, S. Functional differentiation of hepatocyte-like spheroid structures from putative liver progenitor cells in three-dimensional peptide scaffolds. *Differentiation* **71**, 262–270 (2003).

186. Aloy-Reverté, C., Moreno-Amador, J. L., Nacher, M., Montanya, E. & Semino, C. E. Use of RGD-Functionalized Sandwich Cultures to Promote Redifferentiation of Human Pancreatic Beta Cells After In Vitro Expansion. *Tissue Eng. Part A* **24**, 394–406 (2018).

187. Schrader, J. *et al.* Matrix stiffness modulates proliferation, chemotherapeutic response, and dormancy in hepatocellular carcinoma cells. *Hepatology* **53**, 1192–1205 (2011).

188. Markowski, M. C., Brown, A. C. & Barker, T. H. Directing epithelial to mesenchymal transition through engineered microenvironments displaying orthogonal adhesive and mechanical cues. *J. Biomed. Mater. Res. - Part A* **100 A**, 2119–2127 (2012).

189.   Yangben, Y. *et al.* Relative rigidity of cell-substrate effects on hepatic and hepatocellular carcinoma cell migration. *J. Biomater. Sci. Polym. Ed.* **24**, 148–157 (2012).

190.   Leight, J. L., Wozniak, M. A., Chen, S., Lynch, M. L. & Chen, C. S. Matrix rigidity regulates a switch between TGF-β1-induced apoptosis and epithelial-mesenchymal transition. *Mol. Biol. Cell* **23**, 781–791 (2012).

191.   Provenzano, P. P., Inman, D. R., Eliceiri, K. W. & Keely, P. J. Matrix density-induced mechanoregulation of breast cell phenotype, signaling and gene expression through a FAK-ERK linkage. *Oncogene* **28**, 4326–4343 (2009).

192.   Sapudom, J. *et al.* The phenotype of cancer cell invasion controlled by fibril diameter and pore size of 3D collagen networks. *Biomaterials* **52**, 367–375 (2015).

193.   Gill, B. J. *et al.* A synthetic matrix with independently tunable biochemistry and mechanical properties to study epithelial morphogenesis and EMT in a lung adenocarcinoma model. *Cancer Res.* **72**, 6013–6023 (2012).

194.   Wang, C., Tong, X. & Yang, F. Bioengineered 3D brain tumor model to elucidate the effects of matrix stiffness on glioblastoma cell behavior using peg-based hydrogels. *Mol. Pharm.* **11**, 2115–2125 (2014).

195.   Liu, H. Y., Nguyen, H. D. & Lin, C. C. Dynamic PEG–Peptide Hydrogels via Visible Light and FMN-Induced Tyrosine Dimerization. *Adv. Healthc. Mater.* **7**, 1–10 (2018).

196.   Lee, D. S., Kang, J. Il, Hwang, B. H. & Park, K. M. Interpenetrating Polymer Network Hydrogels of Gelatin and Poly(ethylene glycol) as an Engineered 3D Tumor Microenvironment. *Macromol. Res.* **27**, 205–211 (2019).

197.   Puls, T. J., Tan, X., Whittington, C. F. & Voytik-Harbin, S. L. 3D collagen fibrillar microstructure guides pancreatic cancer cell phenotype and serves as a critical design parameter for phenotypic models of EMT. *PLoS One* **12**, 1–25 (2017).

198.   Jang, M. *et al.* Increased extracellular matrix density disrupts E-cadherin/β-catenin complex in gastric cancer cells. *Biomater. Sci.* **6**, 2704–2713 (2018).

199.   Zaman, M. H. *et al.* Migration of tumor cells in 3D matrices is governed by matrix stiffness along with cell-matrix adhesion and proteolysis. *Proc. Natl. Acad. Sci. U. S. A.* **103**, 10889–10894 (2006).

200.   Alonso-Nocelo, M. *et al.* Matrix stiffness and tumor-Associated macrophages modulate epithelial to mesenchymal transition of human adenocarcinoma cells. *Biofabrication* **10**, (2018).

201.   Lee, J. Y. *et al.* YAP-independent mechanotransduction drives breast cancer progression. *Nat. Commun.* **10**, 1–9 (2019).

202.   Chang, J., Pang, E. M., Adebowale, K., Wisdom, K. M. & Chaudhuri, O. Increased Stiffness Inhibits Invadopodia Formation and Cell Migration in 3D. *Biophys. J.* **119**, 726–736 (2020).

203.   Lam, C. R. I. *et al.* A 3D biomimetic model of tissue stiffness interface for cancer drug testing. *Mol. Pharm.* **11**, 2016–2021 (2014).

204.   Guzman, A., Ziperstein, M. J. & Kaufman, L. J. The effect of fibrillar matrix architecture on tumor cell invasion of physically challenging environments. *Biomaterials* **35**, 6954–6963 (2014).

205.   Berger, A. J., Linsmeier, K. M., Kreeger, P. K. & Masters, K. S. Decoupling the effects of stiffness and fiber density on cellular behaviors via an interpenetrating network of gelatin-methacrylate and collagen. *Biomaterials* **141**, 125–135 (2017).

206.   Berger, A. J. *et al.* Scaffold stiffness influences breast cancer cell invasion via EGFR-linked Mena

upregulation and matrix remodeling. *Matrix Biol.* **85–86**, 80–93 (2020).

207. Wei, S. C. *et al.* Matrix stiffness drives epithelial-mesenchymal transition and tumour metastasis through a TWIST1-G3BP2 mechanotransduction pathway. *Nat. Cell Biol.* **17**, 678–688 (2015).

208. Micalet, A., Moeendarbary, E. & Cheema, U. 3D in Vitro Models for Investigating the Role of Stiffness in Cancer Invasion. *ACS Biomater. Sci. Eng.* (2021).

209. Debnath, J., Muthuswamy, S. K. & Brugge, J. S. Morphogenesis and oncogenesis of MCF-10A mammary epithelial acini grown in three-dimensional basement membrane cultures. *Methods* **30**, 256–268 (2003).

210. Kenny, P. A. *et al.* The morphologies of breast cancer cell lines in three-dimensional assays correlate with their profiles of gene expression. *Mol. Oncol.* **1**, 84–96 (2007).

211. Miroshnikova, Y. A. *et al.* Engineering strategies to recapitulate epithelial morphogenesis within synthetic three-dimensional extracellular matrix with tunable mechanical properties. *Phys. Biol.* **8**, (2011).

212. Betriu, N., Recha-sancho, L. & Semino, C. E. Culturing Mammalian Cells in Three-dimensional Peptide Scaffolds. *J. Vis. Exp.* e57259 (2018).

213. Schindelin, J. *et al.* Fiji: An open-source platform for biological-image analysis. *Nat. Methods* **9**, 676–682 (2012).

214. Manders, E. M. M., Stap, J., Brakenhoff, G. J., Van Driel, R. & Aten, J. A. Dynamics of three-dimensional replication patterns during the S-phase, analysed by double labelling of DNA and confocal microscopy. *J. Cell Sci.* **103**, 857–862 (1992).

215. Sastre, D., Estadella, I., Bosch, M. & Felipe, A. Triple-Colocalization Approach to Assess Traffic Patterns and Their Modulation. **2040**, 215–233 (2019).

216. Bolte, S. & Cordelières, F. P. A guided tour into subcellular colocalization analysis in light microscopy. *J. Microsc.* **224**, 213–232 (2006).

217. Mendelsohn, J. & Baselga, J. Epidermal Growth Factor Receptor Targeting in Cancer. *Semin Oncol* **33**, 369–385 (2006).

218. Tan, X., Lambert, P. F., Rapraeger, A. C. & Anderson, R. A. Stress-Induced EGFR Trafficking: Mechanisms, Functions, and Therapeutic Implications. *Trends Cell Biol.* **26**, 352–366 (2016).

219. Oksvold, M. P., Hultfeldt, H. S., Øtvold, A. C. & Skarpen, E. UV induces tyrosine kinase-independent internalisation and endosome arrest of the EGF receptor. *J. Cell Sci.* **115**, 793–803 (2002).

220. Jia Shen, Weiya Xia, Yekaterina. Khotskaya, Longfei Huo, Kotaro Nakanishi, Seung-Oe Lim, Yi Du, Y. W. EGFR modulates microRNA maturation in response to hypoxia through phosphorylation of AGO2. *Nature* **497**, 383–387 (2013).

221. Fang, Y., Tan, J. & Zhang, Q. Signaling pathways and mechanisms of hypoxia-induced autophagy in the animal cells. *Cell Biol. Int.* **39**, 891–898 (2015).

222. Filomeni, G., De Zio, D. & Cecconi, F. Oxidative stress and autophagy: The clash between damage and metabolic needs. *Cell Death Differ.* **22**, 377–388 (2015).

223. Roepstorff, K. *et al.* Differential effects of EGFR ligands on endocytic sorting of the receptor. *Traffic* **10**, 1115–1127 (2009).

224. Henriksen, L., Grandal, M. V., Knudsen, S. L. J., van Deurs, B. & Grøvdal, L. M. Internalization Mechanisms of the Epidermal Growth Factor Receptor after Activation with Different Ligands. *PLoS One* **8**, e58148

(2013).

225. Blandin, A. F. *et al.* Gefitinib induces EGFR and α5β1 integrin co-endocytosis in glioblastoma cells. *Cell. Mol. Life Sci.* **78**, 2949–2962 (2020).

226. Cao, X., Zhu, H., Ali-Osman, F. & Lo, H. W. EGFR and EGFRvIII undergo stress- and EGFR kinase inhibitor-induced mitochondrial translocalization: A potential mechanism of EGFR-driven antagonism of apoptosis. *Mol. Cancer* **10**, 26 (2011).

227. Nishimura, Y., Bereczky, B. & Ono, M. The EGFR inhibitor gefitinib suppresses ligand-stimulated endocytosis of EGFR via the early/late endocytic pathway in non-small cell lung cancer cell lines. *Histochem. Cell Biol.* **127**, 541–553 (2007).

228. Dreier, A., Barth, S., Goswami, A. & Weis, J. Cetuximab induces mitochondrial translocation of EGFRvIII, but not EGFR: Involvement of mitochondria in tumor drug resistance? *Tumor Biol.* **33**, 85–94 (2012).

229. Liao, H. J. & Carpenter, G. Cetuximab/C225-induced intracellular trafficking of epidermal growth factor receptor. *Cancer Res.* **69**, 6179–6183 (2009).

230. Minchinton, A. I. & Tannock, I. F. Drug penetration in solid tumours. *Nat Rev Cancer* **6**, 583–592 (2006).

231. Thakuri, P. S., Liu, C., Luker, G. D. & Tavana, H. Biomaterials-Based Approaches to Tumor Spheroid and Organoid Modeling. *Adv. Healthc. Mater.* **7**, 1–21 (2018).

232. Cui, X., Hartanto, Y. & Zhang, H. Advances in multicellular spheroids formation. *J. R. Soc. Interface* **14**, (2017).

233. Liu, C., Lewin Mejia, D., Chiang, B., Luker, K. E. & Luker, G. D. Hybrid Collagen Alginate Hydrogel as a Platform for 3D Tumor Spheroid Invasion. *Acta Biomater.* **75**, 213–225 (2018).

234. Miyazaki, K., Oyanagi, J., Hoshino, D., Kumagai, H. & Miyagi, Y. Cancer cell migration on elongate protrusions of fibroblasts in collagen matrix. *Sci. Rep.* **9**, 1–15 (2019).

235. Kim, S.-K. *et al.* Phenotypic Heterogeneity and Plasticity of Cancer Cell Migration in a Pancreatic Tumor Three-Dimensional Culture Model. *Cancers (Basel).* **12**, 1–17 (2020).

236. Ricci, C. *et al.* Interfacing polymeric scaffolds with primary pancreatic ductal adenocarcinoma cells to develop 3D cancer models. *Biomatter* **4**, e955386 (2015).

237. Rice, A. J. *et al.* Matrix stiffness induces epithelial-mesenchymal transition and promotes chemoresistance in pancreatic cancer cells. *Oncogenesis* **6**, 1–9 (2017).

238. Marí-Buyé, N., Luque, T., Navajas, D. & Semino, C. E. Development of a Three-Dimensional Bone-Like Construct in a Soft Self-Assembling Peptide Matrix. *Tissue Eng. Part A* **19**, 870–881 (2013).

239. Recha-Sancho, L. & Semino, C. E. Heparin-based self-assembling peptide scaffold reestablish chondrogenic phenotype of expanded de-differentiated human chondrocytes. *J. Biomed. Mater. Res. - Part A* **104**, 1694–1706 (2016).

240. Song, H. *et al.* Three-dimensional culture and clinical drug responses of a highly metastatic human ovarian cancer HO-8910PM cells in nanofibrous microenvironments of three hydrogel biomaterials. *J. Nanobiotechnology* **18**, 1–19 (2020).

241. Buck, E. *et al.* Inactivation of Akt by the epidermal growth factor receptor inhibitor erlotinib is mediated by HER-3 in pancreatic and colorectal tumor cell lines and contributes to erlotinib sensitivity. *Mol. Cancer Ther.* **5**, 2051–2059 (2006).

242. Bryant, K. L., Mancias, J. D., Kimmelman, A. C. & Der, C. J. KRAS: Feeding pancreatic cancer proliferation. *Trends Biochem. Sci.* **39**, 91–100 (2014).

243. Sieminski, A. L., Was, A. S., Kim, G., Gong, H. & Kamm, R. D. The stiffness of three-dimensional ionic self-assembling peptide gels affects the extent of capillary-like network formation. *Cell Biochem. Biophys.* **49**, 73–83 (2007).

244. Hadjipanayi, E., Mudera, V. & R.A, B. Close dependence of fibroblast proliferation on collagen scaffold matrix stiffness. *J. Tissue Eng. Regen. Med.* **3**, 77–84 (2008).

245. Jones, S. *et al.* Targeting of EGFR by a combination of antibodies mediates unconventional EGFR trafficking and degradation. *Sci. Rep.* **10**, 1–19 (2020).

246. Iida, M. *et al.* Sym004, a novel EGFR antibody mixture, can overcome acquired resistance to cetuximab. *Neoplasia* **15**, 1196–1206 (2013).

247. Sobhakumari, A. *et al.* NOX4 mediates cytoprotective autophagy induced by the EGFR inhibitor erlotinib in head and neck cancer cells. *Toxicol. Appl. Pharmacol.* **272**, 736–745 (2013).

248. Zou, Y., Ling, Y., Sironi, J. & Schwartz, E. L. The Autophagy Inhibitor Chloroquine Overcomes the Innate Resistance of Wild-Type EGFR Non-Small-Cell Lung Cancer Cells to Erlotinib. *JTO* **8**, 693–702 (2013).

249. Dragowska, W. H. *et al.* Induction of Autophagy Is an Early Response to Gefitinib and a Potential Therapeutic Target in Breast Cancer. *PLoS One* **8**, 1–20 (2013).

250. Sakuma, Y. *et al.* Enhanced autophagy is required for survival in EGFR-independent EGFR-mutant lung adenocarcinoma cells. *Lab. Investig.* **93**, 1137–1146 (2013).

251. Yoshimori, T., Yamamoto, A., Moriyama, Y., Futai, M. & Tashiro, Y. Bafilomycin A1, a specific inhibitor of vacuolar-type H+-ATPase, inhibits acidification and protein degradation in lysosomes of cultured cells. *J. Biol. Chem.* **266**, 17707–17712 (1991).

252. Mauvezin, C., Nagy, P., Juhász, G. & Neufeld, T. P. Autophagosome-lysosome fusion is independent of V-ATPase-mediated acidification. *Nat. Commun.* **6**, (2015).

253. Melikova, M. S., Kondratov, K. A. & Kornilova, E. S. Two different stages of epidermal growth factor (EGF) receptor endocytosis are sensitive to free ubiquitin depletion produced by proteasome inhibitor MG132. *Cell Biol. Int.* **30**, 31–43 (2006).

254. Albornoz, N., Bustamante, H., Soza, A. & Burgos, P. Cellular responses to proteasome inhibition: Molecular mechanisms and beyond. *Int. J. Mol. Sci.* **20**, (2019).

255. Liu, M. *et al.* Collagen-based three-dimensional culture microenvironment promotes epithelial to mesenchymal transition and drug resistance of human ovarian cancer in vitro. *RSC Adv.* **8**, 8910–8919 (2018).

256. Firuzi, O. *et al.* Role of c-MET inhibitors in overcoming drug resistance in spheroid models of primary human pancreatic cancer and stellate cells. *Cancers* **11**, 638 (2019).

257. Dangi-Garimella, S. *et al.* Three-dimensional collagen I promotes gemcitabine resistance in pancreatic cancer through MT1-MMP-mediated expression of HMGA2. *Cancer Res.* **71**, 1019–1028 (2011).

258. Pinilla-Macua, I., Grassart, A., Duvvuri, U., Watkins, S. C. & Sorkin, A. EGF receptor signaling, phosphorylation, ubiquitylation and endocytosis in tumors in vivo. *Elife* **6**, 1–25 (2017).

259. Heukers, R. *et al.* Endocytosis of EGFR requires its kinase activity and N-terminal transmembrane dimerization motif. *J. Cell Sci.* **126**, 4900–4912 (2013).

260. Ménard, L., Floc'h, N., Martin, M. J. & Cross, D. A. E. Reactivation of mutant-EGFR degradation through clathrin inhibition overcomes resistance to EGFR tyrosine kinase inhibitors. *Cancer Res.* **78**, 3267–3279 (2018).

261. de Wit, M. *et al.* Mutation and drug-specific intracellular accumulation of EGFR predict clinical responses to tyrosine kinase inhibitors. *EBioMedicine* **56**, 1–12 (2020).

262. Beardmore, J. M. & Richards, R. C. Concentrations of epidermal growth factor in mouse milk throughout lactation. *J. Endocrinol.* **96**, 287–292 (1983).

263. Grau, M., Rodríguez, C., Soley, M. & Ramírez, I. Relationship between epidermal growth factor in mouse submandibular glands, plasma, and bile: effects of catecholamines and fasting. *Endocrinology* **135**, 1854–1862 (1994).

264. Mullin, J. M. Epithelial Barriers, Compartmentation and Cancer. *Sci. Signal.* **2004**, pe2–pe2 (2004).

265. Thøgersen, V. B. *et al.* A Subclass of HER1 Ligands Are Prognostic Markers for Survival in Bladder Cancer Patients. *Cancer Res.* **61**, 6227–6233 (2001).

266. Normanno, N. *et al.* The ErbB Receptors and their Ligands in Cancer: An Overview. *Curr. Drug Targets* **6**, 243–257 (2005).

267. Révillion, F., Lhotellier, V., Hornez, L., Bonneterre, J. & Peyrat, J.-P. ErbB/HER ligands in human breast cancer, and relationships with their receptors, the bio-pathological features and prognosis. *Ann. Oncol.* **19**, 73–80 (2008).

268. Siegel, R. L., Miller, K. D., Fuchs, H. E. & Jemal, A. Cancer Statistics, 2021. *CA Cancer J. Clin.* **71**, 7–33 (2021).

269. Kleeff, J. *et al.* Pancreatic cancer. *Nat. Rev. Dis. Prim.* **2**, 16022 (2016).

270. Maccurtain, B. M., Quirke, N. P., Thorpe, S. D. & Gallagher, T. K. Pancreatic ductal adenocarcinoma: Relating biomechanics and prognosis. *J. Clin. Med.* **10**, 2711 (2021).

271. Ferrara, B. *et al.* The extracellular matrix in pancreatic cancer: Description of a complex network and promising therapeutic options. *Cancers (Basel).* **13**, 4442 (2021).

272. Jones, D. P., Hanna, W., Cramer, G. M. & Celli, J. P. In situ measurement of ECM rheology and microheterogeneity in embedded and overlaid 3D pancreatic tumor stroma co-cultures via passive particle tracking. *J. Innov. Opt. Health Sci.* **10**, 1–9 (2017).

273. Carragher, N. O., Levkau, B., Ross, R. & Raines, E. W. Degraded collagen fragments promote rapid disassembly of smooth muscle focal adhesions that correlates with cleavage of pp125(FAK), paxillin, and talin. *J. Cell Biol.* **147**, 619–629 (1999).

274. Genové, E., Betriu, N. & Semino, C. E. β-Sheet to Random Coil Transition in Self-Assembling Peptide Scaffolds Promotes Proteolytic Degradation. *Biomolecules* **12**, 411 (2022).

275. Steele, J. G., Dalton, B. A., Johnson, G. & Underwood, P. A. Adsorption of fibronectin and vitronectin onto Primaria™ and tissue culture polystyrene and relationship to the mechanism of initial attachment of human vein endothelial cells and BHK-21 fibroblasts. *Biomaterials* **16**, 1057–1067 (1995).

276. Moreno-Layseca, P. & Streuli, C. H. Signalling pathways linking integrins with cell cycle progression. *Matrix Biol.* **34**, 144–153 (2014).

277. Mireia Alemany Ribes. Doctoral Thesis. Development of 3D cancer models to obtain mechanistic insights into disease progression. (2016).

278. Jokinen, J. *et al.* Integrin-mediated cell adhesion to type I collagen fibrils. *J. Biol. Chem.* **279**, 31956–31963 (2004).

279. Jiang, H. *et al.* Targeting focal adhesion kinase renders pancreatic cancers responsive to checkpoint immunotherapy. *Nat. Med.* **22**, 851–860 (2016).

280. Vitale, M. *et al.* Incorporation of Natural and Recombinant Collagen Proteins within Fmoc-Based Self-Assembling Peptide Hydrogels. *Gels* **8**, 254 (2022).

281. Grzesiak, J. J. & Bouvet, M. The α2β1 integrin mediates the malignant phenotype on type I collagen in pancreatic cancer cell lines. *Br. J. Cancer* **94**, 1311–1319 (2006).

282. Meltzer, H. & Silberberg, A. Adsorption of collagen, serum albumin, and fibronectin to glass and to each other. *J. Colloid Interface Sci.* **126**, 292–303 (1988).

283. Engvall, E. & Ruoslahti, E. Binding of soluble form of fibroblast surface protein, fibronectin, to collagen. *Int. J. Cancer* **20**, 1–5 (1977).

284. Velez, D. O. *et al.* 3D collagen architecture regulates cell adhesion through degradability, thereby controlling metabolic and oxidative stress. *Integr. Biol.* **11**, 221–234 (2019).

285. Mi, K. *et al.* Influence of a self-assembling peptide, RADA16, compared with collagen I and matrigel on the malignant phenotype of human breast-cancer cells in 3D cultures and in vivo. *Macromol. Biosci.* **9**, 437–443 (2009).